U.S. DEPARTMENT OF COMMERCE
National Technical Information Service

PB-286 893

Sludge Dewatering and Drying on Sand Beds

Massachusetts Univ, Amherst Dept of Civil Engineering

Prepared for

Municipal Environmental Research Labs, Cincinnati, OH

Aug 78

United States
Environmental Protection
Agency

Municipal Environmental Research
Laboratory
Cincinnati OH 45268

EPA-600/2-78-141
August 1978

Research and Development

PB 286893

EPA

Sludge Dewatering and Drying on Sand Beds

REPRODUCED BY
NATIONAL TECHNICAL
INFORMATION SERVICE
U. S. DEPARTMENT OF COMMERCE
SPRINGFIELD, VA. 22161

RESEARCH REPORTING SERIES

Research reports of the Office of Research and Development, U.S. Environmental Protection Agency, have been grouped into nine series. These nine broad categories were established to facilitate further development and application of environmental technology. Elimination of traditional grouping was consciously planned to foster technology transfer and a maximum interface in related fields. The nine series are:

1. Environmental Health Effects Research
2. Environmental Protection Technology
3. Ecological Research
4. Environmental Monitoring
5. Socioeconomic Environmental Studies
6. Scientific and Technical Assessment Reports (STAR)
7. Interagency Energy-Environment Research and Development
8. "Special" Reports
9. Miscellaneous Reports

This report has been assigned to the ENVIRONMENTAL PROTECTION TECHNOLOGY series. This series describes research performed to develop and demonstrate instrumentation, equipment, and methodology to repair or prevent environmental degradation from point and non-point sources of pollution. This work provides the new or improved technology required for the control and treatment of pollution sources to meet environmental quality standards.

This document is available to the public through the National Technical Information Service, Springfield, Virginia 22161.

EPA-600/2-78-141
August 1978

SLUDGE DEWATERING AND DRYING ON SAND BEDS

by

Donald Dean Adrian
Environmental Engineering Program
Department of Civil Engineering
University of Massachusetts/Amherst
Amherst, Massachusetts 01003

Grant No. WP 01239/17070 DZS

Project Officers

James E. Smith, Jr.
Roland V. Villiers
Ultimate Disposal Section
Municipal Environmental Research Laboratory
Cincinnati, Ohio 45268

MUNICIPAL ENVIRONMENTAL RESEARCH LABORATORY
OFFICE OF RESEARCH AND DEVELOPMENT
U. S. ENVIRONMENTAL PROTECTION AGENCY
CINCINNATI, OHIO 45268

DISCLAIMER

This report has been reviewed by the Municipal Environmental Research Laboratory, Cincinnati, Ohio, U. S. Environmental Protection Agency, and approved for publication. Approval does not signify that the contents necessarily reflect the views and policies of the U. S. Environmental Protection Agency, nor does the mention of trade names or commercial products constitute endorsement or recommendation for use.

TECHNICAL REPORT DATA
(Please read Instructions on the reverse before completing)

1. REPORT NO. EPA-600/2-78-141	2.	3. RECIPIENT'S ACCESSION NO. PB286893
4. TITLE AND SUBTITLE Sludge Dewatering and Drying on Sand Beds		5. REPORT DATE August 1978 (Issuing Date)
		6. PERFORMING ORGANIZATION CODE
7. AUTHOR(S) Donald Dean Adrian		8. PERFORMING ORGANIZATION REPORT NO.
9. PERFORMING ORGANIZATION NAME AND ADDRESS Environmental Engineering Program Department of Civil Engineering University of Massachusetts Amherst, Massachusetts 01003		10. PROGRAM ELEMENT NO. 1BC611 11. CONTRACT/GRANT NO. WP-01239/17070-DZS
12. SPONSORING AGENCY NAME AND ADDRESS Municipal Environmental Research Laboratory--Cin., OH Office of Research and Development U.S. Environmental Protection Agency Cincinnati, Ohio 45268		13. TYPE OF REPORT AND PERIOD COVERED Final 6/1/67 - 6/30/74 14. SPONSORING AGENCY CODE EPA/600/14

15. SUPPLEMENTARY NOTES
Project Officer: Roland V. Villiers (513) 684-7664

16. ABSTRACT

Dewatering of water and wastewater treatment sludges was examined through mathematical modeling and experimental work. The various components of the research include: (1) chemical analyses of water treatment sludges, (2) drainage and drying studies of sludges, (3) a mathematical model to describe sludge drainage and drying on sand beds, and (4) a procedure to optimize the size of sand beds.

Computer simulation studies were conducted of wastewater and water treatment sludges. The output of this 20-year simulation under six weather conditions was a random variable, the required dewatering time, and its associated frequency distribution. Of the parameters describing sludge characteristics, solids content had the most important effect on dewatering time, and in most cases dominated the effects of specific resistance.

Economic analyses were applied to the outputs of simulation for finding an optimum system design. Two different approaches were used: the first finds an optimum design that fulfills the target output at a minimum cost among the known alternatives; the second uses the concept of marginal analysis to assign a cash value to the end product (dry solids) of the dewatering process, so that the optimum design is obtained at the point where the cost of inputs (land and operation) is just equal to the marginal value of output.

17. KEY WORDS AND DOCUMENT ANALYSIS

a. DESCRIPTORS	b. IDENTIFIERS/OPEN ENDED TERMS	c. COSATI Field/Group
Cost analysis Dewatering Optimum design Sludge drying Waste treatment Water quality Water treatment	Drying rates Sand drying beds Ultimate disposal Wastewater treatment	13B

18. DISTRIBUTION STATEMENT Release to public	19. SECURITY CLASS *(This Report)* Unclassified	21. NO. OF PAGES 196
	20. SECURITY CLASS *(This page)* Unclassified	22. PRICE PC A09 MF A01

FOREWORD

The Environmental Protection Agency was created because of increasing public and government concern about the dangers of pollution to the health and welfare of the American people. Noxious air, foul water, and spoiled land are tragic testimony to the deterioration of our natural environment. The complexity of that environment and the interplay between its components require a concentrated and integrated attack on the problem.

Research and development is that necessary first step in problem solution and it involves defining the problem, measuring its impact, and searching for solutions. The Municipal Environmental Research Laboratory develops new and improved technology and systems for the prevention, treatment, and management of wastewater and solid and hazardous waste pollutant discharges from municipal and community sources, for the preservation and treatment of public drinking water supplies, and to minimize the adverse economic, social, health, and aesthetic effects of pollution. This publication is one of the products of that research; a most vital communications link between the researcher and the user community.

This report summarizes the results of water and wastewater treatment sludge dewatering studies in which a computer simulation procedure is developed to investigate sludge dewatering time and to optimize the size of sand beds. Such a procedure provides a useful means by which water pollution control agencies may realize greater efficiencies in their efforts to protect the environment.

Francis T. Mayo
Director
Municipal Environmental
Research Laboratory

ABSTRACT

The research program presented in this report was developed to examine sludge dewatering through both theoretical and experimental work. Its various components include formulation of mathematical models for sludge drainage and drying on sand beds, preparation of input data for mathematical models, validation of simulation experiments, and analysis of the outputs generated by simulation so as to prescribe an optimum system design.

Drainage and drying studies were conducted under controlled conditions on a variety of sludges. In some cases water content profiles of sludge cakes and supporting sand layers were determined by a gamma-ray attenuation method. Chemical analyses were performed on sludge, filtrate and decant samples.

A theoretical analysis of gravity dewatering of wastewater sludge is presented, and an equation describing the drainage rate developed. The equation relates the depth of sludge with time, using the parameters of solids content, specific resistance, coefficient of compressibility, dynamic viscosity and density of the filtrate. Extensive bench-scale tests substantiated the theory. The concept of media factor is introduced to account for the role of the supporting media. Potential applications of the equation are discussed.

Computer simulation studies were conducted of water and wastewater treatment sludges. The output of this 20-year simulation under six weather conditions is a random variable, the required dewatering time, and its associated frequency distribution. Of the parameters describing sludge characteristics, solids content had the most important effect on dewatering time and in most cases dominated the effects of specific resistance.

Economic analyses were applied to the outputs of simulation for finding an optimum system design. Two different approaches were used: the first finds an optimum design that fulfills the target output at a minimum cost among known alternatives; the second uses the concept of marginal analysis to assign a cash value to the end product (dry solids) of the dewatering process, resulting in an optimum design obtained at the point where the cost of inputs (land and operation) is just equal to the marginal value of output.

The criteria developed may be used by an engineer to design beds on the basis of climatic conditions and the nature of sludge to be dewatered, while assuring that the system will be economically efficient.

This report was submitted in fulfillment of Grant No. WP 01239/17070 DZS by the Department of Civil Engineering, University of Massachusetts at Amherst, under the sponsorship of the U. S. Environmental Protection Agency. The report covers a period from June 1, 1967 to April 1, 1977. Experimental work was completed as of June 30, 1972.

CONTENTS

Foreword iii
Abstract iv
Figures. ix
Tables xiv
Acknowledgments. xvii

I. Introduction. 1
  References 4
II. Conclusions and Recommendations 5
  Conclusions. 5
  Recommendations. 6
III. Review of the Literature. 8
  References 19
IV. Theoretical Considerations. 20
  Moisture 20
  Derivation of specific resistance. 21
  Derivation of mathematical model for the gravity drainage rate 29
  Evaporation of water 33
  Drying 35
  Diffusion of moisture. 38
  Drying rate. 41
  Critical moisture content. 43
  References 46
V. Materials and Apparatus 49
  Types of sludge examined 49
  Equipment for the gravity drainage study 50
  Equipment for drying, evaporation and complex dewatering studies 50
  Moisture measurement apparatus 53
  Scintillation counting equipment 53
  References 57
VI. Methodology 58
  Sludge characteristics 58
  Gravity drainage study 58
  Evaporation and drying studies 60
  Complex sludge dewatering studies. 62
  Moisture profile 63
  Diffusion. 69
  Discussion of the method 70
  Discussion of the results. 72
  References 78

Preceding page blank

VII. Results 81
Chemical characteristics 81
Results of the gravity drainage study. 86
Results of the evaporation and drying studies. 94
Results of drying. 98
Results of the complex sludge dewatering studies 105
Moisture and solids profile. 113
References 121
VIII. The Effect of Rainfall on Sludge Dewatering on Sand Beds. 122
The effect of rainfall on drying 131
References 136
IX. Simulation of Dewatering on Sand Beds 137
Scope of the simulation. 137
Estimation of the simulation sample size 140
Simulation procedure 141
Verification of simulation 142
Output of simulation 143
References 147
X. Performance of Sand Drying Beds 148
An application of statistical decision theory. 148
Performance index. 150
References 151
XI. Economic Analysis for Sludge Dewatering on Sand Beds. 152
Introduction 152
Simulation approach. 152
Marginal analysis approach 158
References 168

Appendix: Experimental Determination of Specific Resistance and Coefficient of Compressibility. 169
Equipment. 169
Laboratory procedures. 172
Data analysis. 174
Calculation of specific resistance 174
Calculation of coefficient of compressibility. 176

FIGURES

Number Page

1 Loading rate of wastewater sludge at various treatment plants in the United States. 10

2 A plot of Haseltine's data of net bed loading versus initial solids content 10

3 A comparison of a typical soil permeameter to Jeffrey's drainometer. 13

4 Jeffrey's drainage data. 14

5 A plot of sludge moisture content $\underline{w}$ versus $(w/100)^3/(1-w/100)$ showing that K/L is not constant with a change in moisture content. 15

6 The Swanwick relationship of bed loading to specific resistance 16

7 A plot of data accumulated by Logsdon and Jeffrey with dewatering time by gravity versus dewatering time using a vacuum 16

8 Illustration of use of a graphical calculator for predicting time required to dewater sludge on sand drying beds. 18

9 Relationship of relative humidity versus moisture content. . . 22

10 Definition sketch for a stratified filter. 25

11 Schematic representation of filtration of a compressible material on a porous medium. 26

12 A typical graph used to determine the specific resistance of a wastewater sludge at three different vacuums 28

13 Schematic representation of the different terms used in derivation of the mathematical model 29

14 Lake evaporation relation. 36

Number Page

15 Mean annual evaporation (inches) from shallow lakes and reservoirs 37

16 Drying rate curves for various substances. 39

17 Sludge drying relationships, various parameters. 41

18 Moisture content versus slab thickness 44

19 Gravity drainage apparatus with piezometer tubes 51

20 Diagram of environmental chamber 52

21 Schematic diagram of gamma-ray attenuation system. 55

22 Diagram of source shielding and collimation. 56

23 Attenuation relations used in moisture profile measurements. . 64

24 Results obtained from specific resistance tests at each of a range of pressures. (Performed with the same sludge sample at constant temperaturee.) 71

25 Effect of conditioner dosage on digested sludge from Amherst . 77

26 Effect of conditioner dosage on digested sludge from Pittsfield 77

27 Experiment IV, triplicate tests with 20 cm of sludge on Franklin sand. 91

28 Experiment IV, triplicate tests with 20 cm of sludge on Ottawa sand. 91

29 Experiment IV, triplicate tests with 20 cm of sludge on Hermitage sand 92

30 Experiment V, 11 cm of sludge applied on three different sands 92

31 Experiment V, 41 cm of sludge applied on three different sands 93

32 Experiment V, 81 cm of sludge applied on three different sands 93

33 Location of containers in evaporation study. 95

34 Sample mass versus time for Billerica sludge drying at 22° C (72° F) and 38% relative humidity. 97

Number Page

35 Drying rate curves for Billerica sludge drying at 22° C (72 F) and 38% relative humidity 98

36 Four types of water treatment sludge at various solids contents 99

37 Sample mass versus time curves for sludges (D-3) drying at 24° C (75° F) and 60% relative humidity 101

38 Sample mass versus time curves for sludges (D-3) drying at 24° C (75° F) and 60% relative humidity 101

39 Drying rate curves for sludges (D-3) drying at 24° C (75° F) and 60% relative humidity 104

40 Drying rate curves for sludges (D-3) drying at 24° C (75° F) and 60% relative humidity 104

41 Sample mass versus time curves for Albany sludge dewatering at 24° C (75° F) and 46% relative humidity 106

42 Change in depth of Albany sludge dewatering at 24° C (75° F) and 46% relative humidity 106

43 Sample mass versus time curves for drying period of dewatering study DW-2 108

44 Cumulative volume of filtrate versus time for Albany sludge dewatering on Ottawa sand (DW-2) 109

45 Drainage curves for 45.7 cm of Albany sludge (DW-2) dewatering on Ottawa sand 111

46 Sample mass versus time curves for sludges (DW-3) dewatering at 24° C (75° F) and 35% relative humidity 111

47 Sample mass versus time for sludges (DW-3) dewatering at 24° C (75° F) and 35% relative humidity 112

48 Drainage curves for 30.8 cm of sludge (DW-3) dewatering on Ottawa sand 113

49 Energy spectrum for 250 millicuries Cs-137 source 116

50 Variation of the ratio N/N_p with thickness of water at 0.661 Mev 116

51 Profile of water content in sand layers (DWO3) after drainage terminated 117

Number		Page
52	Profiles of water content in sand layers for dewatering study DW-3	117
53	Profiles of water content in sand layers (DW-3) after drainage terminated.	118
54	Variation of solids content with depth for Billerica sludge.	119
55	Error analysis	119
56	Variation of solids profiles with time for Albany sludge (DW-3) drying on Ottawa sand	120
57	Variation of solids profile with time for Billerica sludge (DW-3) drying on Ottawa sand	121
58	Definition sketch of mixing drainage	123
59	Definition sketch of ponding drainage.	128
60	Comparison between mixing and ponding models	130
61	Comparison between mixing drainage model and experimental data	131
62	Sample operation of drainage and drying models	142
63	An input/output relation showing the law of diminishing returns.	160
64	Determination of the optimum input and output.	162
65	Iso-quant curve showing five different combinations of A_n and A_r which yield a constant output of 95% performance index.	164
66	Curves of iso-cost lines	165
67	Diagram illustrating procedure for locating the points of optimum proportions.	166
A-1	Vacuum adaptor	169
A-2a	Funnel adaptor	170
A-2b	Adaptor in place on Buchner funnel (with epoxy cement seal).	170
A-3	Vacuum plug (optional)	170

Number Page

A-4 Schematic flow diagram for specific resistance testing . . . 171

A-5 Sample data and data format for specific resistance test . . 173

A-6 Plot of sample specific resistance data. 174

A-7 Graph for calculating coefficient of compressibility 176

TABLES

Number		Page
1	Properties of water treatment and wastewater sludges	74,75
2	Average values for color, pH, and turbidity for the sludge, filtrate, and decant samples	82
3	Average values for solids for the sludge, filtrate and decant samples	82
4	Average values for total acidity and total alkalinity for the sludge, filtrate and decant samples	84
5	Total hardness, calcium, and magnesium for the sludge, filtrate and decant samples	84
6	Average values for manganese and iron for the sludge, filtrate and decant samples	85
7	Average nitrogen values for the sludge, filtrate and decant samples	85
8	Average values of phosphate and sulfate for the sludge, filtrate, and decant samples	87
9	Biochemical oxygen demand and chemical oxygen demand for sludge, filtrate, and decant samples	87
10	Physical characteristics of supporting sand	90
11	Rate of water loss (gm/hr) of de-ionized water at 24°C (75°F) and 47 percent relative humidity	96
12	Analysis of variance for evaporation data	96
13	Results of Billerica sludge, at two different solids contents, dried at 22°C (72°F) and 38 percent relative humidity for 3.0 cm (1.2 in) initial depths	96
14	Experimental arrangement for drying study D-3 conducted at 24°C (75°F) and 60 percent relative humidity	100

Number Page

15 Summary of results for drying study D-3 conducted at 24^oC (75^oF) and 60% relative humidity. 102

16 Results of Albany sludge, DW-1, dewatering at 24^oC (75^oF) and 46 percent relative humidity. 107

17 Dewatering study DW-3, results for four sludges dewatering at 24^oC (75^oF) and 35% relative humidity. 110

18 Attenuation coefficients at 0.661 Mev for the various materials. 114

19 Particle density values, g/cm^3, for water treatment sludge solids and Ottawa sand.. 114

20 Summary of water content measurements for Ottawa sand by the attenuation method. 115

21 The effect of rainfall on wastewater sludge drying during the falling rate period. 134

22 The effect of rainfall on water treatment sludge drying during the falling rate period 135

23 Characteristics of sludges 138

24 Normal monthly weather data -- selected cities 139

25 Occurrence of freezing at selected cities 140

26 Comparison between computer simulation and field observations for covered beds at various locations.. 144

27 Comparison between 20-year computer simulation results and Haseltine's field observation for open sand beds at Grove City, PA 145

28 Comparison between 20-year computer simulation results and Haseltine's field observation for covered sand beds at Grove City, PA. 145

29 The output of simulation of mixed digested primary and activated sludge dewatering on sand beds at Boise, Idaho with 20 cm application 146

30 Annual cost of sludge dried in Boise, Idaho, at different application depths (sludge removed by hand). 156

31 Annual cost of sludge dried in Boise, Idaho, for different application depths (sludge removed by machine). 157

Number	Page
32 An input/output relation showing the law of diminishing returns.	161
33 The results of optimum sand bed dewatering in Boston with a fixed bed area per capita.	163
34 The cost of sludge dewatering.	167

ACKNOWLEDGEMENTS

The author is indebted to a number of persons for their assistance in this research project. Dr. John H. Nebiker introduced him to research on sludge dewatering, served as co-principal investigator from 1967-1969, and served as a sounding board for various research ideas until distance made this impractical. His imprint on the research remained long after he was no longer an active participant. Philip A. Lutin served enterprisingly as a full time research associate during initiation of the project and established many of the early laboratory practices. He was followed by John F. Ramsay who later changed roles from full time research associate to that of graduate student and research assistant.

The dedicated participation of several graduate students is acknowledged with thanks. PhD candidates Edward E. Clark and Kuang-mei (Bob) Lo made major contributions to the research through their dissertation work. Other PhD candidates Thomas G. Sanders, Donald L. Ray, Peter Meier and Peter Kos contributed to the research in their MS and PhD studies. MS candidates who worked on various aspects of the research were Paul Cummings and George Wan. Undergraduates Thomas Belevieu and Thomas Roule assisted in some of the dewatering studies. Christopher C. Clarkson provided valuable assistance in preparing and editing the final report.

Faculty associates who assisted in development of the project include Dr. Tsuan Hua Feng, Professor of Civil Engineering, Dr. Chin Shu Chen, former Assistant Professor of Agricultural Engineering and Bernard B. Berger, Director of the Water Resources Research Center.

Valuable counsel and advice has been provided by EPA Project Officers: Dr. Robert B. Dean who enlarged the author's knowledge of sludge and its properties; Dr. James E. Smith, Jr. who quietly and sympathetically offered his insights on research programs; and Roland V. Villiers who saw the final report to completion.

Personnel at water treatment plants in Billerica, Lowell, Lawrence, and Amesbury, Massachusetts; Albany, New York; Lebanon and Nashville, Tennessee; and Kankakee, Illinois, were most helpful in providing sludge samples for analysis. Sewage sludge was obtained from Amherst and Pittsfield, Massachusetts.

The persons acknowledged above undoubtedly can see their contributions reflected in portions of this report. Needless to say the author bears responsibility for errors which may appear.

SECTION I

INTRODUCTION

Water for domestic and other general municipal use has traditionally been obtained from the best available supplies consistent with economy. With the advent of physical and chemical water treatment late in the nineteenth century, raw water supplies of lower quality could be upgraded to acceptable levels. The chemical dosage was roughly inversely proportional to the raw water quality while the amount of sludge produced varied with the amount of chemical required.

The central concern of the water utility was the production of ample supplies of potable treated water under the constraint that this production be achieved at a minimum cost. Scant attention was paid to treatment by-products such as filter wash water and sludge from the sedimentation basin. A convenient and low cost disposal site for filter wash water was often the supplying stream. Sludge from the sedimentation basin may also have been discharged to the stream, or, if the stream capacity was low, discharged to a lagoon.

The occasional usage of a sludge lagoon, rather than direct discharge of the sludge to the stream, attested to some concern over degradation of the receiving water quality. However, this mode of operation was subject to the whim of the utility. Moreover, the stream was always available as a disposal site should the lagoon capacity become exhausted. In fact, a report by Louis R. Howson in 1966 indicated that over 90 percent of all water treatment wastes were being returned to the raw water source(1). Gradually, water treatment sludge discharged to a stream has come to be recognized as a pollutant. The concern over water pollution necessitates a re-examination of water treatment sludge handling and disposal methodologies. Lagoon disposal may be a satisfactory solution provided additional lagoon sites are available to replace those which are filled, or provided that the compacted solids can be removed and the lagoon reused. Recent studies point out, however, that lagoons are not well suited to the processing of water treatment clarifier sludges due to the high water content of compacted solids which renders them difficult to handle (2).

In many cases the sludge may be discharged directly to a sanitary sewer where it becomes the concern of the wastewater treatment plant. Unfortunately, lime sludge becomes less acceptable to the wastewater treatment plant as the level of treatment increases. While lime sludge is acceptable to a primary treatment plant, it may be unacceptable to a secondary treatment plant (3), unless incorporated into a phosphate removal process (4).

The relative merits of the choice between augmenting treated supplies by drawing upon waters of lower quality, or conserving existing supplies by concentrating on reduction of water usage have recently become more clearly delineated (5). In many instances an immediate but temporary solution to an insufficiently treated water supply is attained by marked reduction in consumption achieved by eliminating waste or by altering industrial processes. However, long range demand trends have focused increased attention on water renovation, with some processes envisioned as forming a closed system such that complete reuse will be achieved. Complete renovation of a municipal wastewater is beyond the capability of secondary treatment. High quality product water is obtained at the expense of the production of voluminous amounts of dilute sludge or brine, the disposal of which vastly increases the now formidable solids handling problem. Today, water renovation in the sense of complete recycling of wastewater through successive treatment steps until it can be returned to the domestic water supply is accomplished in laboratory and pilot systems. Technological advances suggest that wastewater renovation may be practicable on a large scale in water deficient areas. As treatment methods evolve and are put into practice, the alternatives between development of lower quality new raw water sources or renovation of wastewater for reuse will become more clearly defined, enabling a more informed economic choice.

Wastewater renovation and utilization of lower quality raw waters will become more commonplace in the future. Either choice will increase sludge handling problems. Based on the present day production figures of 6.8 kg (15 lb)/capita/year of dry solids from water treatment plants and 59 kg (130 lb)/capita/year of dry solids from wastewater treatment plants, the per capita quantity of sludge requiring handling will be greater with water renovation than with conventional water treatment (3). The solids from either process will be accompanied by vast quantities of water so that on a wet basis, assuming sludges of 3 percent solids content, a water treatment plant would produce nearly 227 kg (500 lb) of sludge per capita per year while a wastewater treatment plant would produce 1900 kg (4,200 lb) of sludge per capita per year.

Ultimate disposal of the sludge solids requires their discharge to the atmosphere, to the ocean, or to the land. Organic compounds which are oxidizable to carbon dioxide and water vapor are most amenable to atmospheric disposal. Water treatment sludges are low in organic content so that incineration will leave a substantial fraction of ash. Soluble compounds may be carried by streamflow to the ocean. For communities near the shore, direct discharge of sludge into the ocean may be practiced. For the overwhelming majority of communities in the United States, water treatment sludge solids are disposed of on land. Prior to their disposal, volume and weight reduction are necessary to reduce the weight from some 227 kg (500 lb)/capita/year on a wet basis to approximately 6.8 kg (15 lb)/capita/year on a dry basis. This can be achieved by removing water from the sludge.

Reduction of the water content of sludge may be carried out by a variety of mechanical or non-mechanical methods such as compaction and decantation in lagoons, or gravity drainage and evaporation on drying beds. Selection among these alternatives is based on economics. Exhaustive studies by the city of Chicago on wastewater sludge shows the cost of various combinations of dewatering, drying, and disposal methods varies from approximately \$12/ton (900 kg) to \$80/ton on a dry solids basis (6). The most economic method was dewatering, drying, and disposing of the solids on land.

Although land disposal is widely utilized at small treatment plants, there is a paucity of reliable design data available with which to design a sand dewatering and drying bed for sludge. Mechanical dewatering methods, although less economic than sand beds, have become increasingly popular with design engineers because of the ready availability of design data. A typical example is the vacuum filter for sludge dewatering. Sludge solids content, specific resistance of the sludge cake, and its coefficient of compressibility are related to the desired dewatered sludge cake characteristics through the machine operating variables. Variation of the machine operating parameters permits selection of the optimum vacuum filter. No such procedure is available to the engineer faced with designing a sand dewatering bed. While he can resort to some empirical rules-of-thumb or practice at operating installations or intuition, none of these are as satisfactory as a functioning mathematical model, verified adequately for reliability, which clearly delineates the role of each parameter. There is a great need for such a mathematical model describing the operation of a sludge dewatering and drying bed. Additionally, rigorous economic analysis is not feasible without a satisfactory model.

The purpose of the study herein reported was to develop methods of approach applicable to the previously cited problems of land disposal of water treatment sludges. The general objective was to develop rational design formulations which would enable an engineer to design dewatering and drying beds for water treatment sludges.

To this end, liaison was established with several water treatment plants treating raw water from several sources by a variety of treatment methods. Sludge samples were characterized by such classification tests as specific resistance, coefficient of compressibility, and solids content. The problem of sludge dewatering and drying was analyzed under a variety of meteorological conditions in order to postulate hypotheses which would permit formulation of mathematical models describing these processes.

Formulation of the relation between loading rates of water treatment sludge applied to filter beds and to subsequent drainage and drying of the sludge forms the core of the engineering analysis reported in this study. The sections which follow present the essential aspects of filtration theory of a compressible material, drainage theory, evaporation and drying theory, dewatering practice, current design practice, effect of rainfall on sludge dewatering, and simulation of dewatering on sand beds.

REFERENCES

1. Howson, L. R. Problems of Pollution. In: Waste Disposal-Water Treatment Plants, Joint Discussion. Journal American Water Works Association, September, 1966.

2. McWain, J. D. Dewatering by Lagoons and Drying Beds. In: Proceedings of the Tenth Sanitary Engineering Conference. University of Illinois, Urbana, Illinois, February, 1968.

3. Hudson, H. E., Jr. How Serious is the Problem? In: Proceedings of the Tenth Sanitary Engineering Conference. University of Illinois, Urbana, Illinois, February, 1968.

4. Dean, R. B. Disposal to the Environment. In: Proceedings of the Tenth Sanitary Engineering Conference. University of Illinois, Urbana, Illinois, February, 1968.

5. Stephan, D. G. and Weinberger, L. W. Wastewater Reuse--Has It Arrived? Paper presented at the 40th Annual Conference of the Water Pollution Control Federation, New York, New York, October, 1967.

6. Dalton, F. E., et al. Land Reclamation--Possibly the Complete Solution of the Sludge and Solids Disposal Problem. Paper presented at the 40th Annual Conference of the Water Pollution Control Federation, New York, New York, October, 1967.

SECTION II

CONCLUSIONS AND RECOMMENDATIONS

CONCLUSIONS

A theoretical model (Equation 47) developed in this research and verified experimentally describes gravity dewatering of wastewater sludge. Experiments also suggest the existence of a dimensionless media factor which relates sludge dewaterability on sand and other filter media, to dewaterability in the Buchner funnel. It is not clear whether the media factor is a multiplier, as used in this research, or if it applies better in the model as an additive factor. The model can be used to calculate bed loadings, and to determine the area needed to dewater a given amount of sludge by gravity drainage alone. Used in conjunction with models describing evaporation and drying, the environmental engineer is provided with a rational means by which to determine sand bed areas. Additionally, it provides a basis upon which to compare drying bed performance with other means of dewatering, and a means by which to measure the effectiveness of the many chemical coagulants.

Drainage times of water treatment sludges may also be predicted which provide a good estimate for design purposes. Drying durations can be calculated from the drying equations examined (Eq. 134). Evaporation ratios for each particular type of sludge and average local weather conditions provide drying rates for any locality or climate. The moisture gradient in water treatment sludge is constant during most of the drying period, indicating that evaporation from the surface--not internal diffusion--presents the major resistance to drying. Under normal conditions, water treatment sludges can be removed from drying beds while in the constant rate drying period.

The gamma-ray attenuation method is applicable to sludge drying studies but needs some refinement to cover the dewatering period after lateral shrinkage of the sludge cake becomes pronounced. After the critical moisture content is reached the moisture profile provides information on the moisture content and the moisture transport mechanisms during the falling-rate period.

Although the water treatment sludges tested resulted in a wide range of values for specific resistance, they were all within one order of magnitude. The water treatment sludges tested were homogeneous, inorganic, and void of filamentous binders, thus it is not unreasonable to expect that water treatment sludges will lend themselves to a variety of dewatering techniques. Somewhat higher coefficients of compressibility were obtained for the water treatment sludges than are cited in the literature for wastewater sludges. This indicates that water treatment sludges produce a more compressible cake than wastewater sludges.

Computer simulation techniques were utilized to develop design criteria with which an engineer can design dewatering beds based upon climatic conditions and the nature of sludge to be dewatered. Economic analyses are applied to the outputs of simulation in developing an optimum system design: the first explores the optimum system design which fulfills projected output at minimum cost among known alternatives; the second utilizes marginal analysis to assign a cash value to the end product (dry solids) of the dewatering process to determine the point at which cost of inputs equals the marginal value of output.

Further work in this area would be enhanced by more rigorous scientific evaluation of the quality of water drainable from different sludges, and by a greater availability of sand dewatering bed construction cost and operating cost data which would enable more accurate evaluation of the costs of sand bed dewatering.

RECOMMENDATIONS

To obtain improved sand bed system design, it is recommended that:

1. the results of the computer simulation be incorporated into standards for dewatering bed design,
2. the simulation model (or computer program) be included as an alternative to other methods of sludge dewatering determination in any systems analysis approach for water and wastewater treatment plant design,
3. a performance index of 95 percent be adopted as a design criterion for sludge dewatering beds, and,
4. the environmental engineering profession re-evaluate its traditional design approach so as to foster an effective union of engineering and economic analysis.

In addition, this investigation points out areas in which further research is required. Future studies should concentrate on the quantities of sludge produced by waters of various qualities being treated in different ways, and the method of removal of sludge from sedimentation basins. Thickening of certain types of sludge--such as softening sludge--by sedimentation and decantation could remove large amounts of relatively clear water. A study of sludge particle size would lead to development of relationships suitable for determining media factors for the drainage model.

There are not now many wastewater treatment plants able to afford the time or expense required to measure the most effective coagulant dose for sludges to be applied to sand drainage beds. However, with future expansion and centralization of wastewater treatment plants, economies to scale will be enjoyed which will be made possible through more sophisticated plant operation. The mathematical model developed in this research could conceivably be used to determine optimum coagulant dosage at a cost far less than the savings to be realized. Availability of a nomograph (whose development is based on the mathematical model presented) would enable treatment plant operators to make more effective use of available sand beds, with only a modicum of experimental work.

SECTION III

REVIEW OF THE LITERATURE

In 1907, Spillner, one of the early researchers on drying beds (1), discovered that digested sludge from an Imhoff tank dewatered more rapidly than raw sludge. He found that 80.9 percent of the moisture reduction in digested sludge was due to drainage as compared with only 44.4 percent for fresh sludge and concluded that the better drainage of the decomposed sludge was due to a decrease in viscosity, destruction of hydrophilic colloids and organic matter, and the formation of gas bubbles. The effect of gas bubbles lifting the sludge to promote formation of a subnatant was probably the singlemost important factor in improving the drainage rate of digested sludge. The gases allowed the rapid release of filtrate by unclogging pores at the sand surface which would otherwise remain blocked by the sludge floc.

During the 1920's, covering drying beds with greenhouse structures became popular. This increased the rate of drying of the sludge by preventing problems with precipitation and by maintaining higher temperatures. However, enclosure prevented the flow of air which could remove water vapor directly above the sludge. In 1931 Skinner (2) published a paper which questioned the economic feasibility of covered sand beds. He stated that open beds had less construction cost per unit area, and entailed no costs for heat, insurance for glass breakage and maintenance of a fragile superstructure. On the other hand, covered beds needed up to 50 percent less area per capita, reduced the odor nuisance, and had a better appearance.

Skinner developed one of the first empirical equations for the computation of drying bed requirements, covered or uncovered, i.e.,

$$\begin{array}{l}\text{Area of Sand Bed}\\ \text{per capita}\end{array} = (\text{Constant})\ \frac{\begin{bmatrix}\text{Average Annual}\\ \text{Precipitation: in.}\end{bmatrix}\begin{bmatrix}\text{Suspended Sewage}\\ \text{Solids: ppm}\end{bmatrix}}{\begin{bmatrix}\text{Number of Months}\\ \text{in Drying Season}\end{bmatrix}\begin{bmatrix}\text{Mean Annual}\\ \text{Temp.: }^{\circ}\text{F}\end{bmatrix}\begin{array}{c}\text{Mean Wind}\\ [\text{Velocity:}]\\ \text{mph}\end{array}}$$

where the constant depends on the sewage treatment process. For covered beds, the area calculated above is divided by 2. The formula points out the different factors that affect sludge drying.

In 1934, Jones (3) made a survey of existing treatment plants to see how effective the sand beds were for the dewatering and drying of sludge. He found that plant records were reliable and concise for every phase of treatment plant operation except sludge dewatering and disposal. As an example:

> "A total of 44 beds of sludge were drawn off from the tanks during this year and a total of 75 beds of scum. All sludge drawn off was well digested, dried out quickly and had no prominent odor."

There was no mention of depth of application, solids content of sludge from digestor, or solids content of sludge when removed from the beds. Jones indicated that economic advantages could not be characterized and cost per unit area estimates for sand beds could not be made until more complete records were kept at the treatment plants. Based upon the data available to him, Jones concluded that the degree of treatment, type of process, and character of sludge not only affected the volume of sludge produced, but also the rate of dewatering.

During the same years that Jones was doing research on sand beds, Rudolfs and Heukelekian (4) were studying the drainability of sludge versus the degree of digestion. It was found that well digested sludge dewatered faster than a poorly digested sludge, or a well digested sludge which had been stored before being placed on the sand beds. The resulting conclusion, substantiating the work of Spillner, was that the well digested sludge had a large amount of gas which "buoyed" the sludge solids, allowing the subnatant water to drain more rapidly.

For so-called dead sludges (a sludge without entrained or dissolved gases), alum could be added to increase the drainability of the sludge. The alum would react with the carbonates in the sludge forming CO_2 gas which would buoy the sludge solids and increase drainability. Copper sulfate and even dilute sulfuric acid would have the same effect on the sludge. However, addition of alum or any other chemical to a freely gaseous sludge would have no effect on drainability (5). Ferric chloride was tested as a sludge conditioner because of its minimal cost (6), however, the ferric salts were oxidized, clogging the sand pores and allowing less drainage.

It was found in Aurora, Illinois in 1939 (6) that differences in drainage characteristics for the same sludge with the same amount of alum were attributable to the method of adding alum to the sludge. If the alum were completely mixed with prolonged stirring, the sludge would not drain as well as the sludge subjected to a minimum of stirring. This problem was due to a build-up of fines from shearing of the floccules (the same occurs with prolonged pumping). Therefore, in order to minimize stirring but obtain complete mixing, alum was first dissolved in water and then added to the sludge a few feet from the sand bed outlet. Because of turbulence in the pipe, adequate mixing was assured.

The major disadvantage to the use of sand beds as a means of sludge dewatering is the cost of removing dried sludge from the beds. In small sewage treatment plants the removal costs may be inconsequential, being merely an occasional task. However, in a larger plant which may treat 1500-2300 cubic meters (2000-3000 cubic yards) of sludge every day, the cost of sludge removal becomes considerable. As early as 1931, the Sanitation District of Chicago, concerned at the cost of manually removing sludge from drainage beds constructed a self-propelled sludge removing machine (7). The device was capable of removing 3.8 cubic meters (5 cubic yards) of

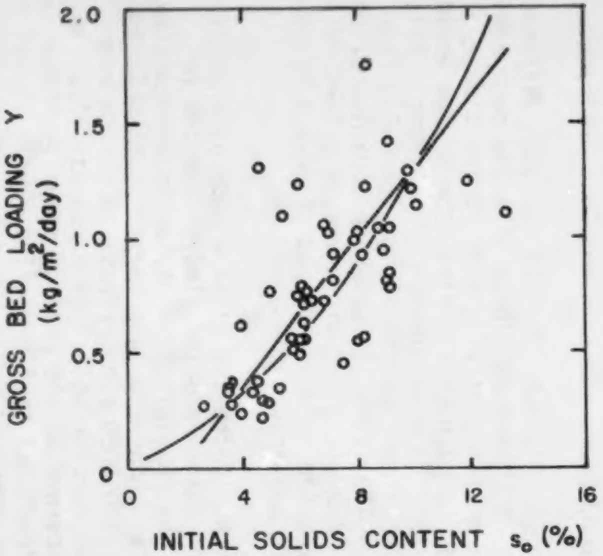

Figure 1: Loading rate of wastewater sludge at various treatment plants in the United States. Shown as a function of the initial solids content , the points and straight line represent the results of Haseltine. The curve is from Vater (10).

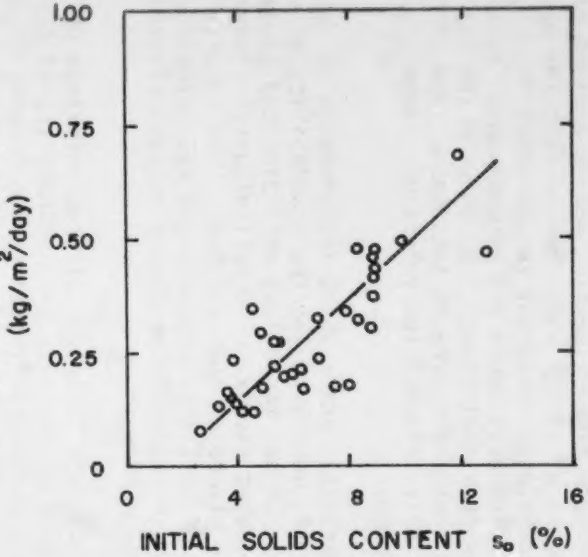

Figure 2: A plot of Haseltine's data of net bed loading versus initial solids content. Data is from American plants. Net bed loading is defined as gross bed loading multiplied by the water content of the sludge removed (9, 10).

sludge per minute and thus could replace the 350-400 men who would have been needed to remove equal amounts of sludge. More recently, a mechanical sludge removing process was installed in 1961 at London's Maple Lodge Works, resulting in a substantial decrease in labor costs (8).

One of the first empirical relationships describing the time required for sludge to dewater on sand drainage beds was developed by Haseltine (9). From field data collected at different treatment plants, he plotted the gross bed loading (kg/m^2/day) versus solids content of the sludge. The resulting equation was determined to be:

$$Y = 0.157\ S_o - 0.286 \qquad (1)$$

where Y = gross bed loading of solids (kg/m^2/day)

S_o = solids content (%)

Vater (10) analyzed the same data used by Haseltine and found that a curve may be fitted using a regression analysis (Figure 1). The relationship thus became exponential and defined by the empirical equation:

$$Y = 0.033\ S_o^{1.6} \qquad (2)$$

where Y = gross bed loading of solids

S_o = solids content (wt %) of sludge charged to the bed

Although both Haseltine's and Vater's relationships appear to fit the data, the curve drawn by Vater seems more realistic since it goes through the origin whereas Haseltine's straight line does not. Clearly, a sludge of zero solids content will yield zero bed loading.

Since final moisture content of the sludge was also to be a determining factor of the sludge drainage and drying capacity of a sand bed, Haseltine defined the term "net bed loading" as the gross bed loading multiplied by the final water content of the dried sludge. The relationship between net bed loading and solids content was found to be (Figure 2):

$$Z = 0.057\ S_o - 0.082 \qquad (3)$$

where Z = net bed loading of solids (kg/m^2/day)

S_o = solids content (%) of sludge charged to the bed

Although Haseltine's equations are strictly empirical, they have been used for the dimensioning of sludge drying beds. Note that the water content is defined as (100 - solids content)/100.

During the first half of the twentieth century there was little progress in formulating drainage and drying relationships which took into account the parameters of sludge characteristics and quantity, and external factors such as the evaporation potential of the air.

Just as there are a number of dewatering methods, there are also a number of types of sludge. However, the differences are usually related to the treatment process without any other classification than solids content. Since primary and secondary sludges with the same solids content but from different treatment plants will not dewater at the same rate, other drainage characteristics intrinsic to each sludge must be present.

Jeffrey (11) studied the relationship between permeability of the sludge, initial head, and time. For his experiment he designed a drainometer (Figure 3) which consisted of a lucite tube 45.7 cm (18 inches) in length covered with a polyethylene film to prevent evaporation. A layer of gravel followed by a 2.2 cm (7/8 inch) layer of sand was placed in the bottom of the lucite tube to simulate a sand drainage bed. An inverted "U" tube drain with a siphon breaker was inserted between the sand and gravel to maintain a water table. Sludge was poured into the column, after which the volume of subnatant collected and the time were noted. Jeffrey observed the relationship for flow through a soil permeameter (see Fig. 3):

$$\ln H/H_o = -kt/L \tag{4}$$

where H_o = initial head at $t = 0$

H = head at any time t

K = permeability coefficient of soil sample

L = length of soil sample

t = time

He then determined from his experiments that the following equation was valid for sludge drainage:

$$\ln W_1/W_o = -Kt/L \tag{5}$$

where W_1 = quantity of filtrate = $V_o - V$ (see Figure 3)

W_o = total quantity of liquor discharged from a drainometer at the time the quantity of discharge over a 24 hour period falls to 1 percent of the total discharge.

K = permeability coefficient of the sludge

L = depth of sludge

t = time

Jeffrey stated that "...the coefficient of permeability, K, is not fixed. Both K and L change with time and apparently at such a rate that the ratio K/L is constant."

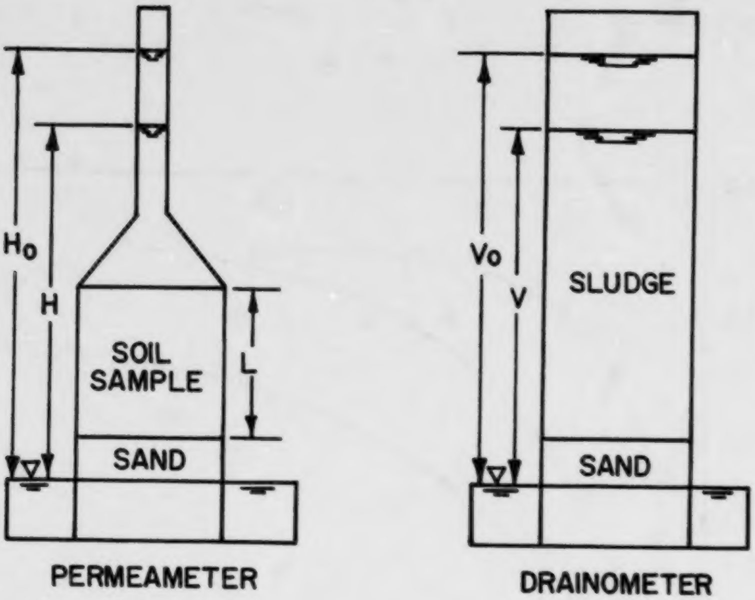

Figure 3. A comparison of a typical soil permeameter to Jeffrey's drainometer (11).

In Figure 4 it is readily apparent that Jeffrey's theoretical curves coincide closely to the actual drainage curves for all three different solids contents. However, it should be noted that the theoretical curve could not be drawn until the actual drainage experiments were near completion since the value of W_0 could not be found until the 24 hour drainage in the column was less than one percent of the total filtrate volume.

Jeffrey based his conclusion, that the ratio K/L was a constant, on his experimental data. The plot of log W_1/W_0 was constant. However, Sanders (12) has shown that K/L is not constant but instead is proportional to the water content of the sludge, such that

$$K/L = B\, w^3/(1-w) \qquad (6)$$

where B = constant

w = moisture content (%)

A plot of w versus $w^3/(1-w)$ produced the curve shown in Figure 5. A small change in w produces a large change in $w^3/(1-w)$ and, by Equation 6, in K/L. Thus, the ratio K/L does not remain constant but instead is a function of water content. Therefore, even though one of Jeffrey's conclusions appears theoretically unjustifiable, he was the first to develop a relationship between head and time.

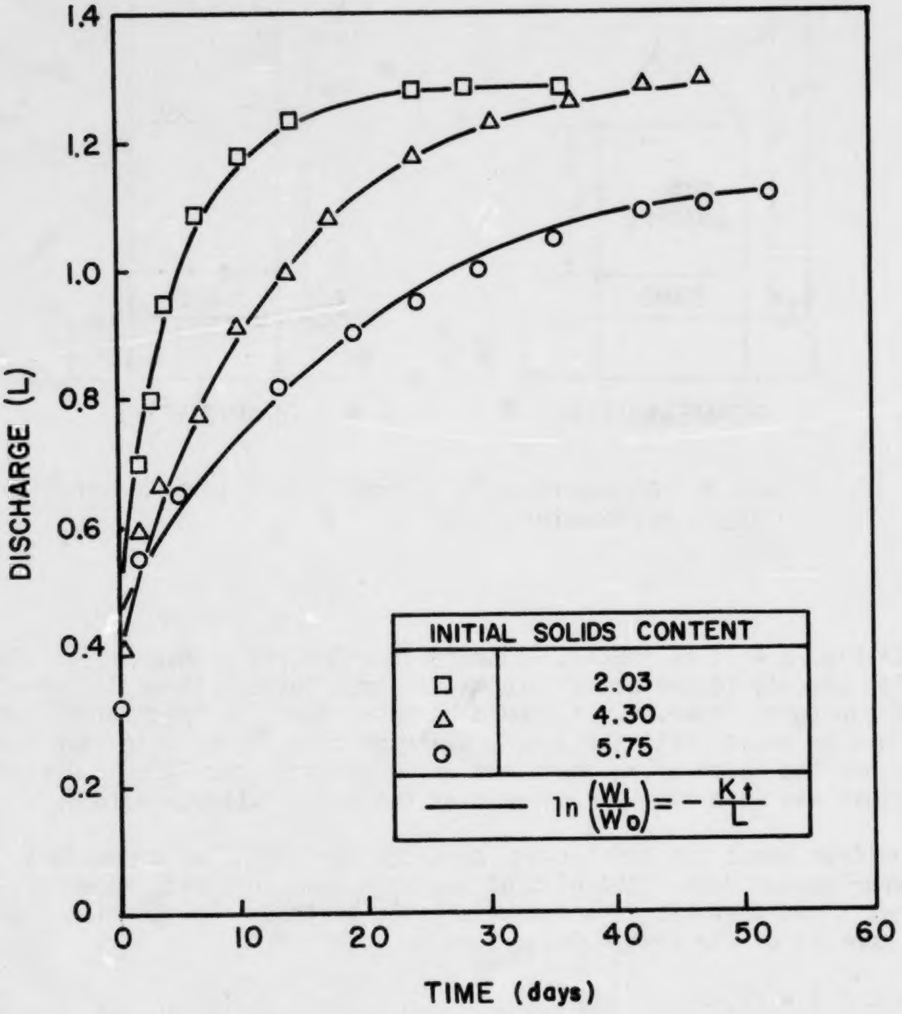

Figure 4: Jeffrey's drainage data. The curves represent Jeffrey's empirically derived equation (11).

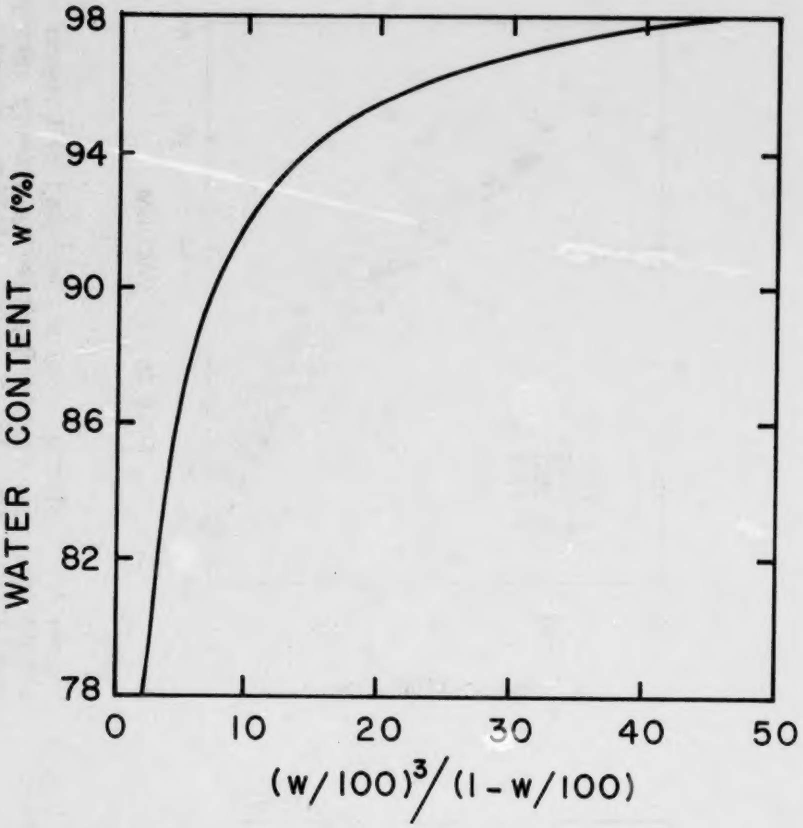

Figure 5: A plot of sludge moisture content W versus (W/100)^3/(1-W/100) showing that K/L is not constant with a change in moisture content.

Pilot plant studies in England on sludge dewatering yielded the conclusion that specific resistance (an intrinsic characteristic of sludge which will be discussed in greater detail later) is related to bed loading (kg/m^2/year). Specific resistance has long been recognized as a functional parameter for use in describing the dewatering rates of sludge submitted to vacuum filtration, but this was the first time that specific resistance was tested as a functional parameter to describe gravity drainage. This is not unreasonable since the processes of vacuum dewatering and gravity drainage differ only in type of pressure exerted on the sludge. In vacuum filtration, the vacuum is constant; and in gravity drainage, the pressure (a function of head) is continually decreasing. A plot of Swanwick's data results in the curve of Figure 6 which is described by the equation (10,13)

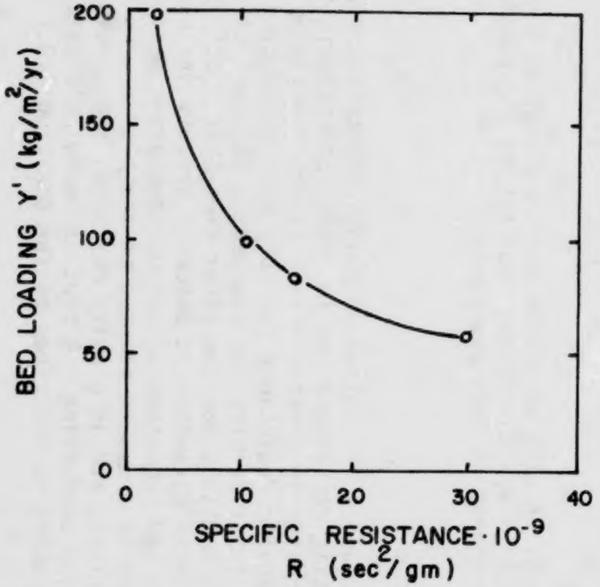

Figure 6: The Swanwick relationship of bed loading to specific resistance. Each point represents the mean of a group of loading values (10, 13).

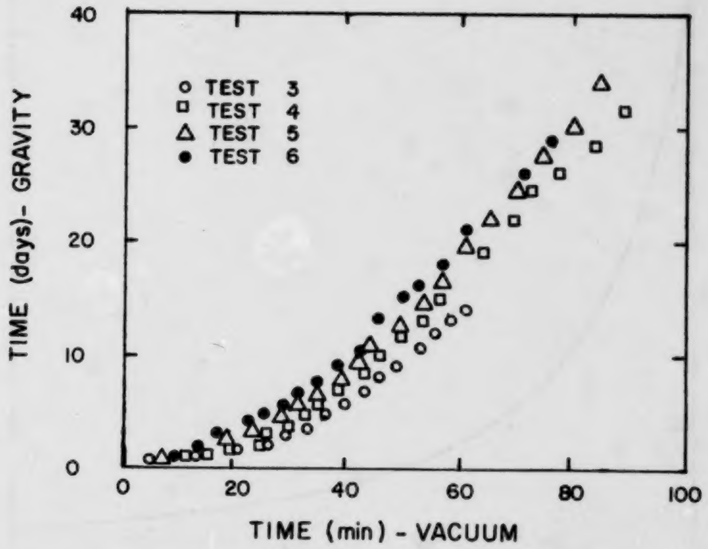

Figure 7: A plot of data accumulated by Losgdon and Jeffrey with dewatering time by gravity versus dewatering time using a vacuum. Solids content of sludge ranges from 2.08% in Test 6 to 3.13% in Test 3 (14).

$$Y' = 10^7/R^{1/2} \quad (7)$$

where Y' = bed loading (kg dry solids/m^2/year)

R = specific resistance at 36.9 cm of mercury (sec^2/gm)

Although it is quite possible that a relationship exists between bed loading and specific resistance, it is highly improbable that this relationship is precisely described by Swanwick's formulation. Other factors which are related to bed loading and unrelated to specific resistance, such as evaporation and freezing temperatures, most certainly play a considerable role in the dewatering of the sludge. Each value plotted in Figure 6 was an average of three tests run in the course of one year, thus establishing some uncertainty as to the reliability of the relationship.

Specific resistance does not take into account moisture removing mechanisms other than drainage. Therefore, evaporation and freezing temperatures must be eliminated from scientific studies for proper correlation of specific resistance with bed loading or other drainage rate parameters.

Logsdon and Jeffrey (14) conducted research to study the relationship between the dewatering time of a sludge on sand, and the vacuum dewatering time (a function of specific resistance) of the same sludge using the Buchner funnel test. Sludges with four different solids contents ranging from 2.08 percent to 3.13 percent total solids were investigated. The times required to remove equal amounts of water by gravity drainage and by filtration were plotted yielding the curves in Figure 7. Even though the vacuum applied to the four sludges varied from 30.5-61.0 cm of mercury, Jeffrey concluded that the vacuums in this range dewatered the sludge at equal rates; therefore, Test 3 through Test 6 could be compared. Since these points on the graph appear to approach a straight line asymptotically, Logsdon and Jeffrey concluded that the dewatering relationship was a straight line with the general equation:

$$d = km + i \quad (8)$$

where: d = number of days the drainometer operates

m = number of minutes the vacuum operates

k = constant = slope of line

i = intercept of abscissa

Weeks are needed to determine the appropriate constants and unfortunately, each sludge must be re-evaluated by these methods to determine the effect of sludge conditioning.

In a 1965 British Water Pollution Research Report (15), the dewatering time for 12 inches (30 cm) of digested sludge was reported as ranging from 12 days to 111 days due to the effects of rainfall on the performance of the drying bed. In order to take this weather effect into account, the Report suggested a graphical method to determine the required bed area. This method depended on estimating the portion of the rainfall drained through the sludge and the portion evaporated. For example, the reported mean values of 15 separate observations suggested that 43 percent of the rainfall drained through the sludge and 57 percent evaporated. In order to predict the drying time, a plot was made of 0.57 x cumulative rainfall against time; the resulting curve then represented the amount of rainfall which would be evaporated from the sludge. Another plot was made on the same (monthly) time scale of 0.75 X cumulative evaporation from a free water surface; this curve represented the evaporation from sludge where the pan evaporation factor was 0.75. From the two plots a graphical calculator was made by cutting away the portion of the evaporation graph below the curve and placing the remaining portion on the rainfall graph. The time scales of both curves are kept coincident and the upper curve is moved in a direction parallel to the rainfall (or evaporation) axis until the two curves cross on the date on which sludge was applied to the bed. The drying time would be found by observing the subsequent date when the two were separated by a distance representing the amount of water to be evaporated from the sludge. The use of this method is illustrated in Figure 8.

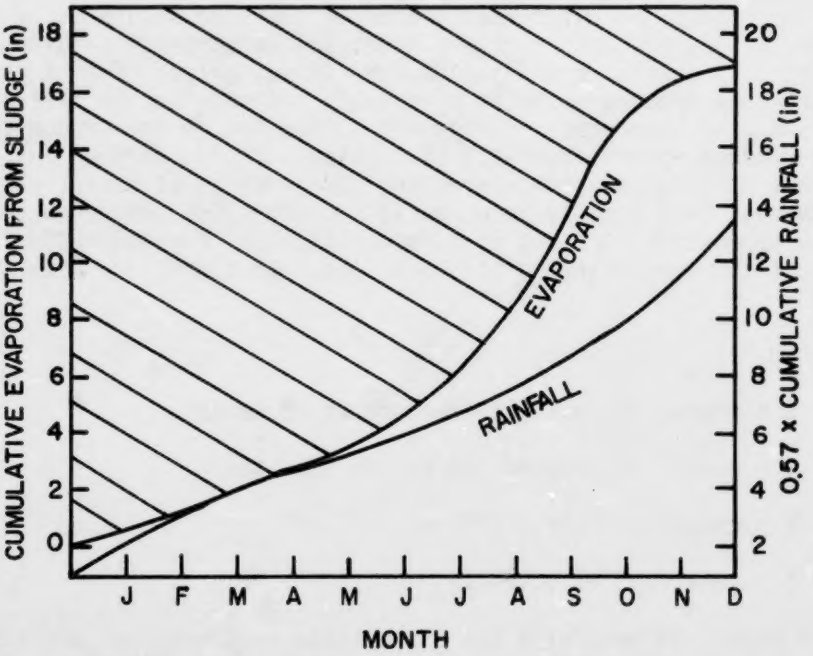

Figure 8: Illustration of use of a graphical calculator for predicting time required to dewater sludge on sand drying beds.

REFERENCES

1. Spillner, F. The Drying of Sludge. Sewage Sludge, London, 1912.

2. Skinner, J. F. Sludge Drying Beds. Sewage Works Journal, 3, No. 3, July, 1931.

3. Jones, F. W. Sludge Dewatering--Sand Filters and Vacuum Filters, Sewage Works Journal, No. 6, November 1934.

4. Rudolfs, W. and Heukelekian, H. Relation Between Drainability of Sludge and Degree of Digestion. Sewage Works Journal, No. 6, November, 1934.

5. Quon, J. E. and Tamblyn, T. A. Intensity of Radiation and Rate of Sludge Drying. Journal of the Sanitary Engineering Division, ASCE, 91, No. SA2, April, 1965.

6. Sperry, W. A. Alum Treatment of Digested Sludge to Hasten Dewatering. Sewage Works Journal, 13, No. 5, September, 1941.

7. Kane, L. P. and Pearse, L. Cleaning Machines for Large Air Drying Sewage Beds. Engineering News Record, January, 1932.

8. Kershaw, M. A. and Wood, R. Sludge Treatment and Disposal at Maple Lodge. J. Proc. Inst. Sew. Purif., 1966.

9. Haseltine, T. R. Measurement of Sludge Drying Bed Performance. Sewage Works Journal, 23, No. 9, September, 1951.

10. Vater, W. Die Entwässerung, Trocknung und Beseitigung von Städischen Klärschlamm. Doctoral dissertation, Hannover Institute of Technology, Hannover, Germany, 1956.

11. Jeffrey, E. A. Laboratory Study of the Dewatering Rates for Digested Sludge in Lagoons. Industrial Waste Conference, Purdue University, May, 1959.

12. Sanders, T. G. Dewatering of Sewage Sludge on Granular Materials. M.S. Thesis in Civil Engineering, University of Massachusetts, Amherst, 1968.

13. Report of the Director, Water Pollution Research, 1962. London, 1962.

14. Logsdon, G. A. and Jeffrey, E. A. Estimating the Gravity Dewatering Rates of Sludge by Vacuum Filtration. Journal WPCF, 38(2), February, 1966.

15. Ministry of Technology. Dewatering of Sludge. Water Pollution Research Report. Ministry of Technology, United Kingdom, 1965.

SECTION IV

THEORETICAL CONSIDERATIONS

Dewatering of water treatment sludge involves several basic operations, not all of which are fully understood. The dewatering process consists of gravity drainage and drying over a wide range of moisture and solids concentration. Sludge initially at 0.5 percent solids (99.5 percent water) undergoing drying and drainage simultaneously may behave as a dilute suspension. The water loss rate by evaporation will approximate that of a free water surface, especially if some sedimentation has occurred exposing clear supernatant to the drying atmosphere. Drainage alone may concentrate the sludge to a gelatin-like mass of 5 to 15 percent solids content in a relatively short time. Drying will further concentrate the sludge causing it to behave like a solid. This stage is accompanied by compression and shrinkage with cracks appearing throughout the sludge cake. Continued drying to equilibrium produces a hard, dry solid having characteristics ranging from those of a dry sand bed to a ceramic. The transition between the various stages is not pronounced and more than one basic mechanism may be present at any one time.

MOISTURE

Different classifications of moisture and water content are used by different disciplines. In environmental engineering the term water content is usually associated with large amounts of water and is defined as the mass of water divided by the total mass (solids plus liquid). Moisture content refers to much smaller amounts of water and is defined as the mass of water per mass of dry solids. The term water content is convenient during the drainage and early stages of water treatment sludge drying, whereas the term moisture content is more convenient during the later stages of drying. The term solids content is also frequently used in sludge dewatering studies. Solids content is defined as the mass of solids divided by the total mass. Thus solids content plus water content is unity.

There is no agreement on the nomenclature of the various kinds of water involved in the various disciplines. According to Spangler (1) one method of classification is the Briggs classification of soil water. Each class of water is referred to according the kind of force primarily controlling its movement. The three types are:

1. Hygroscopic water - water tightly adhering to solid particles in thin films which can be removed only as a vapor.

2. Capillary water - water which is held by cohesion as a continuous film around the soil particles and in the capillary spaces.

3. Gravitational water - water which exists in large pores of soil and which the force of gravity will remove from the soil when conditions for free drainage exist.

Chemical engineering literature usually refers to four types of moisture. The four types as listed by Treybal (2) are:

1. Bound moisture - moisture contained by a substance which exerts an equilibrium vapor pressure less than that of the pure liquid at the same temperature.

2. Unbound moisture - moisture contained by a substance which exerts an equilibrium vapor pressure equal to that of the pure liquid at the same temperature.

3. Equilibrium moisture - the moisture content of a substance when at equilibrium with a given partial pressure of the vapor.

4. Free moisture - that moisture contained by a substance in excess of the equilibrium moisture.

These relationships are shown in Figure 9 for a material exposed to an atmosphere of relative humidity A. Bound water may exist in several conditions. Liquid water in fine capillaries exerts an abnormally low vapor pressure because of the highly concave curvature at the surface. Bound moisture in cell or fiber walls may have a lower vapor pressure due to dissolved solids. Water in many substances is bound by both physical and chemical combination, the nature and strength of which vary with the nature and moisture content of the solid. Unbound water, however, exerts its full vapor pressure and is largely held in the voids of the solid. McCabe and Smith (3) state that the distinction between bound and unbound water depends on the material itself, while the distinction between free and equilibrium moisture depends on the drying conditions.

DERIVATION OF SPECIFIC RESISTANCE

The well known concept of specific resistance initially developed by Carmen and later refined by Coackley and Jones (4), has been proven to adequately describe the dewatering of a compressible material by means of a vacuum filtration unit. Therefore, since the only difference between dewatering by vacuum filtration and dewatering by gravity drainage is that a constant pressure is applied on the sludge in the former and a continually decreasing pressure is applied on the sludge in the latter, the specific resistance concept could well be the basis for a mathematical model describing gravity drainage on a sand bed.

The concept of specific resistance can be developed starting with the classic Darcy-Weisbach equation for the head loss of a fluid moving through

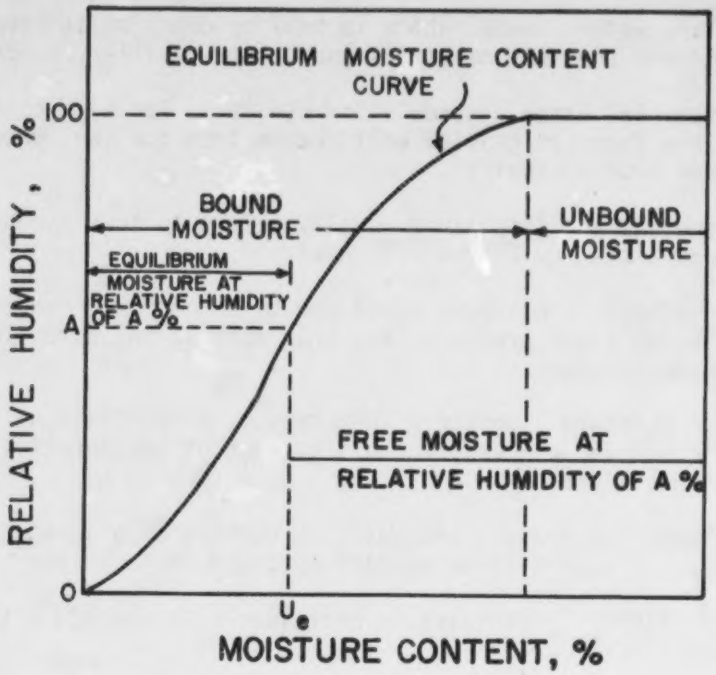

Figure 9: Relationship of relative humidity vs. moisture content.

a pipe.

$$h_f = \Delta P/\rho g = f_1 (L/D)\overline{V}^2/2g \qquad (9)$$

where h_f = head loss (L)
ΔP = pressure drop in pipe ($M\ L^{-1}\ T^{-2}$)
ρ = mass density ($M\ L^{-3}$)
L = length of pipe (L)
$\overline{V}$ = mean velocity ($L\ T^{-1}$)
D = diameter of pipe (L)
g = acceleration due to gravity ($L\ T^{-2}$)
f_1 = friction factor ($M^0\ L^0\ T^0$)

Since the fluid velocity through the pores of a sand bed will be very slow, it is reasonable to conclude that a state of laminar flow will exist. The friction factor in the laminar flow region is related to the Reynolds number:

$$f_1 = 64/R_n \tag{10}$$

where: R_n = Reynolds Number = $D\bar{V}\rho/\mu$ $(M^0L^0T^0)$ $\quad (11)$

μ = dynamic viscosity $(ML^{-1}\ T^{-1})$

For noncircular conduits the hydraulic radius is defined as:

$$R_h = A/P$$

where: R_h = hydraulic radius (L)

A = area (L^2)

P = wetted perimeter (L)

Substituting the area and perimeter of a circular cross section

$$R_h = (\pi D^2/4)/\pi D = D/4$$

$$D = 4R_h \tag{12}$$

Substituting Equations 10, 11 and 12 into Equation 9,

$$h_f = (64/R_n)\ (R_n\mu/DV\rho)(L/4R_h)\ (\bar{V}^2/2g) \tag{13}$$

$$h_f = 2\mu L\bar{V}^2/\bar{V}R_h{}^2\rho g$$

The derivation thus far has been for the head loss through a cross section of measurable dimensions. For flow through incompressible porous media, the conduit cross section must be expressed in terms of the porosity:

$$A_p = \varepsilon A \tag{14}$$

where: A_p = cross-sectional area of pores available to flow. This area is assumed constant throughout the column of sand (L^2)

ε = porosity = V_v/V_{tot} = Void Volume/Total Volume $(M^0L^0T^0)$

Assuming all particles in the porous material to be identical and defining

N = number of particles $(M^0L^0T^0)$

S_p = surface area of each particle (L^2)

V_p = volume of each particle (L^3),

the hydraulic radius may be written as

$$R_h = A_p/P = A\cdot L/P\cdot L = V_v/NS_p \tag{15}$$

Note that:

$$\varepsilon = V_v/V_{tot} = V_v/(V_v + NV_p)$$

Hence

$$V_v = \varepsilon N/(1-\varepsilon)$$

Therefore:

$$R_h = \varepsilon AL/NS_p = \varepsilon NV_p/(1-\varepsilon)NS_p = \varepsilon V_p/(1-\varepsilon)\cdot S_p \qquad (16)$$

The relationship of actual velocity and superficial velocity (Total Flow/Area of Total Cross Section) is required. From continuity considerations:

$$V_s A = \overline{V}A_p$$

$$V_s = \overline{V}A_p/A = \overline{V}A_pL/AL = \overline{V}\varepsilon \qquad (17)$$

where V_s = superficial velocity ($L\ T^{-1}$)

Combining equations 16, 17, and 13,

$$h_f = \frac{(2\mu L)(\frac{V_s}{\varepsilon})(1-\varepsilon)^2\ S_p{}^2}{\rho g \qquad \varepsilon^2\overline{V}_p{}^2} = \frac{2(1-\varepsilon)^2\ V_s\mu LS_p{}^2}{\varepsilon^3 gV_p{}^2\rho} = \frac{\Delta p}{\rho g} \qquad (18)$$

Set

$$\frac{2(1-\varepsilon)^2\ S_p{}^2}{\varepsilon^3\ V_p{}^2} = R \qquad (19)$$

where R = media or filter resistance (L^{-2}), and

$$\frac{h_f\rho g}{L} = \frac{\Delta P}{L} = \mu V_s R \qquad (20)$$

Solving for V_s

$$V_s = \frac{\Delta P}{L\mu R} = \frac{1}{A}\frac{dV}{dt}$$

where dV/dt = Flowrate ($L^3\ T^{-1}$)

Therefore:

$$dV/dt = A\Delta P/\mu LR \qquad (21)$$

Equation 21 may be used for stratified filters where there are two different depths (L) and two different resistances.

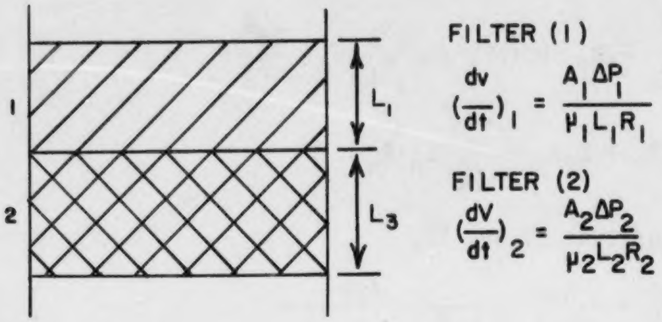
1
2
L_1
L_3
FILTER (1)
$(\frac{dv}{dt})_1 = \frac{A_1 \Delta P_1}{\mu_1 L_1 R_1}$
FILTER (2)
$(\frac{dV}{dt})_2 = \frac{A_2 \Delta P_2}{\mu_2 L_2 R_2}$

Figure 10. Definition sketch for a stratified filter.

Since water is incompressible

$$(\frac{dV}{dt})_1 = (\frac{dV}{dt})_2 = \frac{dV}{dt}$$

$$A_1 = A_2 = A$$

$$\mu_1 = \mu_2 = \mu$$

$$\frac{A\Delta P}{\mu LR} = \frac{A\Delta P_1}{\mu L_1 R_1} = \frac{A\Delta P_2}{\mu L_2 R_2}$$

$$\frac{\Delta P}{LR} = \frac{\Delta P_1}{L_1 R_1} = \frac{\Delta P_2}{L_2 R_2}$$

$$\Delta P_2 = \frac{L_2 R_2}{L_1 R_1} \Delta P_1$$

where $\Delta P = \Delta P_1 + \Delta P_2$

$$L = L_1 + L_2$$

$$\Delta P = \Delta P_1 + \frac{L_2 R_2}{L_1 R_1} \Delta P_1$$

If the filter consists of n number of strata

$$\frac{L_1 R_1}{\Delta P_1} = \frac{L_2 R_2}{\Delta P_2} = \frac{LR}{\Delta P}$$

$$LR = \frac{\Delta P}{\Delta P_1} L_1R_1 = (\Delta P_1 + \frac{L_2R_2}{L_1R_1}\Delta P_1)\frac{L_1R_1}{\Delta P_1}$$

$$LR = L_1R_1 + L_2R_2 + \sum_{n=3}^{n=\infty} L_n \cdot R_n \tag{22}$$

Combining equations 21 and 22,

$$\frac{dV}{dt} = \frac{A\Delta P}{\mu LR} = \frac{A\Delta P}{\mu(L_1R_1 + L_2R_2)} = \frac{A\Delta P}{\mu\sum\limits_{n=1}^{\infty} L_nR_n} \tag{23}$$

Filtration of a compressible material on a porous medium may be described by using the specific resistance concept. The initial filtration rate is governed by the support medium resistance, then a cake gradually forms on the support surface and contributes to the resistance to flow. This cake increases in thickness with increasing volume of filtrate; as each volume of filtrate is separated from the sludge, a portion of this volume (solids) will remain to form a sludge cake with a thickness equal to L_1 (Figure 11).

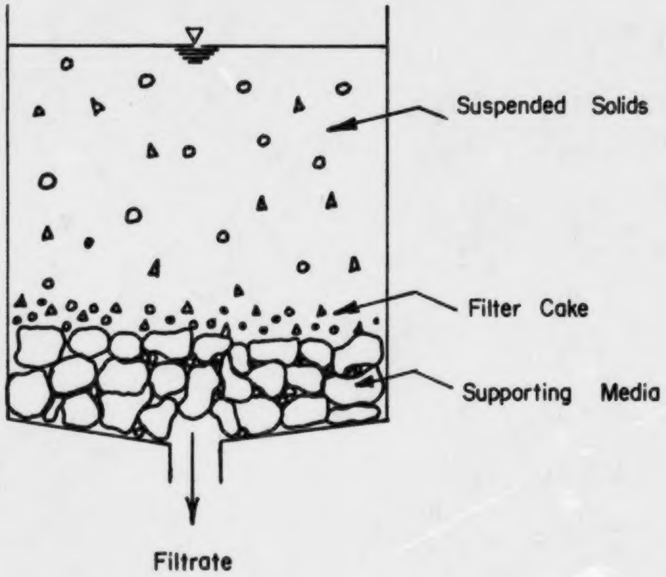

Figure 11: Schematic representation of filtration of a compressible material on a porous medium.

The relationship is expressed as:

$$L_1 = vV/A \tag{24}$$

where: V = volume of filtrate (L^3)
A = area of surface (L^2)
v = volume of cake deposited per unit volume of filtrate ($L^0M^0T^0$)

This accumulation of sludge particles, however, may be more easily expressed and determined if v is replaced by f, the weight of cake solids per unit volume of filtrate ($F\ L^{-3}$). Therefore, substitution into (Eq. 23) will give:

$$\frac{dV}{dt} = \frac{A\Delta P}{\mu(\frac{fVR}{A} + L_2R_2)} \qquad (25)$$

L_2 and R_2 refer to the supporting medium. The resistance of the cake, R, called "specific resistance," has units of T^2M^{-1}.

The characteristics of the supporting incompressible medium may be combined by substituting R_f for the constant L_2R_2 and rearranging

$$dt = \left(\frac{\mu fVR + \mu AR_f}{A^2\Delta P}\right)dV \qquad (26)$$

If ΔP remains constant, the following integration can be made:

$$\int_0^t dt = \int_0^V \left(\frac{\mu fVR}{A^2\Delta P} + \frac{\mu AR_f}{A^2\Delta P}\right) dV$$

$$t = \frac{1}{2}\,\frac{\mu fR}{A^2\Delta P}\,V^2 + \frac{\mu R_f}{A\Delta P}\,V \qquad (27)$$

The experimental data, plotted as (t/V) versus V will yield a straight line on arithmetic paper. The slope b allows calculation of the specific resistance R (Figure 12):

$$R = \frac{2A^2\Delta Pb}{\mu f} \qquad (28)$$

where R = specific resistance of compressible material subjected to a vacuum of ΔP (T^2M^{-1})
ΔP = pressure loss across sludge cake ($F\ L^{-2}$)
A = area of filtration surface (L^2)
μ = dynamic viscosity of filtrate ($M\ L^{-1}\ T^{-1}$)
f = weight of solids per unit volume of filtrate ($F\ L^{-3}$)
b = slope from t/v versus V plot ($T\ L^{-6}$)

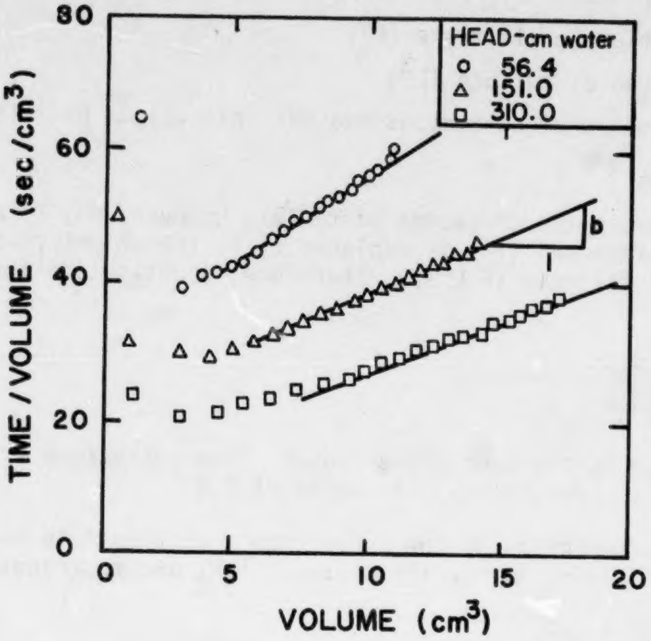

Figure 12: A typical graph used to determine the specific resistance of a wastewater sludge at three different vacuums.

Similarly, the t/v intercept of the line of slope b at V = 0 determines the resistance of the supporting media

$$R_f = \frac{(t/v\ \text{intercept})\ A\Delta P}{\mu}$$

The relationship of specific resistance to head was studied and found to be empirically described by the following equation (5,6):

$$R = R_c(h/h_c)^{\sigma} \tag{29}$$

where R = specific resistance of sludge at head h ($T^2\ M^{-1}$)

R_c = specific resistance when head = h_c (T^2M^{-1})

σ = coefficient of compressibility ($L^0M^0T^0$)

A plot of the log of specific resistance as the ordinate versus the log of the head will yield a straight line with a slope equal to the coefficient of compressibility σ.

DERIVATION OF MATHEMATICAL MODEL FOR THE GRAVITY DRAINAGE RATE

Using the specific resistance concept, a mathematical model can be derived for determining the gravity drainage rate of a sludge or other compressible material on a drainage bed. Referring to Equation 23

$$\frac{dV}{dt} = \frac{A\Delta P}{\mu(L_1R_1 + L_2R_2)} \qquad (23)$$

and knowing that

$$L_2R_2 = R_f$$

$$L_1 = fV/A \text{ and}$$

$$\Delta P = \rho hg$$

substitution of R (Eq. 29) for R_1 (Eq. 23) and rearrangement gives:

$$\frac{dV}{dt} = \frac{A^2 \rho hg}{\mu[fVR_c(h/h_c)^\sigma + AR_f]} \qquad (30)$$

Because the specific resistance of a wastewater sludge is much greater than the resistance of the supporting sand or soil media, ($R >> R_f$) the term AR_f can be assumed negligible. Therefore it follows that

$$\frac{dV}{dt} = \frac{A^2\rho hg}{\mu fVR_c \, (h/h_c)^\sigma}$$

Since

$$\frac{dV}{dt} = -A\frac{dh}{dt}$$

And

$$V = A(H_o - h)$$

$$H_o = \text{initial head (L)}$$

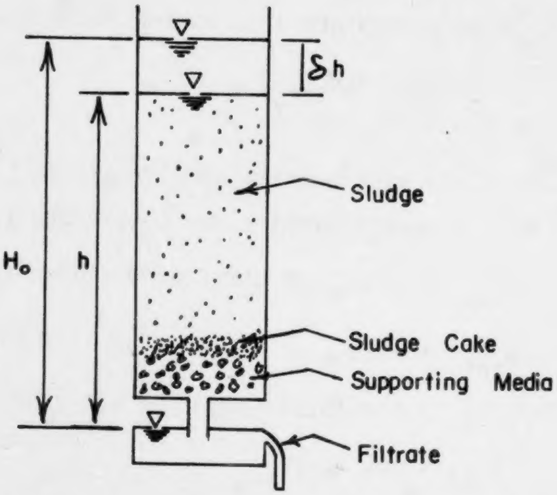

Figure 13: Schematic representation of the different terms used in derivation of the mathematical model.

Therefore:

$$\frac{dh}{dt} = - \frac{\rho g h(h_c/h)^{\sigma}}{\mu f R_c(H_o - h)} \qquad (31)$$

Reorganizing and integrating to the proper limits will yield

$$\int_0^t dt = - \frac{R_c \ \mu f}{\rho g(h_c)^{\sigma}} \int_{H_o}^{h} (H_o - h)^{\sigma - 1} dh \qquad (32)$$

$$t = - \frac{\mu R_c f}{\rho g(h_c)^{\sigma}} \left\{ \left[\frac{H_o h^{\sigma}}{\sigma}\right]_{H_o}^{h} - \left[\frac{h^{\sigma+1}}{\sigma+1}\right]_{H_o}^{h} \right\}$$

$$t = - \frac{\mu R_c f}{\rho g(h_c)^{\sigma}} \left\{ \frac{H_o}{\sigma} (h^{\sigma} - H_o^{\ \sigma}) - \frac{h^{\sigma+1} - H_o^{\ \sigma+1}}{\sigma+1} \right\}$$

$$t = \frac{\mu R_c f}{\rho g(h_c)^{\sigma}(\sigma+1)} \left\{ h^{\sigma+1} - \frac{\sigma+1}{\sigma} H_o h^{\sigma} - H_o^{\ \sigma+1} + \frac{\sigma+1}{\sigma} H_o^{\ \sigma+1} \right\} \qquad (33)$$

The value of f, solids deposited per unit volume of filtrate, requires further analysis in order to simplify Equation 33.

If no solids are lost during filtration the volume of filtrate is

$$V = \frac{(W_{tot_o} - W_{tot_f})}{\rho g} \qquad (34)$$

where ρ = mass density of filtrate ($M \ L^{-3}$)

g = acceleration due to gravity ($L \ T^{-2}$)

W_{tot_o} = weight of unfiltered sludge ($M \ L \ T^{-2}$)

W_{tot_f} = weight of filtered cake ($M \ L \ T^{-2}$)

Referring to the total weight in terms of solids content:

$$W_{tot} = 100 \ W_{TS}/F_o \qquad (35)$$

W_{tot} = total weight of sludge ($M \ L \ T^{-2}$)

W_{TS_o} = weight of solids in unfiltered sludge ($M \ L \ T^{-2}$) = W_{TS}

W_{TS_f} = weight of solids in filtered cake ($M \ L \ T^{-2}$) = W_{TS}

F_o = solids content (%)

Therefore the volume of filtrate may be written as:

$$V = \left(\frac{W_{TS}\cdot 100}{F_o} - \frac{W_{TS}\cdot 100}{F_f}\right)/\rho g \qquad (36)$$

where F_o = solids content of sludge at beginning of test (%)

F_f = solids content of sludge at end of test (%)

which simplifies to

$$V = 100\,\frac{W_{TS}}{\rho g}\left(\frac{1}{F_o} - \frac{1}{F_f}\right) \qquad (37)$$

It has been previously defined that f is equal to the weight of dry solids deposited per unit volume of filtrate.

$$f = W_{TS}/V \qquad (38)$$

Therefore, by substitution of (Eq. 37) into (Eq. 38)

$$f = W_{TS}/\left[\frac{100\,W_{TS}}{\rho g}\left(\frac{1}{F_o} - \frac{1}{F_f}\right)\right] \qquad (39a)$$

which reduces to

$$f = \rho g/\left(\frac{100}{F_o} - \frac{100}{F_f}\right) \qquad (39b)$$

F_o will be much less than F_f since dewatering will decrease the solids content of a dilute sludge 10-15 times. Therefore, the term $100/F_f$ may be neglected. Dropping the subscript:

$$f = \rho g F/100 \qquad (40)$$

Equation 40 may now be substituted into Equation 33, resulting in

$$t = \frac{\mu R_c F}{100(h_c)^{\sigma}\,(\sigma+1)}\left[h^{\sigma+1} - \frac{\sigma+1}{\sigma} H_o h^{\sigma} - H_o{}^{\sigma+1} + \frac{\sigma+1}{\sigma} H_o{}^{\sigma+1}\right] \qquad (41)$$

Equation 41 is dimensionally correct with the gravity drainage time defined by basic parameters -- specific resistance R_c at a given head loss h_c, coefficient of compressibility σ, initial solids content F, initial head H_o, and dynamic viscosity of the filtrate μ.

Equation 41 has been used to predict the drainage times for wastewater sludges. Laboratory determinations of σ, F_o, and R comprise the laboratory operations. It is the basic equation used by Sanders (28) and Nebiker et al. (29) in predicting drainage times for wastewater sludges.

The specific resistance, R, in Equation 41 is determined by the Buchner funnel or fritted glass funnel method. Standard laboratory procedures for measuring specific resistance by the various methods have been reported by Lutin et al. (30). An adjustment to the specific resistance so determined is necessary to account for the pressure variation across the cake in the funnel. In the Buchner or fritted glass funnel the specific resistance is a function of pressure where

$$R(P) = R_c \left(\frac{P}{P_c}\right)^{\sigma} \tag{42}$$

where P = pressure at time t $(ML^{-1}t^{-2})$

P_c = reference pressure at R_c $(ML^{-1}t^{-2})$

The pressure varies from near zero at the surface of the cake to ΔP at the outlet of the testing funnel. An average value R is measured by the funnel and could be defined as:

$$\overline{R} = \frac{1}{\Delta P} \int_{0}^{\Delta P} R(P)\, dP \tag{43}$$

where R(P) is the local specific resistance at each horizon in the sludge cake. Substituting the value of R(P) from Equation 42 into Equation 43 and performing the integration

$$\overline{R} = \frac{R_c}{P_c^{\sigma}} \frac{1}{\sigma + 1} (\Delta P)^{\sigma} \tag{44}$$

or rearranging,

$$\overline{R} = \frac{1}{\sigma + 1} R_c \left(\frac{\Delta P}{P_c}\right)^{\sigma} \tag{45}$$

Then from Equation 42, Equation 45 may be written as

$$\overline{R} = \frac{1}{\sigma + 1} R(P) \tag{46}$$

This indicates that the values for t determined from Equation 41 should be multiplied by the term $1/(\sigma + 1)$ so that proper account is taken of the specific resistance of the sludge cake.

It is interesting to note that Nebiker et al. (29) in a study of the drainage time required for sludge applied to sand columns found it necessary to multiply the drainage times predicted from Equation 41 by a media factor, a function of the ratio of the size of the sludge particle to the size of the sand particle. Media factors of magnitude 0.45, 0.60 and 0.75 for three different sands were used so that the theoretical equation would agree with experimental values. They used the unadjusted specific resistance values instead of $\overline{R}$. The sludges studied had coefficients of compressibility ranging from 0.63 to 0.64, which would yield values of the correction $1/(\sigma + 1)$ of 0.62. Clearly much of the discrepancy between the theoretical formulation and their experimental values was due not to the media used, but to using the unadjusted specific resistance.

The assumption that the final solids content term can be ignored in Equation 39 may be invalid for water treatment sludges. In water treatment sludges the initial and final solids content may be on the order of 0.5 and 1.5 percent, respectively. Using Equation 39 for f, employing the media factor, and correcting for the variation of specific resistance with pressure, the equation for drainage of water treatment sludge may be expressed as

$$t = \frac{m\, R_c\, F_o\, F_f\, \mu}{(\sigma+1)\ (100F_f - 100F_o)\ H_c^{\sigma}} \left[\frac{H^{\sigma+1} - H_o^{\sigma+1}}{\sigma + 1} + \frac{H_o^{\sigma+1} - H_o H^{\sigma}}{\sigma}\right] \qquad (47)$$

where: m = media factor (dimensionless).

EVAPORATION OF WATER

A net input of thermal energy to a flat free-water surface increases the free kinetic energy of the water molecules to the point where some are able to escape across the liquid-gas interface. The amount of heat absorbed by a unit mass of water while passing from the liquid to the vapor state at constant temperature is called the latent heat of evaporation or latent heat of vaporization (7). Molecules of water that leave the liquid surface cannot readily re-enter due to a decrease in kinetic energy. Under equilibrium conditions water vapor may be treated as an ideal gas yielding the following equation:

$$p = \rho_v\, R_v\, T \qquad (48)$$

where p = partial pressure of water vapor $(ML^{-1}\ T^{-2})$

ρ_v = mass density of water vapor (ML^{-3})

R_v = gas constant for water $(L^2T^{-2}T^{-1})$

T = absolute temperature (T)

Further vaporization causes a continued increase in p in the air above the liquid until condensation begins. When the rate of condensation and the rate of vaporization become equal the air is saturated with vapor and molecules cross the interface in both directions at the same rate. The partial pressure of the vapor in the air at which this equilibrium takes place is known as the saturation vapor pressure, or simply the vapor pressure of the liquid. This vapor pressure is an increasing function of the liquid temperature. Equilibrium never exists under natural conditions since the volume of air into which vaporization takes place is essentially infinite. Also, various convective transport processes will operate to transport the vapor both parallel and perpendicular to the liquid surface, thus preventing equilibrium from occurring.

Laboratory studies on evaporation from free water surfaces have been reported by many investigators in various disciplines. Boelter et al.(8) presented the following empirical equation, developed under laboratory conditions, for evaporation rate into a quiescent atmosphere.

$$E_w = K_e (p_i - p_g) \quad (49)$$

where E_w = evaporation rate ($ML^{-1}T^{-3}$)

K_e = evaporation transfer coefficient (T^{-1})

p_i = partial pressure of water at interface ($ML^{-1}T^{-2}$)

p_g = partial pressure of water in main gas ($ML^{-1}T^{-2}$)

The value of K_e is 0.054 when pressures are reported in inches of mercury. Other investigators found similar values for K_e.

When evaporation is taking place from a free-water surface, it is helpful to assume that a thin film of vapor saturated air forms adjacent to the water surface. The film temperature is assumed to be the temperature of the water. Whenever the saturation vapor pressure at film temperature is greater than the partial pressure of the water vapor in the air immediately above the film a gradient in vapor pressure will exist. The evaporation function may be written as

$$E_r = -K\, dp_g/dZ \quad (50)$$

where E_r = evaporation rate (LT^{-1})

Z = elevation(L)

K = transfer coefficient ($M^{-1}L^3T$)

The dependence of E_r upon total atmospheric pressure and salinity as well as upon temperature is implied through variation of p_g with these variables. The presence of wind will have a major effect on E_r, since by convection it will remove the vapor-laden air, thereby keeping the film thin and maintaining a high transfer rate. Other factors influencing the evaporation rate, either directly or indirectly, are solar radiation, air temperature, and vapor pressure.

The depression of the evaporation rate due to salinity or dissolved solids can be formulated by Henry's law which may be written as

$$P_a = C_h\, x \quad (51)$$

where P_a = partial pressure of component a ($ML^{-1}T^{-2}$)

C_h = Henry's law constant ($ML^{-1}T^{-2}$)

x = mole fraction of component a in liquid phase (dimensionless)

Since χ is defined as the ratio of moles of component a (in this case water) to the total moles, a dilute solution will exert a higher vapor pressure and the driving force $(p_i - p_g)$ in Equation 49 will approach the maximum (that of pure water). For increasing values of χ (dense solutions), the driving force decreases, hence the evaporation rate decreases.

According to Eagleson (7) there are two fundamental approaches to the theoretical study of evaporation from a free water surface. The diffusion method involves a mass-transfer process by which vapor is removed from the liquid surface. The energy-balance method involves determining an average rate of water loss by evaporation over a given time interval. Penman(9) first utilized the best features of both of the theoretical approaches in order to derive a water-surface evaporation relation which is dependent upon a limited number of fairly easily measured meteorological variables. Kohler et al. (10) further developed Penman's model to obtain a graphical method as shown in Figure 14 which allows prediction of daily water surface evaporation.

In order to apply the concepts of Figure 14 to natural water bodies, adjustments must be made for advected energy and for changes in heat storage. This adjustment is in the form of a pan coefficient which is the ratio of the rate of evaporation in a pan of water to the rate of evaporation in a large body of water. Measurements are somewhat simplified by using a standard circular pan which may be installed on the ground (land pan) or in the water (floating pan). The average coefficient for the land pan is about 0.7 and for the floating pan, 0.8. Complete instructions for making these measurements are given by the U. S. Weather Bureau (11).

Average annual evaporation rates for lakes in the United States have been compiled by the U. S. Weather Bureau. The average annual lake evaporation, in inches, for the period 1946-1955 is presented in Figure 15 as taken from Kohler et al. (12).

DRYING

When a solid dries, two fundamental and simultaneous processes occur. These are: transfer of heat to evaporate liquid and transfer of mass as internal moisture and evaporated liquid. Drying of solids encompasses two different types of material: porous and nonporous. It is customary to assume that a drying solid is either porous or nonporous although McCabe and Smith (3) state that most solids are intermediate between the two extremes. Either type may also be hygroscopic or nonhygroscopic. The drying of a solid may be studied from the standpoint of how the drying rate varies with external conditions such as temperature and humidity or with changes in moisture in the interior of the solid. Internal liquid flow may occur by several mechanisms, depending on the structure of the solid. Some of the possible mechanisms as listed by Marshall and Friedman (13) are as follows: (1) diffusion in continuous homogeneous solids, (2) capillary flow in granular or porous solids, (3) flow caused by shrinkage and pressure gradients, (4) flow caused by gravity, and (5) flow caused by a vaporization-condensation sequence. In general, one mechanism predominates at a given time during drying in a solid and it is not uncommon to find different mechanisms predominating at

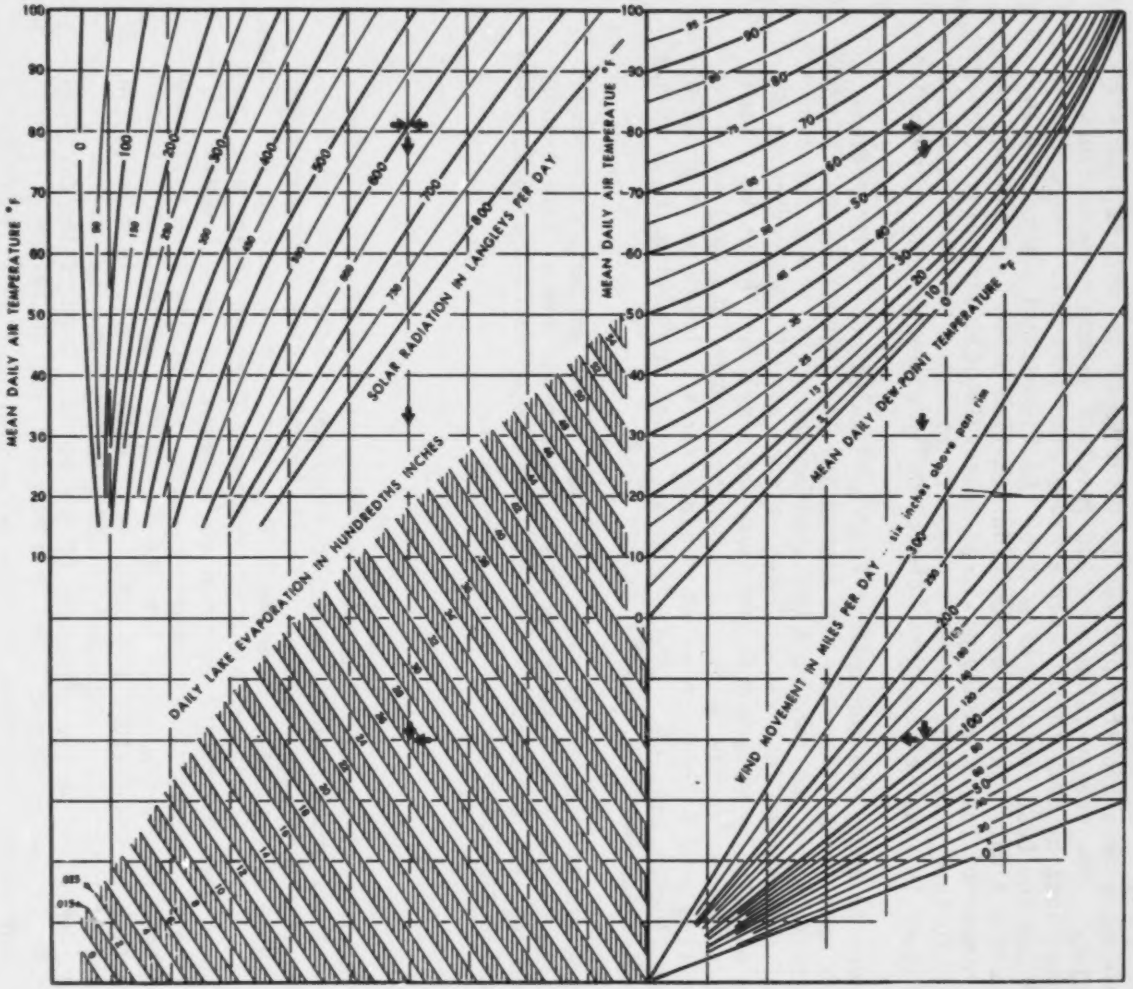

Figure 14: Lake evaporation relation (adapted from Figure 6 of Ref. 12).

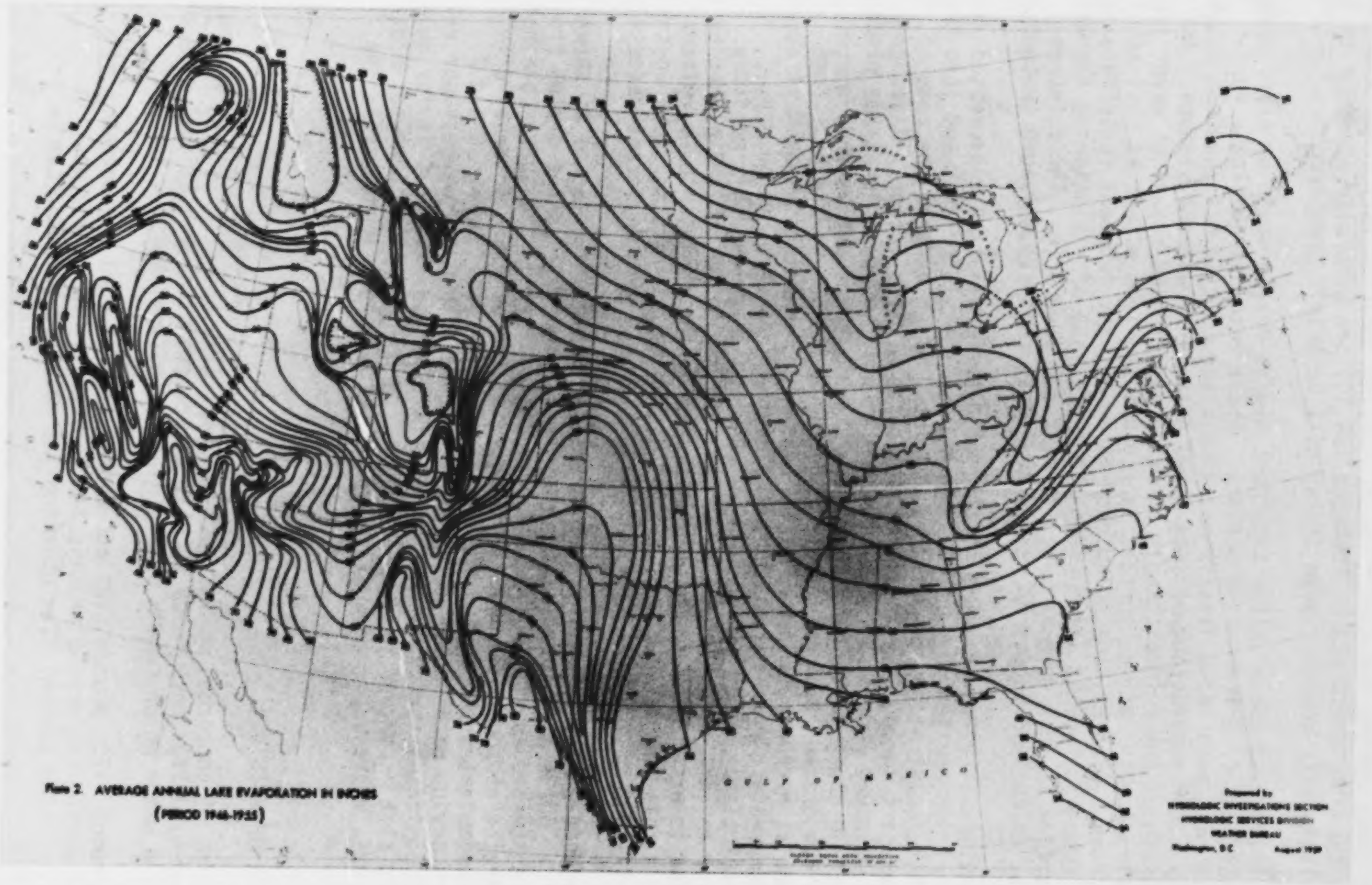
Plate 2. AVERAGE ANNUAL LAKE EVAPORATION IN INCHES
(PERIOD 1946-1955)
GULF OF MEXICO
Prepared by
HYDROLOGIC INVESTIGATIONS SECTION
HYDROLOGIC SERVICES DIVISION
WEATHER BUREAU
Washington, D.C.
August 1959

Figure 15: Mean annual evaporation (inches) from shallow lakes and reservoirs(Ref. 12).

different times during the drying cycle. Drying theories vary somewhat, however, the theories presented by Sherwood (14,15) are generally accepted and their applicability toward sludge drying will be briefly reviewed.

The initial stages of water treatment sludge drying would be expected to approximate that of a free water surface. Ample water is available for evaporation and some sedimentation may take place. It is not uncommon to see relatively clear supernatant on some types of water treatment sludges. As drying continues the volume changes in proportion to the amount of water lost. A thin film of water at the surface is replenished from within as fast as it can evaporate. Eventually a solid cake forms and the internal resistance to moisture movement becomes large enough that the rate of replenishing the water at the surface is less than the rate the air can absorb it. The moisture content at which this occurs is called the first critical moisture content.

Additional drying continues at the solid surface but at a decreased rate. The zone of evaporation may gradually move into the sludge mass and into the pores of the walls of any cracks that develop. At this stage the rate of vapor transport through the empty pores becomes a major factor. A second critical moisture content is often reached at which evaporation takes place solely within the interior of the solid. At this point and beyond, resistance to evaporation from surfaces of individual solids dominates. Some water such as hygroscopic water and hydrate water cannot be removed at atmospheric temperature even though the solid may be considered to be dry. Significant elevation of temperature is required to remove this moisture. During the falling rate drying period the rate may be determined either by the resistance to water removal at the surface or by the resistance to moisture movement within the material. A plot of drying rate versus moisture content for the falling rate period will vary significantly with different materials.

Sherwood (16) presented drying curves for various substances as shown in Figure 16. Curve A is for porous ceramic plate and follows the drying process as described above. Curve B represents the drying-rate curve obtained in the drying of soap and wood. This case is typical where internal diffusion predominates throughout the falling-rate period. Curves C and D represent drying-rate curves which may be obtained in cases where vapor removal predominates throughout the falling-rate period. Curve C is for sulfite pulp slab. Curve D represents the drying of newsprint, bond, or blotting papers, where vapor removal and not internal diffusion controls the drying.

DIFFUSION OF MOISTURE

Drying of nonporous solids such as soap, glue and plastic clay have been described by diffusion. These substances are essentially colloidal gels of solids and water which retain considerable amounts of bound water.

Sherwood (17), Newman (18) and Luikov (19) studied the movement of moisture during the drying process for various drying conditions and materials. The general flux equation for moisture movement can be presented as:

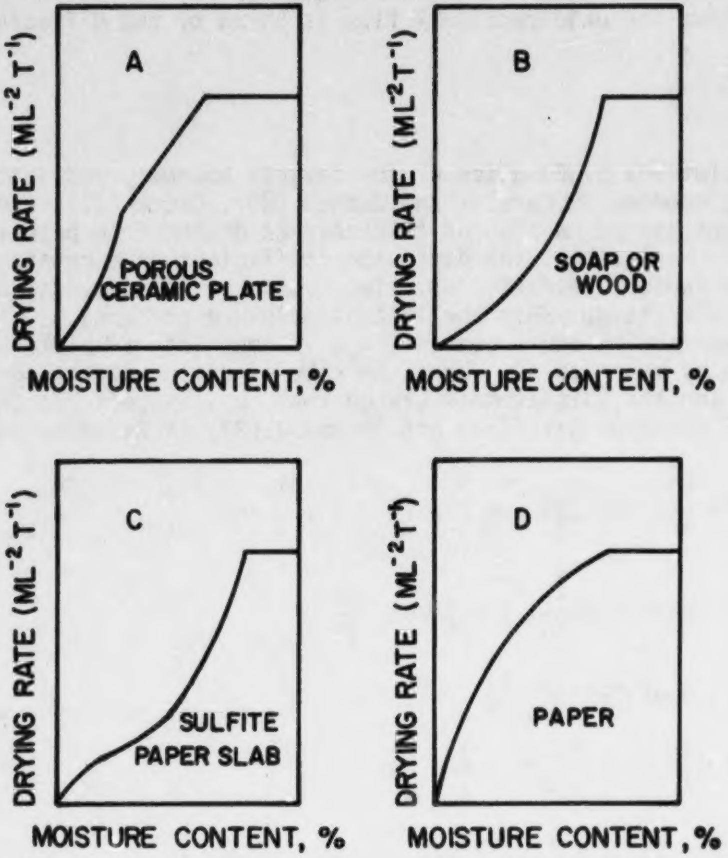

Figure 16: Drying rate curves for various substances.

$$I = -\frac{1}{A}\frac{dW_w}{dt} = D\rho\,\frac{\partial U}{\partial x} \qquad (52)$$

where I = drying rate ($ML^{-2}T^{-1}$)

A = area (L^2)

W_w = mass of water (M)

t = time

D = constant diffusion coefficient (L^2T^{-1})

ρ = density (ML^{-3})

U = average moisture content, dimensionless

x = distance (L)

The general partial differential equation for variation in moisture content with time for unidirectional flow is given by the diffusion equation

$$\frac{\partial U}{\partial t} = D \frac{\partial^2 U}{\partial X^2} \qquad (53)$$

The solutions of Equation 47 for several boundary and initial conditions have been presented by Carslaw and Jaeger (20), Crank (21), and Ozisik (22). All solutions assume a slab of thickness 2ℓ drying from both surfaces, where shrinkage is negligible, the diffusion coefficient is a constant, and all moisture is subject to diffusion. Two common cases encountered in the literature are cited. When the initial moisture content, U_o, is uniform and where the surface moisture content, U_s, is constant, a solution of Equation 53 is given by Equation 54. When the rate of drying at the surface is constant, I_c, and the initial moisture content, U_o, is uniform, the solution of Equation 52 given by Gilliland and Sherwood (23) is Equation 55.

$$\frac{U-U_s}{U_o-U_s} = \frac{4}{\pi} \{[\cos \frac{\pi x}{2\ell} \exp [-Dt(\frac{\pi}{2\ell})^2] - \frac{1}{3} \cos \frac{3\pi x}{2\ell}$$

$$\exp[-9Dt(\frac{\pi}{2\ell})^2] + \frac{1}{5} \cos \frac{5\pi x}{2\ell} \qquad (54)$$

$$\exp[-25Dt(\frac{\pi}{2\ell})^2] \; . \; . \; .$$

$$(U_o-U) (\frac{D\rho}{I_c}\ell) = [\frac{(x-\ell)}{2\ell^2} - \frac{1}{6} + \frac{Dt}{\ell^2}$$

$$- \frac{2}{\pi^2} \sum_{1}^{\infty} \frac{(-1)^n}{n^2} \exp(-n^2 \pi^2 \frac{Dt}{\ell 2})\cos-(n\pi \; (x-\ell)/\ell\}] \qquad (55)$$

The main limitations to describing moisture movement by diffusion during drying are the assumptions of constant diffusion coefficient and negligible shrinkage (constant thickness). Hougen et al. (24) and Ceaglske and Hougen (25) found that diffusivity varied with moisture content for various solids such as paper pulp and sand. Variable diffusivities for wood and other building materials are also reported by Luikov (19).

If diffusivity is a function of the moisture content, the moisture transport rate may be written

$$\text{Moisture Flux Rate} = -D(U)\frac{\partial U}{\partial x} \qquad (56)$$

which, when combined into a conservation of mass equation, yields

$$\frac{\partial U}{\partial t} = \frac{\partial}{\partial x} [D(U) \frac{\partial U}{\partial x}] \qquad (57)$$

as the concentration dependent diffusion equation. The variation of the diffusion coefficient with moisture content must be evaluated from experimental data.

DRYING RATE

The drying-rate approach presents a less fundamental study of internal moisture conditions, however, it is experimentally straight-forward and its application is not sensitive to problems of shrinkage.

The drying-rate method makes calculation of drying times straightforward. Drying studies can often be conducted under conditions identical to those the materials will be exposed to during actual processing. Moisture-time curves can be constructed requiring only an initial moisture content measurement and measurements of the loss of water at various times. The time to dry the material to any desired moisture concentration can then be read from the moisture-time curve directly. Such a curve is shown in Figure 17. Note that the sludge mass-time curve is the only experimental curve, the others being constructed from the data. The general case involves predicting drying times for materials under a variety of drying conditions only a few of which need be simulated in the laboratory.

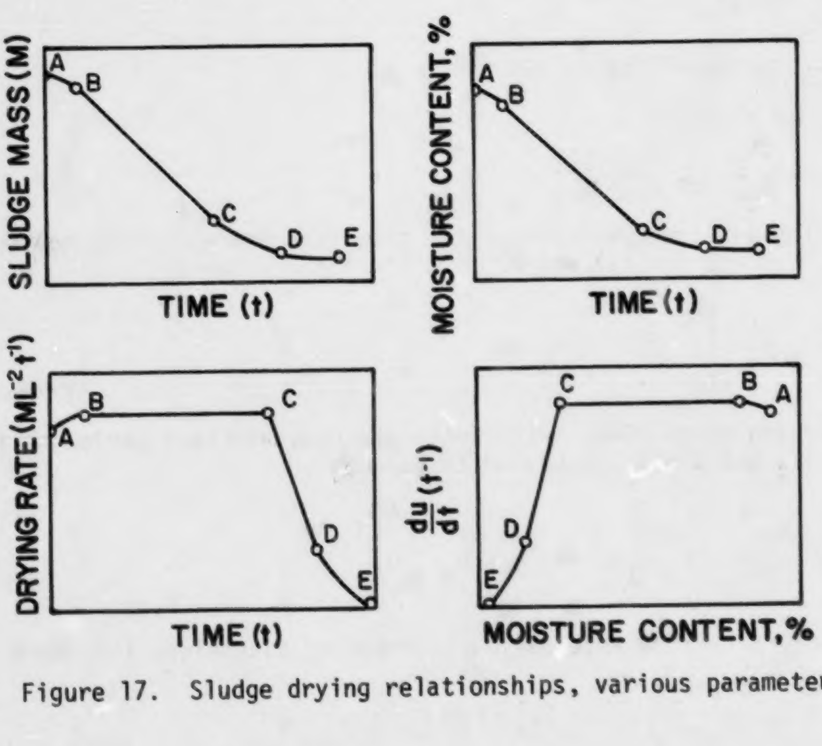

Figure 17. Sludge drying relationships, various parameters.

The evaporation of unbound moisture from a solid exposed to constant drying conditions has been explained by Treybal (2). Since evaporation of moisture absorbs latent heat, the liquid surface will come to and remain at an equilibrium temperature such that the rate of heat flow from the surroundings to the surface equals the rate of heat absorption. If the solid and liquid surface are at a different temperature than the surroundings, the evaporation rate will vary until equilibrium conditions are reached as shown by points A and B. The vapor pressure at the surface thereafter remains constant causing the rate of evaporation to remain constant. This period is the constant-rate drying period previously described and shown between points B and C.

When the average moisture content reaches the first critical moisture content (point C), the surface film of moisture is so reduced by evaporation that dry spots appear upon the surface. This gives rise to the first falling-rate period (point C to point D). The moisture content at point D is the second critical moisture content and the second falling-rate period is shown between points C and D. The moisture content at point E is the equilibrium moisture content and is the minimum moisture content obtained under this drying condition.

This method was used by Nebiker (26) to describe the drying of digested sewage sludges on open air drying beds. Since the expression for moisture content is

$$U = 100 \frac{W_s}{W_{TS}} \tag{58}$$

where W_{TS} = mass of dry solids (M)

the rate of drying is

$$I = -\frac{dW_w}{Adt} = -\frac{W_{TS}}{100A}\frac{dU}{dt} \tag{59}$$

Rearranging and integrating over the time interval while the moisture content changes from its initial value U_o to its final value U_t,

$$t = \frac{W_{TS}}{100A}\int_{U_t}^{U_o} \frac{dU}{I} \tag{60}$$

If the drying takes place entirely in the constant rate period so that U_o and $U_t > U_{CR}$ and $I = I_c$, Equation 60 becomes

$$t = \frac{W_{TS}}{100AI_c}(U_o - U_t),\ \text{for } U_o > U_t \geq U_{CR} \tag{61}$$

If the entire falling rate period is taken as a straight line then

$$I_f = I_c \frac{(U_t - U_e)}{(U_{CR} - U_e)}\ ;\ \text{for } U_{CR} > U_t > U_e \tag{62}$$

where U_e = equilibrium moisture content (dimensionless).

Upon substitution of Equation 62 into Equation 60 the following is derived:

$$t_f = \frac{W_{TS}(U_{CR} - U_e)}{A\ I_c \quad 100} \ln \frac{(U_{CR}-U_e)}{(U_t-U_e)} \tag{63}$$

If the equilibrium moisture content is negligibly small, Equation 63 may be written as

$$t_f = \frac{W_{TS}}{A\ I_c} \frac{U_{CR}}{100} \ln \frac{U_{CR}}{U_t}, \text{ for } U_{CR} > U_t > U_e \tag{64}$$

For a material drying in both the constant and falling rate periods, the total drying time would be

$$t = t_c + t_f$$

$$= \frac{W_{TS}}{100AI_c} [U_o-U_{CR} + U_{CR} \ln (\frac{U_{CR}}{U_t})], \text{ for } U_o \geq U_{CR} \geq U_t \tag{65}$$

CRITICAL MOISTURE CONTENT

The importance of the first critical moisture content is evident from inspection of the previous equations. Most of the relationships to predict the critical moisture content were derived using the diffusion method of moisture movement in the interior of the solid. Methods to calculate the critical moisture content have been presented by Sherwood and Gilliland (23), Luikov (19), and Broughton (27).

Broughton derived a relationship for the critical moisture content on the assumption that the surface-free moisture concentration at the critical point is dependent on the nature of the material but not the drying conditions. If the constant-rate period is long enough the steady state is achieved and Equation 53 results in a parabolic moisture distribution across the slab as shown in Figure 18, the equation for which is

$$\frac{U_m-U_x}{U_m-U_s} = \frac{(x-\ell)^2}{\ell^2} \tag{66}$$

where U_s = moisture control at the surface (dimensionless)

U_m = moisture content at the midplane (dimensionless)

Differentiating and substituting $x = 0$ and $x = 2\ell$ gives gradients at the surface as

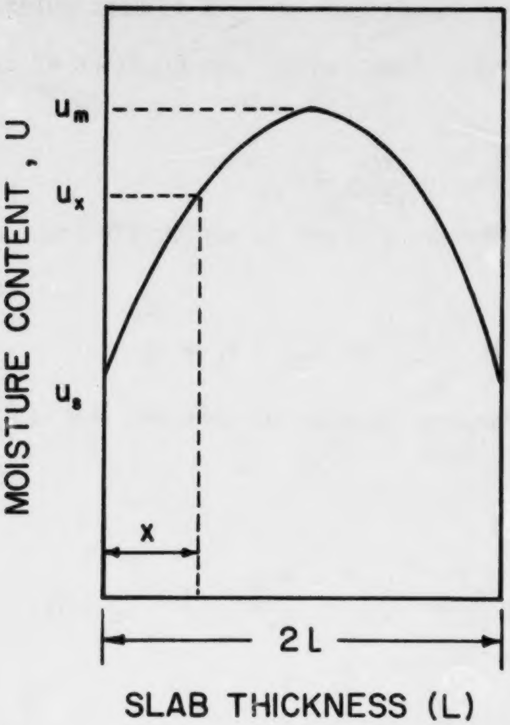

Figure 18. Moisture content vs. slab thickness.

$$\frac{(dU_x)_s}{(dx)_s} = \pm \frac{2(U_m-U_s)}{\ell} \tag{67}$$

U can be determined from

$$U = \frac{1}{\ell} \int_0^{\ell} U_x \, dx \tag{68}$$

where U_x = moisture content at a specific location (dimensionless).

Substituting U from Equation 66 into Equation 68 and integrating,

$$U-U_s = \frac{2}{3} (U_m-U_s) \tag{69}$$

Equations 52, 58, 67, and 69 may be combined to give

$$\ell p \frac{dU}{dt} = \frac{3D(U-U_s)}{\ell} \tag{70}$$

which when integrated results in

$$U_{CR} = U_o + \frac{I_c \ell}{3\rho D} \ln\left(\frac{U_{CR}-U_s}{U_o-U_s}\right) \tag{71}$$

where I_c = the constant drying rate $(ML^{-2}\ T^{-1})$

The diffusion coefficient, D, would be expected to depend on the nature of the material and the viscosity of the liquid. Assuming that D varies inversely as the viscosity and using the fact that the variation of viscosity of water is inversely proportional with temperature

$$D = \frac{K}{\nu} = K(a + b\ T_a) \tag{72}$$

where ν = dynamic viscosity $(ML^{-1}T^{-1})$

K = constant (MLT^{-2})

a = constant $(M^{-1}LT)$

b = constant $(M^{-1}LT\theta^{-1})$

T_a = temperature (θ)

Using the dry bulb temperature of the air and substituting for D in Equation 71,

$$U_{CR} = U_o + \left(\frac{\ell}{3\rho K}\right) \frac{(I_c)}{(a+b\ T_a}) \ln \left(\frac{U_{CR}-U_s}{U_o-U_s}\right) \tag{73}$$

The main limitations to Equation 71 are the assumptions of no shrinkage and mechanism of diffusion. The applicability of this to predicting the critical moisture content in water treatment sludge drying is questionable.

Nebiker (26) simplified the above procedure by assuming thickness to be a function of the mass of solids, allowing Equation 71 to be expressed as

$$U_{CR} = f\ (I_c,\ W_{TS}/A) \tag{74}$$

Nebiker also assumed a constant diffusivity and a negligible equilibrium moisture content. For open-air drying of wastewater sludges the following empirical equation was developed from Equation 74:

$$U_{CR} = 500\ (I_c \cdot W_{TS}/A)^{1/2} \tag{75}$$

Values of U_{CR} from Equation 75 when used with Equation 65 gave calculated drying times which compared favorably with actual drying times.

REFERENCES

1. Spangler, M. G. Soil Water. Soil Engineering. 2nd Ed., International Textbook Co., Scranton, PA, 1960, pp. 84-90.

2. Treybal, R. E. Drying. Mass-Transfer Operations. McGraw-Hill Co., New York, 1955, pp. 524-583.

3. McCabe, W. L., and Smith, J. C. Unit Operations of Chemical Engineering, 2nd Ed., McGraw-Hill Co., New York, 1967, pp. 512-515.

4. Coackley, P. and Jones, B. R. S. Interpretation of Results by the Concept of Specific Resistance. Sewage and Industrial Wastes, August, 1956.

5. Eckenfelder, W. A. and O'Connor, D. J. Biological Waste Treatment. Pergamon Press Ltd., New York, 1961.

6. Rich, L. G. Unit Operations of Sanitary Engineering. John Wiley & Sons, Inc., New York, 1961.

7. Eagleson, P. S. Evaporation and Transpiration. Dynamic Hydrology. McGraw-Hill Co., New York, 1970, pp. 211-241.

8. Boelter, L.M.K., *et al*. Free Evaporation into Air of Water from a Free Horizontal Quiet Surface. Industrial and Engineering Chemistry, 38(6), June, 1946.

9. Penman, H. L. Natural Evaporation from Open Water, Bare Soil, and Grass. Proceedings, Royal Society (London), Ser. A, Vol. 193, 1948, pp. 120-145.

10. Kohler, M. A., *et al.* Evaporation from Pans and Lakes. Research Paper No. 38. U.S. Weather Bureau, 1955.

11. Instructions for Climatological Observers. U.S. Department of Commerce, Weather Bureau, Circular B, 10th Ed., Washington, D.C., October, 1955.

12. Kohler, M. A. *et al*. Evaporation Maps for the United States. Technical Paper No. 37, U.S. Department of Commerce, Weather Bureau, Washington, D. C., 1959.

13. Marshall, W. R., and Friedman, S. J. Drying. *Chemical Engineers Handbook,* 3rd ed., J. H. Perry, ed., McGraw-Hill Co., New York, 1950, pp. 799-884.

14. Sherwood, T. K. The Drying of Solids--I. Industrial and Engineering Chemistry, 21(1):12-16, January, 1929.

15. _____. The Drying of Solids--II. Industrial and Engineering Chemistry, 21(10):976-980, October, 1929.

16. _____. The Air Drying of Solids. Transactions, American Institute of Chemical Engineers, 32:150-168, 1936.

17. _____. Application of Theoretical Diffusion Equations to the Drying of Solids. Transactions, American Institute of Chemical Engineers, 27:190-202, 1931.

18. Newman, A. B. The Drying of Porous Solids: Diffusion and Surface Emission Equations. Transactions, American Institute of Chemical Engineers, 27:203-217, 1931.

19. Luikov, A. V. Heat and Mass Transfer in Some Engineering Processes. *Heat and Mass Transfer in Capillary-Porous Bodies*, 1st English ed., Pergamon Press, New York, 1966, pp. 341-376.

20. Carslaw, H. S. and Jaeger, J. C. *Conduction of Heat in Solids*, 2nd ed., Oxford University Press, London, 1959.

21. Crank, J. *The Mathematics of Diffusion*. Oxford University Press, London, 1956.

22. Ozisik, M. N. *Boundary Value Problems of Heat Conduction*. International Textbook Co., Scranton, PA, 1968.

23. Gilliland, E. R. and Sherwood, T. K. The Drying of Solids--VI: Diffusion Equations for the Period of Constant Drying Rate. Industrial and Engineering Chemistry, 25(10):1134-1136, October, 1933.

24. Hougen, D. A., *et al.* Limitations of Diffusion Equations in Drying. Transactions, American Institute of Chemical Engineers, 36:183-209, 1940.

25. Ceaglske, N. H. and Hougen, D. A. The Drying of Granular Solids. Transactions, American Institute of Chemical Engineers, 33:283-312, 1937.

26. Nebiker, J. H. The Drying of Wastewater Sludge in the Open Air. Journal WPCF, 39(4):608-626, April, 1967.

27. Broughton, D. B. The Drying of Solids-- Prediction of Critical Moisture Content. Industrial and Engineering Chemistry, 37(12):1184-1185, December, 1945.

28. Sanders, T. G. A Mathematical Model Describing the Gravity Dewatering of Wastewater Sludge on Sand Drainage Beds. Master's Degree thesis, University of Massachusetts, Amherst, 1968.

29. Nebiker, J. H., et al. An Investigation of Sludge Dewatering Rates. Presented at the 23rd Annual Meeting of the Purdue Industrial Waste Conference, Purdue University, Lafayette, Indiana, May, 1968.

30. Lutin, P. A., et al. Experimental Refinements in the Determination of Specific Resistance and Coefficient of Compressibility. Proceedings, 1st Annual New England Anti-Pollution Conference, University of Rhode Island, Kingston, Rhode Island, 1968.

SECTION V

MATERIALS AND APPARATUS

TYPES OF SLUDGE EXAMINED

Sludge resulting from four different types of water treatment was used for drying and complex dewatering studies. Various wastewater treatment sludges were also used for detailed study of gravity drainage. The four different types of water treatment sludge studied represented the following treatment processes: softening, alum coagulation, alum coagulation with iron removal, and alum collection with activated carbon. A brief description of each plant follows.

Albany. The raw water supply for Albany, New York, consists of two impounding reservoirs, Alcove and Basic, which contain 47.4 and 3.79 million cubic meters (12.5 and 1.0 billion gallons), respectively. The Alcove watershed has an area of 8370 hectares (32.33 square miles) with a flooded area of 580 hectares (1440 acres). The Basic watershed has a drainage area of 4200 hectares (16.37 square miles) with a flooded area of 107 hectares (265 acres). Water from the Basic reservoir passes into the Alcove reservoir by means of a tunnel 975 meters (3200 feet) long. The impounding reservoirs are treated with copper sulfate at times of sudden onset of algal blooms.

The filtration plant in Fuera Bush is of the conventional rapid sand type, with aeration, alum coagulation-flocculation and sedimentation, and filtration followed by chlorination. There is provision for pH stabilization with lime, and taste and odor control with activated carbon, however, the sludge samples collected for this investigation contained only alum. Sludge is stored in sedimentation tanks for approximately 6 months and then discharged to a nearby receiving stream.

Amesbury. The raw water supply for the Town of Amesbury, Massachusetts, is a well field consisting of some 300 shallow wells of 5 to 23 cm (2 to 9 inches) diameter. The raw water contains an abundance of iron and treatment thus consists of aeration; flocculation with alum and caustic soda followed by addition of activated carbon; sedimentation in a manually cleaned basin; filtration through manually cleaned slow sand filters; and chlorination. The sludge is decanted before being discharged twice a year into a nearby lagoon where it dewaters for approximately six months.

Billerica. The raw water for the Billerica, Massachusetts, water treatment plant is the Concord River. Various industrial wastes are discharged into the river causing the water to be very turbid and to promote algal growth. Treatment consists of flocculation with alum and activated carbon, sedimentation in a continuously mechanically cleaned basin, rapid sand filtration, and chlorination. The sludge is discharged daily to a nearby lagoon. The capacity of the lagoon is exceeded by the sludge discharges. The overflowing sludge flows directly into the Concord River.

Murfreesboro. The raw water supply for Murfreesboro, Tennessee, is the East Fork of Stones River. The intake is on the back water from Walter Hill Dam which marks the beginning of Percy Priest Reservoir. The raw water contains a hardness of approximately 67 mg/l. The treatment process includes softening, sedimentation, rapid sand filtration and chlorination. Chemicals added during the treatment process include ferric sulfate, lime, soda ash, and activated carbon. Sludge is continuously transferred from the softening and settling basins to two lagoons. The lagoons are used alternately, each having approximately two years capacity. Supernatant is withdrawn from the lagoons by means of an overflow weir and discharged to the river.

EQUIPMENT FOR THE GRAVITY DRAINAGE STUDY

In order to obtain statistically significant and accurate results,nine columns (Figure 19) were fabricated for the first phase of the research project. The column diameter, not a determining factor in the results as pointed out by previous investigators (1), was 10.2 cm (4.0 in) I.D., large enough to insert a hand but small enough so that only a minimal amount of sludge would be needed for the experiment. The corrosion resistant acrylic columns were 0.6 cm (.25 in) thick and 91.5 cm (36 in) long. Flanges were fastened at each end of the columns, so that acrylic plates could be bolted in place with an O-ring seal to prevent leakage of water and air. Nickel-plated nozzles attached to the plates connected at each end of the column were the only outlets. O-ring seals were also used to prevent leakage from the nozzle connection.

Placed directly below each column were 1000 ml lucite cylinders, graduated to 2 milliliters. A No. 12 rubber stopper with two holes was placed in each graduated cylinder with 0.6 cm (1/4 in) I.D. Tygon tubing connected to a glass tube in the stopper and to the lower nozzle of the column. Tygon tubing was also connected to the top nozzle of the column which ran to another glass tube in the stopper, thus preventing evaporation and maintaining a saturated humidity. No pressure differences could exist in the column and the cylinder, for the filtrate displaced the same volume of air in the graduated cylinder as would be needed by the volume vacated by the filtrate in the column.

EQUIPMENT FOR DRYING, EVAPORATION, AND COMPLEX DEWATERING STUDIES

Two types of containers were used in the drying and evaporation studies. Drying studies utilized glass pans, 0.5 cm (0.2 in) thick. The inside dimensions of the pans were 22 x 35 x 4.5 cm (8.7 x 13.8 x 1.8 in) and

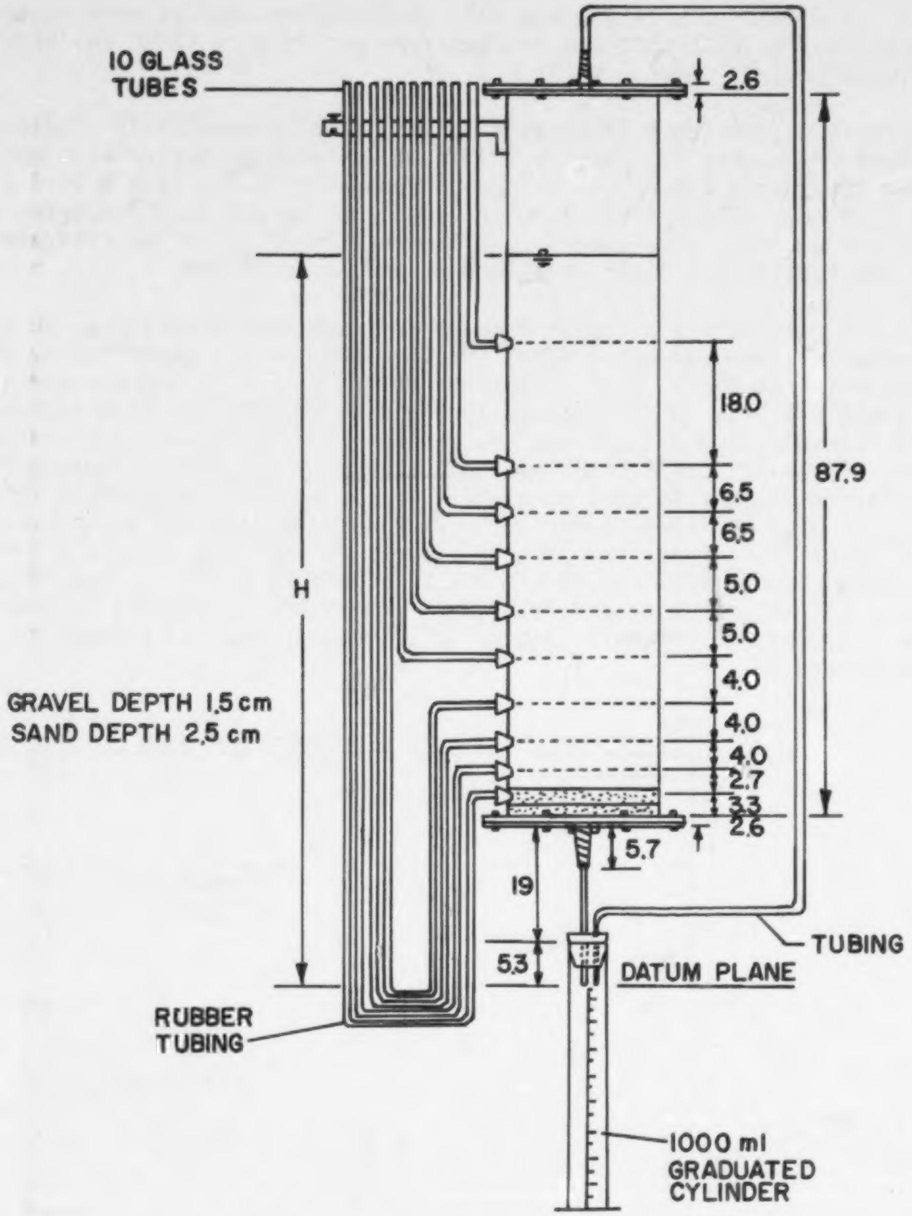

Figure 19. Gravity drainage apparatus with piezometer tubes. The supporting filter media consists of 2.5 cm of sand underlain by approximately 1.5 cm of coarse gravel. The top sand surface lies 30.9 cm above the datum. All dimensions are in centimeters.

19 x 30 x 4.5 cm (7.5 x 11.8 x 1.8 in). Evaporation studies were conducted in plastic pails, 27.5 cm (10.8 in diameter) and 35.5 cm (14.0 in) high (inside dimensions).

Plastic columns were fabricated for the complex dewatering studies. The column walls were 1.3 cm (1/2 in) thick and were connected with machine screws. The inside dimensions of the columns were 12.7 x 12.7 x 91.4 cm (5 x 5 x 36 in). The columns were arranged continuously and supported by a metal stand. This arrangement permitted measurements of the filtrate volume and facilitated other measurements and observations.

In order to maintain constant known environmental conditions, an environmental chamber was constructed and utilized for all evaporation, drying, and dewatering studies. This chamber consisted of a room approximately 4.3 x 4.9 x 3 m (14 x 16 x 10 ft), specially modified to minimize heat and moisture losses. Constant temperature and low relative humidities were maintained by a 31,000 BTU/hr air conditioner with electric heat and reheat capabilities. High relative humidities were maintained by two humidifiers, each with a capacity of 36.4 kg (80 lbs) per day. An electronic control system was capable of maintaining relative humidity between 30 and 80 ± 2 percent and temperature between 18.3 and 29.4 ± 1.1°C (65 and 85 ± 2°F). A continuous record of both temperature and relative humidity was maintained by a wall-mounted recorder. A schematic diagram of the environmental chamber is show in Figure 20.

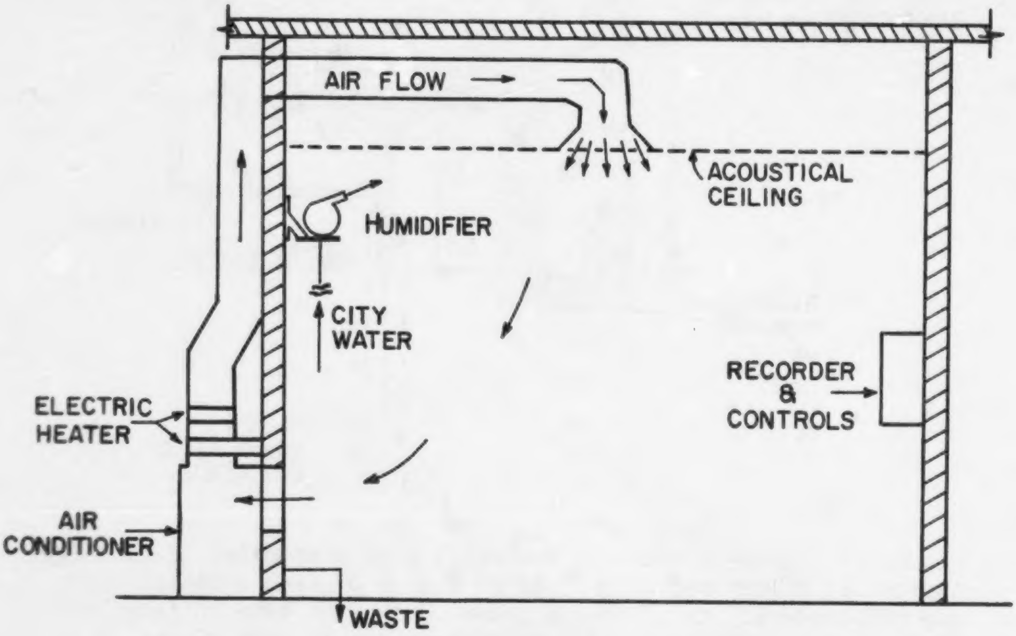

Figure 20. Diagram of environmental chamber.

Some of the drying experiments were conducted with slight wind velocities in order to facilitate drying and enhance air circulation in the tall dewatering columns. Air was provided by a 0.04 cubic meters per minute (1.5 cfm) blower and an 11.4 x 3.8 cm (4-1/2 x 1-1/2 in) duct served as a manifold supply. Equally spaced 1 cm (3/8 in) diameter holes provided a uniform air stream to each column.

MOISTURE MEASUREMENT APPARATUS

The basic equipment for measuring moisture profiles by gamma-ray attenuation included scintillation, detection, and counting equipment; shielding; and auxiliary equipment arranged as shown in Figure 21.

A rigid structural truss assured alignment of the detector with the source beam. All were mounted on a hydraulic fork lift, permitting measurements at any elevation desired. The entire apparatus could be moved forward manually along the support for measurement at the various columns.

In order to assure repetitive measurements at a particular vertical location on a column, machined metal spacers of various thicknesses were placed on the vertical shaft of the hydraulic cylinder of the fork lift. The weight of the apparatus would be supported by the spacers when hydraulic pressure was released, thus fixing the vertical position of the source and detector. A tape measure mounted on the side of the fork lift allowed measurements of the vertical elevation to millimeter accuracy.

Five plastic boxes were fabricated to obtain attenuation coefficient measurements of sludge and water. These boxes were constructed of 1.3 cm (0.5 in) plastic, carefully machined, with all connections made with machine screws. The plastic boxes had inside dimensions of 12.7 x 10.2 cm (5 x 4 in), with widths of 3.8, 7.6, 11.4, 15.2, and 19.1 cm (1.5, 3.0, 4.5, 6.0 and 7.5 in).

SCINTILLATION COUNTING EQUIPMENT

The scintillation counting system included a scintillation-photomultiplier assembly, high voltage supply, voltage stabilizer, linear amplifier, discriminator, and scaler-timer.

A gamma-ray photon, or ionizing event, struck the crystal in the detector and generated photons which caused a flash of light. These photons were reflected by the crystal housing to the photocathode of the photomultiplier tube. The photomultiplier multiplied the initial number of electrons by a factor of about one million and delivered a charge proportional to the radiant energy spent in the scintillator. The preamplifier received the charge from the photomultiplier, gave it added gain, and served as an impedance matching device to assure the maximum transfer of the signal from the detector to the amplifier. The amplifier accepted the voltage input pulse and increased it in a linear manner, thus the relative sizes of the pulses were preserved. A differential discriminator followed the linear amplifier and provided analysis of the pulse height information, sorted out pulses which satisfied the present requirements, and rejected those which did not. The difference in energy levels between the upper limit and the baseline was the window width. The scaler-timer served as the point for all the information from the detector. The timer determined the interval during which pulses from the discriminator were collected. The high voltage supply furnished the required dynode voltages to the photomultiplier tube.

The amplifier, single channel analyzer, and scaler-timer were of the RIDL series, manufactured by Nuclear-Chicago Corporation. The amplifier was a model 30-23. The scaler-timer was a model 49-25. The scaler portion was composed of three cascaded transistorized decades which drove a four-digit mechanical register with a total storage of up to 10^7 counts. The register responded to a maximum input rate of 20,000 pulses per second on a continuous basis. A mechanical timing dial could be set manually for any desired time, and then operated electrically to return its indicators to zero during the elapsed time for which it was set.

The voltage stabilizer, manufactured by the Raytheon Corporation, had an input voltage range of 95-130 volts, with an output voltage of 115 volts. The high voltage supply was of the 2 KV type, manufactured by the Harshaw Company. The scintillator-photomultiplier system, a 5.1 x 5.1 cm (2 in x 2 in) Na(Tl) crystal, also was manufactured by the Harshaw Company. A Baird-Atomic survey meter and Nuclibadge film-badge service provided additional monitoring devices.

Shielding and Collimation

The shielding consisted of a specially constructed lead block for collimating the gamma beam and providing radiation safety to operating personnel. The shielding and scintillation detection equipment were positioned by means of the hydraulic fork lift previously described.

Since the weight of the lead shield was not an important factor, the shielding was designed to reduce the radiation to values only slightly greater than background levels. According to Gardner (2) normal background varies from 0.01 to 0.03 mR (milliroentgen) per hour. One milliroentgen is approximately equal to one millirad (mrad), the unit of physical radiation dose. The dose rate in mrad per hour at a distance z in cm from a point source of gamma radiation at strength A_s in mc (millicuries) is calculated by

$$D.R.(z,z') = 2.134 \times 10^6 \, B(\mu,z) \frac{\mu_a}{\rho} E_o \frac{A_s}{4\pi z^2} \exp(-\mu z') \qquad (76)$$

where D.R. = radiation dose rate (L^2T^{-3})

$B(\mu_a,z)$ = buildup factor

μ_a/ρ = mass-attenuation coefficient $(M^{-1}L^2)$

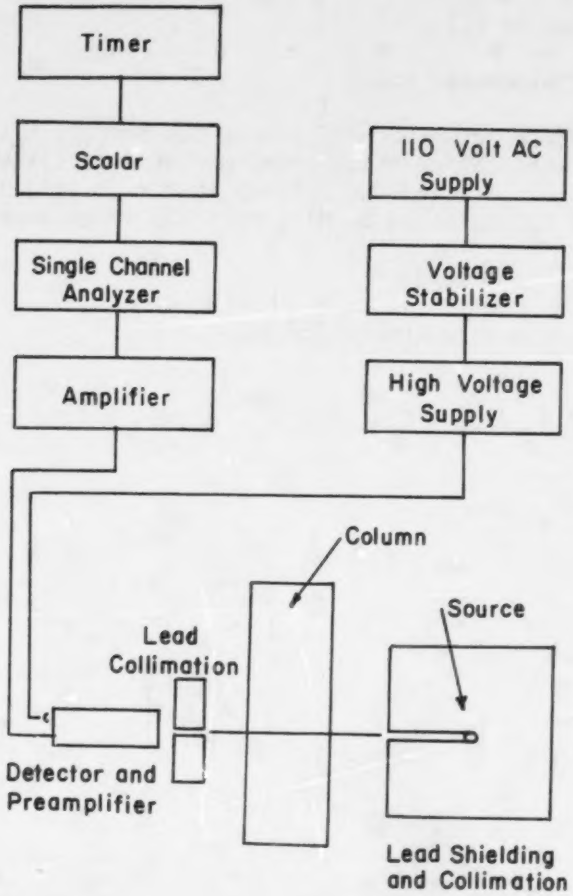

Figure 21. Schematic diagram of gamma-ray attenuation system.

μ = attenuation coefficient ($M^{-1}L^{2}$)

E_o = energy, Mev ($ML^{2}T^{-2}$)

A_s = radiation strength (T^{-1})

z = distance, cm (L)

z' = shield thickness, cm(L)

For gamma radiation from a Cs-137 source the energy, E_o, is primarily 0.661 Mev. The mass attenuation coefficient measured in tissue is about 0.0317 cm^2/gm, μ is 1.134 cm^{-1} and the buildup factor (B ,z') for lead (from 3 to 20 cm thick) is approximated by Blizard's (3) relationship

$$B(\mu, z') = 1.2 + 0.13z' \tag{77}$$

Therefore, the dose rate in mrad/hr is:

$$D.R.(z,z') = (4.27 + 0.463z')10^{3} \frac{A_s}{z^2} \exp(-1.134z') \tag{78}$$

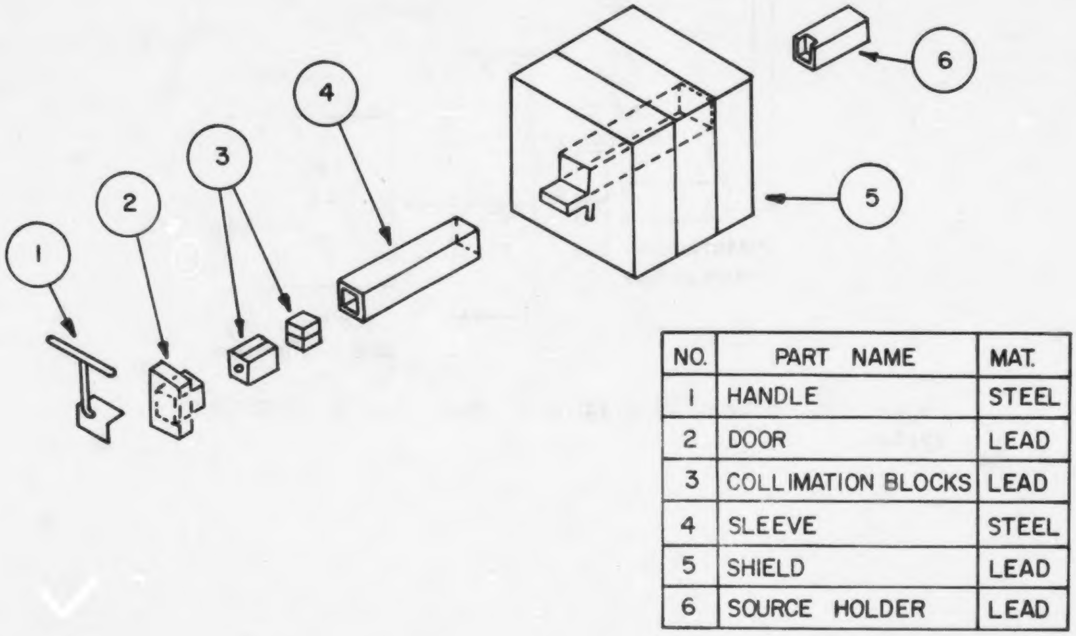

NO.	PART NAME	MAT.
1	HANDLE	STEEL
2	DOOR	LEAD
3	COLLIMATION BLOCKS	LEAD
4	SLEEVE	STEEL
5	SHIELD	LEAD
6	SOURCE HOLDER	LEAD

Figure 22. Diagram of source shielding and collimation.

For the 250-mc Cs-137 source with 14 cm minimum lead thickness, the radiation at the surface was approximately 0.017 mrad/hr, well below normal background values (0.01 to 0.03 mrad/hr). In addition to adequate thickness, care must be exercised in the design to minimize radiation leakage. A diagram of the shielding used in this method is shown in Figure 22. "Good Geometry" conditions are required for successful gamma-ray attenuation measurements. Gamma rays from the source should be collimated so that only a narrow beam strikes the absorber. A collimation slit of 0.1 x 1.9 cm (0.04 x 0.75 inches) provided a narrow beam from the source, and a detector collimation slit of 0.2 x 1.9 cm (0.08 x 0.75 inches) minimized buildup due to scatter.

REFERENCES

1. Quon, J. E. and Tambyln, T. A. Intensity of Radiation and Rate of Sludge Drying. Journal of the Sanitary Engineering Division, ASCE, 91, No. SA2, April, 1965.

2. Gardner, W. H. Water Content. Methods of Soil Analysis: Part 1, C. A.Black, ed., Academic Press, Madison, Wisconsin, 1965, pp. 82-127.

3. Blizard, E. P. Nuclear Radiation Shielding. Nuclear Engineering Handbook, H. Etherington, ed., McGraw-Hill Co., New York, 1958.

SECTION VI

METHODOLOGY

A number of sludge related characteristics were measured in this investigation. Chemical analyses were performed on sludge, decant, and filtrate samples. Dewatering studies required measurement of gravity drainage rates, evaporation rates of water, drying rates of thin layers of sludge, drying rates of thick layers of sludge on sand, and dewatering (drying plus drainage) rates of sludge on sand. All studies were conducted in the environmental chamber under controlled temperature, relative humidity, and wind conditions.

Moisture profile studies required refinements in the gamma-ray attenuation method and determination of required physical parameters. These parameters were attenuation coefficients of dry sand, dry sludge solids and water as well as particle densities of the sand and sludge.

SLUDGE CHARACTERISTICS

Representative sludge samples were used to determine chemical characteristics of the sludge, decant, and filtrate. Physical properties such as total solids, particle density and specific resistance were determined for each individual study. Samples of the clear supernatant which resulted from sedimentation were taken as representative decant samples. Filtrate samples were collected during the drainage studies. The filtrate had passed through 9.0 cm of Ottawa sand. Unless otherwise specified, all analyses were performed according to Standard Methods (1) and FWPCA Methods for Chemical Analysis of Water and Wastes (2). In some cases standard procedures were not available and it was necessary to develop suitable methods of analysis. Six separate experiments were undertaken for which the average value of triplicate analyses is reported.

Solids analyses were determined by heating the samples for 8 hours at 103°C to determine total solids and 20 minutes at 600°C to determine total volatile solids. Experimental determination of specific resistance and coefficient of compressibility is presented in detail.

GRAVITY DRAINAGE STUDY

In order to demonstrate that the drainage rate of sludge on a sand bed is a function of specific resistance, coefficient of compressibility, initial solids content, and initial head, interference from outside factors which affect the rate of moisture removal but which are unrelated to gravity drainage had to be eliminated. These factors include evaporation and flotation.

Evaporation, if not eliminated, would reduce the moisture of the sludge at some unknown rate so that determination of head from the volume of filtrate collected would be impossible. Therefore, the experimental apparatus was designed as a closed system to prevent the entrance or exit of moisture.

Each column was initially calibrated with water by noting the time required for the water surface elevation to drop from 110 cm (43 in) to 30 cm (11.8 in). Minor adjustments were made until the time deviation between columns was 1.9 percent. Addition of the sand, gravel, and the chromel 16 mesh (24 B&S gage) wire screen decreased discharge rates in each column equally. Total drainage time using water was approximately 2 minutes, hence, permeability of the supporting media was so large relative to the permeability of the sludge that it could be disregarded in the computations.

It is important to note that the effective drainage head was the distance from the upper sludge surface to the tip of the discharge tube. The distance from the discharge tube to the sand surface approximated the standard design depths for sand in a drying bed. The additional head created is thought realistically to approach the operation of properly constructed drying beds in which, as the sand becomes rapidly saturated, a vacuum tends to form on the bottom of the sludge-sand interface, as was created also by the discharge system of the experimental columns.

Three different sands were utilized for the experiments. To provide a basis for later corroboration by other researchers, A.S.T.M. Standard Ottawa sand was used. To develop information of practical value, sands from drying beds of two treatment plants (Hermitage Hills, and Franklin,Tennessee) were tested. These sands were coded as types O, H, and F, and were sieve analyzed.

Prior to each of the six experiments, all equipment including the acrylic columns, graduated cylinders, and Tygon tubing was thoroughly washed and rinsed with distilled water to avoid the possible problem of biological or chemical contamination. Furthermore, all sand and gravel used in previous experiments was replaced with clean material. Lastly, to prevent impedance of flow due to the presence of air pockets, sand in the column was saturated with distilled water before addition of sludge.

Experiments I-III were designed to test a settled sludge condition. Sludges were introduced to the columns with an additional depth of supernatant applied, thus providing a greater potential filtrate volume, and, in essence, simulating conditions in a lagoon.

Experiments IV-VI used a homogeneous charge of sludge without an applied supernatant. All nine columns of Experiment IV had an initial head of 54 cm, with Franklin, Ottawa, and Hermitage sands used as the supporting media in columns 1-3, 4-6, and 7-9, respectively. In Experiment V, Franklin sand was again the supporting media for columns 1, 2, and 3; Ottawa sand for columns 4, 5, and 6; and Hermitage sand for columns 7, 8, and 9. However, the initial head varied--44 cm for columns 1, 4, and 7; 74 cm for columns 2, 5, and 8; and 114 cm for columns 3, 6, and 9.

Once all nine columns were brought up to the proper head, the stoppers were released so that drainage could begin. *During the course of the six* experiments the volume of filtrate drained from the sludge in each column was measured and recorded three times daily. The length of each experiment varied from 20 to 57 days depending upon the time required for the drainage of filtrate to cease in the majority of the columns and leave a dewatered sludge cake.

For Experiment VI, only one column was used. Nine piezometer tubes were placed along the length of the column so that the pressure at different depths of sludge could be studied. To prevent the sludge from clogging the piezometer tubes, the column was filled with distilled water, thereby filling the piezometer tubes. The tubes were stoppered, causing the distilled water to remain in them after the column had been emptied. Sludge was then poured into the column after which the stoppers on the piezometer tubes were released. The initial head was 96 cm.

EVAPORATION AND DRYING STUDIES

1 establish a control, evaporation studies were conducted to determine evaporation rates from free water surfaces. Cylindrical plastic pails 27.5 cm (10.8 in) diameter and 35.5 cm (14 in) high (inside dimensions) were filled with water at depths of 9.6, 19.3, and 29.1 cm (3.8, 7.6 and 11.5 in). The pails were placed at three locations within the environmental chamber. The mass of containers plus water was determined to the nearest gram on a triple-beam balance at intervals of approximately 1.5 days.

Since a plot of mass of water versus time is linear for constant drying conditions, the slope is equal to the drying rate (MT^{-1}). This allows comparison of drying rates using the method of comparison of regression lines. The procedure utilized was taken from Hald (3). Straight lines were fitted to the data by linear regression analysis. The hypothesis that the theoretical variances of the two populations are equal was tested by means of the variance ratio. If the test did not reveal a significant difference between the two variances, the slopes of the two regression lines were compared by means of a t-test of $f = N_1 + N_2 - 4$ degrees of freedom, such that

$$\tau = \frac{\beta_1 - \beta_2}{S} \Big/ \left[\frac{1}{SSD_{x_1}} + \frac{1}{SSD_{x_2}}\right]^{1/2} \qquad (79)$$

where $SSD_{t_i} = \Sigma N(t_i - \overline{t})^2$

β = slope (80)

If τ exceeded the significance limit the test hypothesis was rejected and the two lines were considered to have different slopes.

If τ was not significant the two regression lines were considered parallel. A common estimate of the slope β was obtained by forming the weighted mean of the two slopes β_1 and β_2, using the reciprocal values of the variances as

$$\beta = \frac{SPD_{t_1w_1} + SPD_{t_2w_2}}{SSD_{t_1} + SSD_{t_2}} \tag{81}$$

where $$SPD_{t_1w_1} = \Sigma(t_i-t)\ (w_i-\bar{w}) \tag{82}$$

and $$\bar{t} = \frac{1}{N}\ \Sigma t_i \tag{83}$$

An analysis of variance was also performed which considered average evaporation rates as variables.

Two methods were considered in the data analyses of water treatment sludge drying studies. The first method consisted of taking the derivative of the sludge mass-time data. Various relationships were then fitted to certain portions of the data. The second method considered the sludge mass-time curve only.

The first method is the traditional one for analyzing drying data in environmental and chemical engineering equations. The equation for obtaining the derivative of a function W = f(t) for unequal spacing of the independent variable t, as given by Salvadori and Baron (4) may be written:

$$\frac{dW}{dt}\,(t_n) = \frac{1}{a(a+1)h}\,[W_{n+1} - (1-a^2)W_n - a^2W_{n-1}] \tag{84}$$

where a is the ratio between the spacings of the three points t_{n-1}, t_n, t_{n+1} written as:

$$a = (t_{n+1} - t_n)/(t_n-t_{n-1}) \tag{85}$$

and

$$h = t_{n+1} = t_n \tag{86}$$

Moisture content may be obtained from the relationship

$$U = (\frac{W-W_{TS}}{W_{TS}})100 = 100(\frac{W}{W_{TS}} - 1) \tag{87}$$

where W_{TS} = mass of sludge solids (M).

The evaporation ratio E, in percent, is defined as the rate of evaporation of sludge divided by the rate of evaporation of water. The shape of the drying rate curve and the rate of change of moisture content curve are the same since

$$I = \frac{W_{TS}}{100A} \frac{dU}{dt} \qquad (88)$$

when W_{TS} and A are assumed constant.

It is known from theory that a constant-rate drying period should occur under certain conditions. Thus the mass of water, W_w, is a direct function of time,

$$\frac{dW_w}{dt} = \frac{d(W-W_{TS})}{dt} = B(\text{constant}) \qquad (89)$$

The mass versus time curve is therefore the integral of Equation 89 or a straight line of the form

$$W_w = A + Bt \qquad (90)$$

In some cases the falling rate portion of the drying curve has been shown to be approximately linear in the form

$$\frac{dW_w}{dt} = D + Et \qquad (91)$$

Equation 91 indicates that the weight-time curve for the falling-rate portion should be of the form

$$\int dW_w = \int (D+Et)dt \qquad (92)$$

therefore

$$W_w = C + Dt + Et^2 \qquad (93)$$

Statistical analyses of the constant-rate portions of the curves were conducted by the same procedure used for the evaporation studies.

COMPLEX SLUDGE DEWATERING STUDIES

The primary methodology for complex sludge dewatering studies was to determine the amount of water lost by gravity drainage, the solids content at the end of drainage, and the solids content at the end of dewatering (drainage plus drying).

All dewatering studies were conducted in plastic columns supported by a metal frame. Temperature and relative humidity were carefully controlled during the experiments. All sludges were dewatered on an 8.9 cm (3.5 in) layer of saturated Ottawa sand, supported by a 2.5 cm (1 in) layer of washed stone. Each sludge was thoroughly mixed in large quantities in a 115 liter

(30 gallon) capacity concrete mixer for a minimum of 20 minutes. The sludge was carefully placed in the columns by means of a specially constructed splash rod which prevented damage to the sand bed while charging the columns. (Aliquot samples were taken simultaneously for laboratory analyses). Initial mass of container (tare), tare plus mass of dry sand, and tare plus mass of saturated sand were recorded. Sludge surface elevations, volume of filtrate, and mass of sludge were recorded at various intervals. The sludge mass and time were both recorded when drainage stopped. Samples of the filtrate were taken for chemical analyses after drainage had continued for some time. This insured a more representative sample since the sand and other media were previously saturated with distilled water.

The columns were permitted to drain throughout the entire dewatering study. The total filtrate collected when drainage ceased consisted of water drained from the sludge and the distilled water used to saturate the sand beds initially. The procedure for calculating the solids content at the end of drainage was as follows: the percentage of the total filtrate which came from the sludge (excluding the water to saturate the support media) was determined from

$$V_f = 100(1-V/V_t) \tag{94}$$

where V_f = volume of filtrate (L^3)
V = volume of distilled water (L^3)
V_t = total volume collected (L^3)

The corresponding drainage time for V_f was then determined from the cumulative filtrate-time curve and the corresponding sludge mass was determined from the sludge mass-time curve. The solids content at the end of sludge drainage was calculated as the mass of total solids (previously determined) to the total sludge mass.

MOISTURE PROFILE

Gamma-ray attenuation techniques have been used widely to follow the rapid water content change in soil columns undergoing wetting (5,6,7,8). More recently, this method was used by Tang (9) to determine moisture profiles in sewage sludges. Because gamma-ray attenuation provides a convenient, rapid, non-destructive method for repeatedly measuring the solids or moisture content of sludges, it was selected for determining in situ the solids and moisture profiles in columns of water treatment sludge undergoing dewatering.

Attenuation Equations. Evans (10) relates the intensity of monoenergetic gamma rays after passing through several layers of material to their incident intensity:

$$N = N_0 \exp(-\Sigma\ \mu_i\ \rho_i\ L_i) \tag{95}$$

where N = intensity of transmitted beam (dimensionless)

N_o = intensity of incident beam (dimensionless)

μ_i = attenuation coefficient of material i ($M^{-1}L^2$)

ρ_i = density of material i (ML^{-3})

L_i = thickness of material i (L)

As an example, consider a plastic column which contains sludge and is subjected to a monoenergetic beam of gamma rays as shown in Figure 23. The gamma ray beam traverses the two column walls, each of thickness L_p, and the sludge of thickness L_s. The applicable attenuation relation is

$$N = N_o \exp - (2 \mu_p\rho_pL_p + \mu_s\rho_sL_s) \tag{96}$$

where μ_p = attenuation coefficient of plastic ($M^{-1}L^2$)

ρ_p = density of plastic (ML^{-3})

μ_s = attenuation coefficient of sludge ($M^{-1}L^2$)

ρ_s = density of sludge (ML^{-3}).

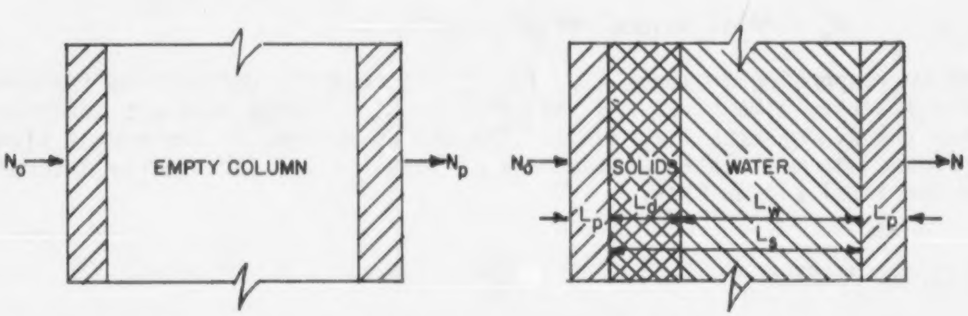

Figure 23: Attenuation relations used in moisture profile measurements.

Since sludge consists of water and solids, Equation 96 can be expanded to

$$N = N_o \exp -(2\mu_p\rho_pL_p + \mu_w\rho_wL_w + \mu_d\rho_dL_d) \tag{97}$$

where the subscripts p, w, and d refer to plastic, water and solids, respectively. Attenuation of the plastic is described by the equation

$$N_p = N_o \exp (-2\mu_p\rho_pL_p) \tag{98}$$

where N_p = intensity of beam transmitted through plastic ($M^oL^oT^o$)

Division of Equation 97 by Equation 98 results in a simplified form:

$$N = N_p \exp - (\mu_w \rho_w L_w + \mu_d \rho_d L_d) \tag{99}$$

Adrian (11) showed that a relationship between L_w, L_d, L_S, and the water content, w, can be derived from the basic relationship

$$L_s = L_w + L_d \tag{100}$$

and the definition of solids content

$$\frac{S}{100} = \frac{W_{TS}}{W_w + W_{TS}} = \frac{\rho_d \cdot V_d}{\rho_w V_w + \rho_d V_d} \tag{101}$$

where S = percent solids content (dimensionless)

W_{TS} = mass of solids (M)

W_w = mass of water (M)

V_d = volume of solids (L^3)

V_w = volume of water (L^3).

Solving Equation 101 for V_d results in

$$V_d = \frac{S \rho_w V_w}{100 \rho_d (1 - S/100)} \tag{102}$$

The respective volumes are related by Area A and Equation 100, by the relation

$$V_T = AL_s = A(L_w + L_d) = V_w + V_d \tag{103}$$

so the distance through the water may be expressed as

$$L_w = L_s \left[\frac{\rho_d (1 - S/100)}{(S/100)\rho_w + \rho_d (1-S/100)}\right] \tag{104}$$

The distance through the solids becomes

$$L_d = L_s \left[\frac{(S/100\rho_w)}{(S/100)\rho_w + \rho_d (1-S/100)}\right] \tag{105}$$

The distance L_s can be readily measured. Therefore, a combination of Equations 102, 104, and 105 are related to the counting measurements N and N_p through the equation

$$N = N_p \exp\left\{ - \rho_d \rho_w L_s \left[\frac{\mu_w - S/100\ (\mu_d - \rho_w)}{\rho_d + S/100\ (\rho_w - \rho_d)}\right]\right\} \qquad (106)$$

Equation 106 can be rearranged as

$$\frac{S}{100} = \frac{\rho_d[\mu_w \rho_w L_s - \ln\ (N_p/N)]}{(\rho_w - \rho_d)\ \ln\ (N_p/N) + \rho_w \rho_d L_s (\mu_w - \mu_d)} \qquad (107)$$

and since moisture content

$$U = 100(\frac{100}{S} - 1) \qquad (108)$$

Equation 107 may be expressed in terms of moisture content as

$$\frac{U}{100} = [\frac{(\rho_w - \rho_d)\ \ln\ (\frac{N_p}{N}) + \rho_w \rho_d L_s (\mu_w - \mu_d)}{\rho_d\ (\mu_w \rho_w L_s\ -\ \ln\ (N_p/N))}] -1.0 \qquad (109)$$

Equations 107 and 109 were the equations used for moisture profile measurements in this investigation. Attenuation coefficients were determined by measuring the attenuation of gamma-rays through small plastic boxes filled with water or dry solids. The particle density of sludge solids was measured by standard soil testing procedures for specific gravity. Specific gravity, the ratio of the unit weight of solid per unit weight of water at 4°C, is numerically equal to density in the cgs system. Values for the density of water were taken from reference tables.

Radiation Counting. The radioisotope source emitted a complete energy spectrum rather than monoenergetic gamma rays assumed for the attenuation theory. Therefore a differential discriminator was used to permit measurements over a narrow energy range. The advantages and disadvantages of using a Cs-137 source for attenuation studies have been discussed by Van Bavel et al.(12). The long half life (30 yr) of Cs-137 eliminates any need for compensating for radioactive decay. The cesium spectrum with the well defined peak at 0.661 Mev facilitated attenuation measurements. The base-line discriminator was calibrated to read directly in kilo electron volts (kev) using the procedure outlined by Chase and Rabinowitz (13). Thus the channel number corresponded directly with energy. For this investigation width was set to accept gamma radiation of 0.661 ± 0.13 Mev.

The average number of radiation counts for a given time interval must be known. An estimate of the average true number of counts was obtained from single observations of the number of counts, N, in a given time period, t. Since the radioactive decay process is a Poisson distribution, Kohl et al. (14) gives the standard deviation as

$$\sigma(N) \cong (N)^{1/2} \qquad (110)$$

The relative standard deviation, R.S.D. is defined as

$$\text{R.S.D.} = \frac{\sigma(N)}{N} = \frac{(N)^{1/2}}{N} = \frac{1}{(N)^{1/2}} \qquad (111)$$

Since the number of observed counts depends on the counting interval, the R.S.D. can be decreased by extending the counting time.

The counting rate observed during a time t was defined as

$$n = \frac{N}{t} \qquad (112)$$

where n = counting rate (T^{-1})

Excluding errors in the measurement of time t, the standard deviation of the counting rate would be

$$\sigma(n) = \frac{\sigma(N)}{t} \cong \frac{(N)^{1/2}}{t} = \frac{(nt)^{1/2}}{t} = \left(\frac{n}{t}\right)^{1/2} \qquad (113)$$

A counting time of 16 minutes was chosen for this study and provided a standard deviation of $(n)^{1/2}/4$ for the counting rate. To reduce the standard deviation by half, i.e., to $(n)^{1/2}/8$, would have required a counting time of 64 minutes.

The radioactivity detection instruments have finite resolving times within which two occurring events may be distinguished and recorded separately. Thus some counts are missed; the fraction lost increases with increasing counting rate. A coincidence correction allows the mean number of counts occurring to be calculated by the method given by Kohl et al. (14) as

$$n_o = \frac{n}{1 - nt_r} \qquad (114)$$

where n_o = mean count rate occurring (T^{-1})

n = mean count rate recorded (T^{-1})

t_r = resolving time (T)

The number of lost counts is

$$n_o - n = n\, n_o\, t_r \qquad (115)$$

and

$$n_{max} \rightarrow 1/t_r \qquad (116)$$

All count rates in this investigation were corrected for coincidence losses using the previous equations and the published value for the counting equipment of $t_r = 1\mu$ sec.

Attenuation Coefficient Measurements. Values for the attenuation coefficients for water and dry solids are needed in the gamma-ray attenuation equations. The basic attenuation equation as used by Davidson et al. (6) can be written as

$$N = N_p \exp [- (\mu_d \rho_b + \mu_w \theta) L] \tag{117}$$

where ρ_b = bulk density of the dry material (ML^{-3})

θ = water content (ML^{-3})

L = thickness of sample (L).

For distilled water, Equation 117 reduces to

$$N = N_p \exp (-\mu_w \rho_w L) \tag{118}$$

where ρ_w = density of water (ML^{-3})

Equation 118 can be written as

$$\ln N/N_p = -\mu_w \rho_w L \tag{119}$$

or in linear fashion

$$Y = BX \tag{120}$$

where $Y = \ln(N/N_p)$

$B = -\mu_w$

$X = \rho_w L = L$

since the density of water in the cgs system is approximately 1.0.

Plastic boxes of various thicknesses were used for making several measurements of Y. The term B was found by regression analysis for a line passing through the origin (15):

$$B = \frac{\Sigma X_i Y_i}{\Sigma X_i^2} \tag{121}$$

the variance

$$\sigma^2 = \frac{1}{N-1} \Sigma (Y_i - BX_i)^2 \tag{122}$$

and the correlation coefficient r from

$$r = \frac{\Sigma X_i Y_i}{(\Sigma X_i^2 \Sigma Y_i^2)^{1/2}} \tag{123}$$

Attenuation coefficients for dry sludge solids or dry sand required measuring the attenuation of the dry material for a constant thickness at various bulk densities. To this end the sludges were slowly dried on a water bath, pulverized with a mortar and pestle, placed in uniform layers, and compacted by shaking or with a standard number of strokes with a blunt instrument. The bulk density was the weight of material divided by the volume of the box. Counting times for both the dry material and the empty box were 16 minutes, with counts taken at various locations.

Particle Density. Particle density measurements were made on all sludges studied as well as the Ottawa sand used for drainage media. Particle density, the mass of solid per unit volume, is numerically equivalent to the specific gravity of a soil, and is defined by Lambe (16) as the ratio of the weight in air of a given volume of soil particles to the weight in air of an equal volume of distilled water at 4°C. The specific gravities of the sludges were determined using laboratory procedures presented by Lambe (16).

Moisture Profile Determinations. The moisture profiles of both sludge and supporting sand layers were determined periodically during the dewatering studies. Equations 107 and 109 were used to obtain moisture or solids profiles in the sludge layers. The method for determining the moisture content of the sand was identical to that of sludge, however, the amount of water in the sand was calculated differently, because when water left the sand layer the pores were filled with air, changing the effective thickness of the sample. Equation 107 and 109 were thus not valid for drying sand since the derivation assumed the entire sample to be either solid or water. Equation 117 was used to determine the water content of sand.

DIFFUSION

Measurements of the diffusion coefficient were made in order to determine the applicability of the diffusion model to water treatment sludge drying. Recent work in the soil sciences examining moisture movement in soils found the diffusion coefficient to be a function of the moisture content. Covey (17) and Wakabayashi (18,19) reported experimental values for D(U) for soils.

Where D is a function of U only, Boltzman (20) has shown that if $U=U(\eta)$, where $\eta = xt^{-1/2}$, the concentration dependent diffusion equation

$$\frac{\partial U}{\partial t} = \frac{\partial}{\partial x}\left[D(U)\,\frac{\partial U}{\partial x}\right] \tag{124}$$

can be written as an ordinary nonlinear differential equation

$$\frac{d^2U}{d\eta^2} + \frac{\eta}{2D(U)}\,\frac{dU}{d\eta} + \frac{1}{D(U)}\,\frac{dD(U)}{dU}\left(\frac{dU}{d\eta}\right)^2 = 0 \tag{125}$$

The initial and boundary conditions for Equation (124)

$$U\,(x,0) = U_1;\quad U(0,t) = U_s \text{ and } U\,(\infty,t) = U_1 \tag{126}$$

Reproduced from best available copy.

transform to two conditions for Equation 125

$$U(0) = U_s \text{ and } U(\infty) = U_i \tag{127}$$

Equation 125 may be written as

$$\frac{d}{d\eta}\left[D(U)\frac{dU}{d\eta}\right] = -\frac{\eta}{2}\frac{dU}{d\eta} \tag{128}$$

and upon integration, rearranged as

$$D(U)_x = -\frac{1}{2t}\left(\frac{dx}{dU}\right)_{U_x}\int_{U_i}^{U_x} x\,dU \tag{129}$$

Obtaining D(U) requires measurements of U vs. X for t constant, or nearly constant. These measurements must be made experimentally by determining the moisture content along a column containing drying sludge.

After evaluating the variation of the diffusion coefficient with moisture content and using the proper boundary conditions the basic diffusion equation, Equation 124, can be solved for U at any time t by numerical techniques. This also permits calculation of the time required to dry the material to any desired moisture content.

DISCUSSION OF THE METHOD

In order to obtain reliable results for both specific resistance and the coefficient of compressibility, computer handling of data was employed whenever possible. One aspect, however, which is hardly applicable to computer techniques is human variation in basic specific resistance testing.

Although Swanwick and Davidson (21) noted very high replicability in their experimentation, a series of tests was devised to measure the reproducibility of results on the newly designed equipment and techniques being employed. Triplicate specific resistance tests were performed on the same sludge, at each of three different pressures in a constant temperature room. The elapsed time from the beginning of the first test to the end of the last was held to an absolute minimum.

The results as shown in Figure 24 are indeed gratifying because in addition to corroborating the work of Swanwick and Davidson (21) the reliability of past and future testing with later generation equipment and techniques has been substantiated.

Swanwick et al. (21) have proposed several refinements to the testing methods. Of primary concern was the determination of the filter area of a Buchner funnel. It was reasoned that the entire filter paper area was not the effective filter area because of the relatively wide spacing of the drain holes in the filter paper support plate of the funnel. Swanwick noted that the filter area appears as a squared term in the evaluation of specific resistance, and hence a faulty evaluation of area could lead to a significant

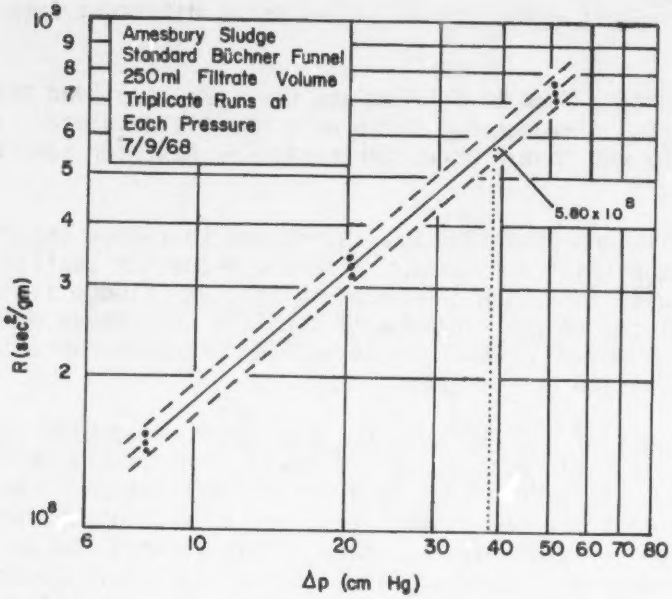

σ	Correlation Coefficient	Std. Error of Computed R
0.87401	0.99880	0.03436

Pressure (cm Hg)	Computed R (sec^2/gm)	95% Confidence Limits	
		Upper	Lower
50.8	7.44×10^8	7.97×10^8	6.95×10^8
20.0	3.30×10^8	3.53×10^8	3.08×10^8
8.0	1.48×10^8	1.59×10^8	1.38×10^8

Legend

——— Regression Line
------ 95% Confidence Limits

Figure 24: Results obtained from triplicate specific resistance tests at each of a range of pressures. (Performed with the same sludge sample at constant temperature.)

error. He corrected the apparatus by placing a gauze wire mesh between the paper and plate and delineating the filter area using Perspex rings clamped onto the filter paper. However, no difference in results was found using this arrangement over the previous method. However, Swanwick did notice a difference in specific resistance values using different types of filter paper.

The consulting firm of O'Brien and Gere (22) modified the testing procedure by placing diatomaceous earth onto the filter plate. The reasoning here apparently was that a more representative test for sand bed drainage could be made.

Baskerville and Gale (23) have attempted to reduce the time required to determine specific resistance. A simple automatic capillary suction apparatus is used for which the readings indicate sludge filterability. These readings can be correlated with specific resistance units. However, accuracy was apparently low, and no method for coefficient of compressibility determination was included.

The approach of O'Brien and Gere (22) appears to have considerable merit for measuring specific resistance and coefficient of compressibility of sludges to be gravity drained. Nebiker, Sanders, and Adrian (24) noted that the classic Buchner funnel results required a correlation factor for use with their gravity dewatering equation. This factor, the so-called media factor, approximated 75 percent, and depended on the characteristics of the filter in the Buchner funnel test, and on the characteristics of the supporting media used in gravity dewatering. A closer analysis of the media factor appeared justified. A promising procedure would be to test the actual drainage media along with the sludge in the Buchner funnel apparatus. This may then allow elimination of the media factor in the computations required to predict gravity dewatering rates.

The results of preliminary filtrations made through the standard funnel with a dilute slurry of sludge indicated a concentration of solids on the filter paper around each individual perforation in the filter disk. Since, as previously described, this was not a true representation of gravity thickening, alternative filtration equipment was sought. A simple solution was found by substituting for a perforated filter disk a fritted glass disk which allows filtration across the entire filter surface, thus eliminating the localized phenomenon observed in the standard funnel (25). An additional advantage of the fritted funnel is the transparency of the filter walls which allows observation of the entire filtration process.

In the technique employed in specific resistance testing on bulk filter media the fritted funnel is filled to a predetermined depth with media. The sand is then washed, repacked, and flooded with sludge. A vacuum is then applied to the system. With a coarse media such as Ottawa sand, there is likely to be some penetration of sludge into the media at higher vacuums. The sand depth is experimentally adjusted to insure against sludge penetration through the filter disk.

DISCUSSION OF THE RESULTS

Units

As pointed out by Swanwick and Davidson (21), early investigators reported specific resistance in units of sec^2/gm. These units resulted from interpreting pressure in units of gm/cm rather than $dynes/cm^2$. The laboratory data presented in Table 1 is in a form for ready comparison to results reported by previous investigators. These units are dimensionally correct when considering c as the WEIGHT of sludge solids per unit volume of filtrate (rather than the MASS of sludge solids per unit volume of filtrate). Simple multiplication of specific resistance (in sec^2/gm) by g (980 cm/sec^2) results in units of cm/gm and implies that c is considered as the mass of sludge solids per unit volume of filtrate.

The laboratory data of specific resistance and coefficient of compressibility obtained for various sludges are compared with the data published by other authors in Table 1.

Specific Resistance

It is evident from the laboratory data and the results from O'Brien and Gere (22) presented in Table 1 that for the most part water treatment sludges have lower specific resistance values than wastewater sludges. The water treatment sludges tested were homogeneous, inorganic, and devoid of filamentous binders.

The specific resistances of the pulp and paper activated sludge (2 percent $FeCl_3$) reported by O'Brien and Gere (22) point out the fact that chemical conditioning may be of significant value in lessening the resistance of sludge to filtration.

Although the water treatment sludges tested resulted in a wide range of values for specific resistance, they were all within one order of magnitude. The specific resistances of Billerica and Lawrence sludges determined using 100 ml filter samples compare favorably with those obtained using 250 ml filter samples.

Coefficient of Compressibility

O'Brien and Gere (22) do not report values for the coefficients of compressibility of water treatment sludges tested, so no comparable data are available with which to compare values obtained with Massachusetts water treatment sludges. Somewhat higher coefficients of compressibility were obtained for the water treatment sludges than are cited in the literature for wastewater sludges. This indicates that water treatment sludges produce a more compressible cake than wastewater sludges.

Sludge Conditioning

Efforts to improve gravity dewatering by conditioning date back over half a century. Alum, ferric salts, and lime all had been used to accelerate dewatering rates of what was then solely primary sludge. Ferric salts were reported to oxidize and clog the sand beds. The most successful conditioner,

TABLE 1. PROPERTIES OF WATER TREATMENT AND WASTEWATER SLUDGES

Sludge	Solids Content %	Sample Volume (ml)	Coefficient of Compressibility	R @ ΔP = 38.1 cm Hg (sec^2/gm)	Reference
Digested Wastewater	15.0	NA	0.63	23.8×10^9	Coackley (29)
Digested Wastewater	15.0	NA	0.56	18.7×10^9	Coackley (29)
Digested Wastewater	4.9	NA	0.76	4.07×10^9	Niemitz (30)
Raw Wastewater	NA	NA	0.54	4.70×10^9	Eckenfelder & O'Connor (31)
Pulp & Paper Activated Sludge 2% $FeCl_3$	NA	NA	0.80	0.165×10^9	Eckenfelder & O'Connor (31)
Digested Wastewater	6.35	100	0.51	72.4×10^9	Nebiker, Sanders, & Adrian (24)
Digested Wastewater	4.89	100	0.74	14.0×10^9	Nebiker, Sanders, & Adrian (24)
Digested Wastewater	3.70	100	0.66	48.0×10^9	Nebiker, Sanders, & Adrian (24)
Water Treatment 3.0 mg/l Lime	1.00	NA	NA	0.098×10^9	O'Brien & Gere (22)
Water Treatment 2.0 mg/l Lime	1.00	NA	NA	1.29×10^9	O'Brien and Gere (22)

TABLE 1. PROPERTIES OF WATER TREATMENT AND WASTEWATER SLUDGES (continued)

Sludge	Solids Content %	Sample Volume (ml)	Coefficient of Compressibility	R @ ΔP = 38.1 cm Hg (sec^2/gm)	Reference
Water Treatment	1.00	NA	NA	1.85×10^9	O'Brien & Gere (22)
Water Treatment Billerica (x)	4.65	100	1.21	2.49×10^9	Laboratory Data
Water Treatment Lawrence (y)	0.944	100	1.02	10.4×10^9	Laboratory Data
Water Treatment Lowell (z)	3.81	100	0.886	4.23×10^9	Laboratory Data
Water Treatment Amesbury	2.06	250	0.802	1.04×10^9	Laboratory Data
Water Treatment Billerica	4.65	250	0.831	3.48×10^9	Laboratory Data
Water Treatment Lawrence	0.944	250	1.32	9.85×10^9	Laboratory Data

x = average of 3 sets

y = average of 5 sets

z = average of 4 sets

alum, in addition to providing larger floc, hence larger pores and easier paths of egress for the filtrate, provided additional flotation by production of carbon dioxide (26).

The effect of conditioning on drainage was noted most vividly by Templeton (27). Here aluminum chlorohydrate was added to one sample at a dosage of 10 percent based on dry solids. During the first ten days, the treated sludge dewatered at twice the rate of the untreated sludge. Furthermore, the treated sludge dewatered from 6.7 percent solids to 14.3 percent, whereas the untreated sludge dewatered to but 7.6 percent solids.

In spite of such impressive results, few treatment plants presently utilize chemical conditioning to aid gravity dewatering. A powerful deterrent to chemical use resides in the belief that the metals in conditioned sludge are deleterious to certain plant life, hence proscribing sludge disposal on farmland (28). The use of organic polymer conditioners promises to quiet such objections; thus, the role of conditioning in gravity dewatering bears closer scrutiny in the future. Evaluation of conditioner performance must be simplified, however, over methods such as outlined by Templeton (27). In this regard, the applicability of the specific resistance concept to gravity dewatering can prove of great value.

Two wastewater sludges were selected for experimentation to determine conditioner performance. The Amherst, Massachusetts treatment plant provided a primary digested sludge. Pittsfield, Massachusetts, served as a source of a digested mixed primary and trickling filter sludge. Samples of each sludge were flash mixed with doses of polymer conditioners at 100 rpm for one minute. The effectiveness of each dosage and conditioner was noted qualitatively after one minute of gentle stirring at 30 rpm, with attention being paid to floc structure and depth of supernatant. Two conditioners were eventually selected as being sufficiently effective to warrant specific resistance tests.

Samples of each sludge were prepared with conditioner dosages of 0, 100, 200, 300, 400, and 500 mg/ℓ, each sample being readied according to the manufacturer's instructions. One hundred ml of sludge was then poured into a 12 cm I.D. Buchner funnel, previously fitted with a wetted Whatman No.5 filter paper. The vacuums applied were 18, 38, and 60 cm of mercury, each held constant during each separate filter run. Three repetitions were run throughout. The duration of each run was never in excess of 17 minutes, which was sufficient at the higher vacuums to provide a solid cake. Cakes generally did not develop at the lowest pressures, and because of theoretical justification, the top liquid sludge was poured off and the solids content of the remaining cake measured.

Regression analysis provided the values for specific resistance and the coefficient of compressibility in Figures 25 and 26. As can be seen, the specific resistance decreased in both cases with increasing conditioner concentration. Statistical tests proved the variation of specific resistance with concentration was significant (>90 percent certainty). The apparent increase in the coefficient of compressibility with dosage, however, could not be statistically proven. This was believed to be caused by the erratic values of specific resistance measured at the lowest heads, possibly resulting from unrepresentative cake samples. For instance, if cake material were to be poured off with the unfiltered sludge at the end of the experiment, the final solids content of the cake would be too high, with inflated values of specific resistance resulting. Nonetheless, all regression lines had a correlation coefficient of better than 0.98.

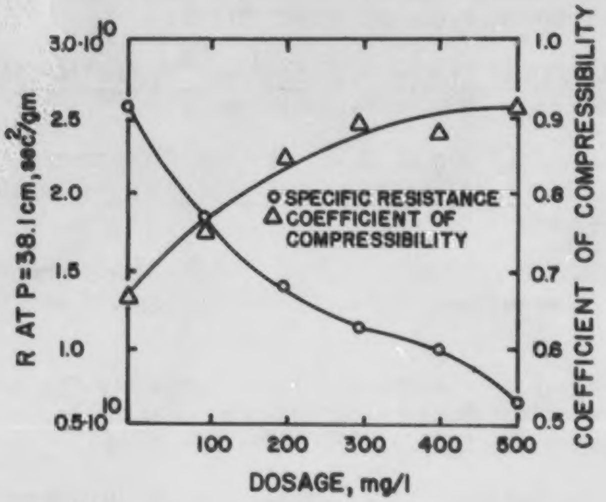

Figure 25: Effect of conditioner dosage on digested sludge from Amherst. The specific resistance values are at a vacuum of 38.1 cm of mercury. Initial solids content = 9.5%.

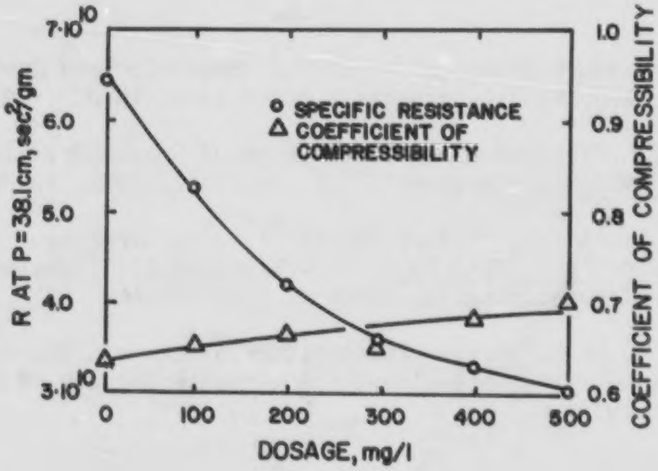

Figure 26: Effect of conditioner dosage on digested sludge from Pittsfield. Specific resistance values are for vacuums of 38.1 cm of mercury, initial solids content of 4.9%.

REFERENCES

1. Standard Methods for the Examination of Water and Wastewater, 12th Ed., American Public Health Association, New York, 1965.

2. FWPCA Methods for Chemical Analysis of Water and Wastes, Federal Water Pollution Control Administration, U.S. Department of the Interior, Washington, D.C., November 1969.

3. Hald, A. Statistical Theory With Engineering Applications. John Wiley and Sons, Inc., New York, 1952, pp. 571-584.

4. Salvadori, M. G., and Baron, M. L. Finite Differences and Their Applications. Numerical Methods in Engineering. Prentice-Hall Inc., New York, 1952, pp. 45-75.

5. Reginato, R. J. and Van Bavel, C.H.M. Soil Measurement with Gamma Attenuation. Proceedings, Soil Science Society of America, 28(6);721-724, 1964.

6. Davidson, J. M. et al. Gamma Radiation Intensity for Measuring Bulk Density and Transient Water Flow in Porous Materials. Journal of Geophysical Research, 68(16):4777-4783, 1963.

7. Ferguson, H. and Gardner, W. H. Water Content Measurement in Soil Columns by Gamma Ray Adsorption. Proceedings, Soil Science Society of American, 26(1):11-14, 1962.

8. Gurr, C. G. Use of Gamma Rays in Measuring Water Content and Permeability in Unsaturated Columns of Soil. Soil Science, 94:224-229, 1962.

9. Tang, W. Moisture Transport in Sludge Dewatering and Drying on Sand Beds. Ph.D.Thesis, Vanderbilt University, 1969.

10. Evans, R. D. Attenuation and Absorption of Electromagnetic Radiation. The Atomic Nucleus, McGraw-Hill Co., New York, 1955, pp. 224-229.

11. Adrian, D. D., et al. Source Control of Water Treatment Waste Solids. Report No. EVE-7-58-1, Department of Civil Engineering, University of Massachusetts, Amherst, April, 1968.

12. Van Bavel, C. H. M. et al. Transmission of Gamma Radiation by Soils and Soil Densitometry. Proceedings, Soil Science Society of America, 21:588-591, 1957.

13. Chase, C. G. and Rabinowitz, J. L. Scintillation Techniques of Nuclear Emulsions. *Principles of Radioisotope Methodology*, 3rd Ed., Burgess, Minneapolis, 1967, pp. 283-323.

14. Kohl, J., *et al.* *Radioisotope Applications Engineering,* Van Nostrand Co., New York, 1961.

15. Steel, R.G.D. and Torrie, J. H. *Principles and Procedures of Statistics,* McGraw-Hill Co., New York, 1951, pp. 15-19.

16. Lambe, T. W. Specific Gravity Test. *Soil Testing for Engineers*, John Wiley and Sons, New York, 1951, pp. 15-19.

17. Covey, W. Mathematical Study of the First Stage of Drying of a Moist Soil. Proceedings, Soil Science Society of America, 27(2): 130-134, 1963.

18. Wakabayashi, K. Moisture Diffusion Coefficient of Solids During Drying Process. Kagaku Kogaku (abridged ed.), 2(2):132-136, 1964.

19. ______________. Calculation of Moisture Distribution in Clay During Drying Process. Kagaku Kogaku, 2(2):146-149, 1964.

20. Ames, W. F. *Nonlinear Partial Differential Equations in Engineering.* Academic Press, New York, 1965, p. 34.

21. Swanwick, J. D. and Davidson, M. F. Determination of Specific Resistance to Filtration. The Water and Waste Treatment Journal, July/August, 1961.

22. O'Brien and Gere. Waste Alum Sludge Characteristics and Treatment. Research Report No. 15, New York State Department of Health, 1966.

23. Baskerville, R. C. and Gale, R. S. A Simple Automatic Instrument for Determining the Filterability of Sewage Sludges. Journal of the Institute of Water Pollution Control, 2, 1968.

24. Nebiker, J. H. *et al.* An Investigation of Sludge Dewatering Rates. Proceedings of the 23rd Purdue Industrial Waste Conference, May, 1968.

25. Lutin, P. A., Nebiker, J. H. and Adrian, D. D. Experimental Refinements in the Determination of Specific Resistance and Coefficient of Compressibility. Proceedings of the Annual North Eastern Regional Anti-Pollution Conference, University of Rhode Island, Kingston, July, 1968.

26. Sperry, W. A. Sewage Works Journal, September, 1941, pp. 855-867.

27. Templeton, W. E. J. Proc. Inst. Sew. Purif., 1959, pp. 223-226.

28. Downing, A. L. and Swanwick, J. D. J. Instn. Municipal Engineers, 94:81-86, March, 1967.

29. Coackley, P. and Jones, B.R.S. Interpretation of Results by the Concept of Specific Resistance. Sewage and Industrial Wastes, August, 1956.

30. von Niemitz, W. and Fuss, K. "Der spezifische Filterwiderstand und die Kompressibilitat von Klarschlammen," Wasser-Abwasser 106 Jahrg, Jeft 28, 16 (Juli, 1965).

31. Eckenfelder, W. A. and O'Connor, D. J. Biological Waste Treatment. Pergamon Press Ltd., New York, 1961.

SECTION VII

RESULTS

CHEMICAL CHARACTERISTICS

Chemical characteristics of the sludge, decant, and filtrate samples are presented for four water treatment sludges. Physical properties such as particle density, specific resistance, and total solids were determined for each individual study and are not included here. Samples of the clear supernatant which resulted from sedimentation were taken as representative decant samples. Filtrate samples were collected during the dewatering studies from the column effluent. The average value of triplicate analyses is reported.

Color-turbidity-pH. Color, turbidity, and pH were determined for all samples. The average values are tabulated in Table 2.

Color was determined by a Helige Aqua Tester on unfiltered samples. This method gave values for the apparent color. The sludges exhibited a dark black color with the exception of the softening sludge. The softening sludge was reddish-brown. The dark color of the three clarifier sludges was probably due to the activated carbon and minute amounts of organic material. Both the filtrate and decant were relatively clear, exhibiting low color values.

Turbidity was determined by the Jackson turbidity meter. The presence in the sludge of suspended solids which could settle out rapidly may have given false high readings. The turbidity values for the sludges therefore have less significance than the values for decant and filtrate. Relatively low turbidity values were obtained for the filtrate samples with the exception of Billerica sludge which had an average pH of 4.3. During the time interval of transferring samples from the treatment plants to the laboratory and subsequent handling, neutralization, such as from loss of CO_2, could have taken place.

Solids. Total solids, total volatile solids, and suspended solids were determined. No established procedure for determining solids in sludge samples exists, however Standard Methods (1) and extensive solids analysis investigations at the University of Massachusetts (2) served as guidelines. Total solids were determined by heating the samples for 8 hours at 103°C and total volatile solids were determined by heating the total solids residue at 600°C for 20 minutes. Samples for the suspended (nonfilterable solids determinations were processed by filtering through a standard glass fiber filter. The results of the solids determinations are presented in Table 3.

TABLE 2. AVERAGE VALUES FOR COLOR, pH, AND TURBIDITY FOR THE SLUDGE, FILTRATE, AND DECANT SAMPLES

Sample	Color, (color units)	pH	Turbidity, (JTU)
Albany			
Sludge	black	7.0	1200
Filtrate	0.03	7.5	6.0
Decant	0.10	7.7	36
Amesbury			
Sludge	black	8.0	3600
Filtrate	0.01	8.3	4.0
Decant	0.02	7.9	3.0
Billerica			
Sludge	black	4.3	2200
Filtrate	0.10	7.4	65
Decant	0.12	8.3	22
Murfreesboro			
Sludge	reddish-brown	8.0	1700
Filtrate	0.02	7.6	8.0
Decant	0.02	7.6	2.0

TABLE 3. AVERAGE VALUES FOR SOLIDS FOR THE SLUDGE, FILTRATE, AND DECANT SAMPLES

Sample	Total Solids, %	Volatile Solids as a % of Total Solids	Suspended Solids, mg/l
Albany			
Sludge	1.45	46.0	13500
Filtrate	0.029	40.0	1.5
Decant	0.024	53.0	2.0
Amesbury			
Sludge	3.83	43.8	37200
Filtrate	0.041	12.5	0.11
Decant	0.029	11.0	0.08
Billerica			
Sludge	6.30	58.0	62000
Filtrate	0.104	34.8	2.14
Decant	0.050	40.8	2.58
Murfreesboro			
Sludge	4.80	2.2	47000
Filtrate	0.036	26.0	1.44
Decant	0.326	19.0	0.90

The four sludges had a wide variation in total solids, the range extending from 1.45 percent for Albany sludge to 6.30 percent for Billerica sludge. The sludges were approximately 50 percent volatile solids with the exception of Murfreesboro (softening) sludge which was only 2.15 percent volatile solids. A portion of the high values (50 percent) for volatile solids may be attributed to bound water which would be retained on the solid particle at lower temperatures but driven off at higher temperatures. Suspended material accounted for 98.5 percent of the total solids for the four sludges. The filtrate and decant samples were relatively clear. Note that suspended solids cannot be compared directly with total solids since two different analytical methods were utilized. The total solids are reported on a mass-mass (percent) basis while the suspended solids are reported as mass-volume (mg/l). The two are comparable only when the specific gravity of the sample is unity. Values for specific gravity for the sludges ranged from 1.95 to 2.75.

Acidity and Alkalinity. Total acidity and total alkalinity were determined by potentiometric titration. The results are tabulated in Table 4. Billerica sludge had total acidity of 2753 mg/l (as $CaCO_3$), the maximum obtained. The maximum alkalinity obtained was for the Murfreesboro (softening) sludge and was 12,950 mg/l (as $CaCO_3$).

Calcium-Magnesium-Total Hardness. Total hardness and calcium were determined by the EDTA titrimetric method. Magnesium was determined by subtracting calcium from total hardness since hardness is usually considered to be primarily composed of calcium and magnesium. The results are presented in Table 5.

Iron and Manganese. Iron and manganese were determined for the samples and the results are shown in Table 6. The Amesbury and Murfreesboro sludges contained the highest concentrations of iron, 3080 and 1990 mg/l, respectively. The Amesbury water treatment plant practices iron removal by oxidizing ferrous iron to the insoluble ferric state. A similar removal process would be produced during softening at the Murfreesboro plant. As shown by the low values for iron in the filtrate and decant samples, most of the iron was in the insoluble ferric state. Manganese often is present with iron in surface water supplies and is generally removed concurrently with iron. A large percentage of manganese in the Albany and Billerica sludges was in the insoluble form.

Nitrogen. Nitrogen analysis consisted of organic nitrogen, ammonia, nitrite, and nitrate. Ammonia was analyzed by the direct nesslerization method. Organic nitrogen was determined by performing total Kjeldahl and then subtracting the value obtained for ammonia. Nitrate was obtained by the phenoldisulfonic acid method which determined both nitrate and nitrite. The values for nitrate were then determined by subtracting the values previously obtained for nitrite. The results of the nitrogen analyses are presented in Table 7.

The Albany and Billerica sludges contained 479 and 612 mg/l organic nitrogen, respectively. The filtrate and decant for both sludges contained significantly less organic nitrogen, indicating the organic nitrogen was

TABLE 4. AVERAGE VALUES FOR TOTAL ACIDITY AND TOTAL ALKALINITY FOR THE SLUDGE, FILTRATE, AND DECANT SAMPLES

Sample	Total Acidity, mg/l as $CaCO_3$	Total Alkalinity, mg/l as $CaCO_3$
Albany		
Sludge	360	832
Filtrate	44.2	147
Decant	25.2	87.4
Amesbury		
Sludge	612	1,975
Filtrate	16.7	158.5
Decant	-	-
Billerica		
Sludge	2,753	-
Filtrate	14.0	88.0
Decant	253.5	2.6
Murfreesboro		
Sludge	-	12,950
Filtrate	6.0	74.5
Decant	7.5	82.5

TABLE 5. TOTAL HARDNESS, CALCIUM, AND MAGNESIUM FOR THE SLUDGE, FILTRATE, AND DECANT SAMPLES

Sample	Total Hardness, mg/l as $CaCO_3$	Calcium mg/l as Ca	Magnesium mg/l as mg
Albany			
Sludge	12,900	3,960	715
Filtrate	195	68	6
Decant	153	58	2
Amesbury			
Sludge	2,360	790	92
Filtrate	182	68	3
Decant	165	64	1
Billerica			
Sludge	10,900	2,560	1,100
Filtrate	458	172	7
Decant	452	170	7
Murfreesboro			
Sludge	15,100	3,990	1,240
Filtrate	180	62	6
Decant	182	62	7

TABLE 6. AVERAGE VALUES FOR MANGANESE AND IRON FOR THE SLUDGE, FILTRATE, AND DECANT SAMPLES

Sample	Manganese, mg/l	Iron, mg/l
Albany		
Sludge	70.0	89.2
Filtrate	12.3	0.07
Decant	13.8	1.27
Amesbury		
Sludge	57.6	308
Filtrate	5.4	0
Decant	0	
Billerica		
Sludge	31.0	541
Filtrate	7.4	2.38
Decant	18.8	5.55
Murfreesboro		
Sludge	5.6	1990
Filtrate	0	0
Decant	0	0

TABLE 7. AVERAGE NITROGEN VALUES FOR THE SLUDGE, FILTRATE, AND DECANT SAMPLES

	mg/l Nitrogen found as			
Sample	Organic N	Free NH_3	NO_2	NO_3
Albany				
Sludge	479	58.8	0.126	2.65
Filtrate	41.8	12.6	3.15	0.450
Decant	25.3	24.8	11.2	2.80
Amesbury				
Sludge	4.70	10.5	0.019	0.13
Filtrate	1.50	10.7	0.004	0.22
Decant	1.06	8.49	0.004	0.38
Billerica				
Sludge	612	89.2	0.002	0.98
Filtrate	10.6	41.4	0.065	0.22
Decant	15.2	72.8	0.011	0.27
Murfreesboro				
Sludge	35.8	2.00	0.019	0.23
Filtrate	9.1	1.65	0.027	0.15
Decant	15.0	3.66	0.006	0.37

adsorbed to the sludge solids. The organic nitrogen in the Amesbury and Murfreesboro sludges was considerably less at 4.70 and 35.8 mg/l, respectively. The Albany, Amesbury, and Billerica samples contained significant amounts of free ammonia. Nitrite and nitrate values of all samples were comparatively small. The decant samples in general contained more nitrogen than the filtrate samples. The two might normally be considered equal except for the amount adsorbed to any suspended particles in the decant. Filtrate and decant samples for Albany and Billerica had a higher concentration of NO_2 than the sludge samples. The filtrate and decant samples were separated from any bacteria that was present in the original sludge samples. Since the amount of each of the different forms of nitrogen is greatly influenced by microbial activity, the rates of oxidation reduction of the filtrate and decant samples were not equal to the oxidation reduction rates of the sludge samples.

Phosphate. Phosphate determinations consisted of orthophosphate and polyphosphate analyses. Orthophosphate was determined by the stannous chloride method. Polyphosphates were determined by subtracting orthophosphate from the total inorganic phosphate. The phosphate results are summarized in Table 8.

Polyphosphate comprised the larger portion of phosphates in all samples except for the Murfreesboro sludge sample. The filtrate and decant samples contained much less phosphate than the sludge samples which indicates that phosphates were adsorbed to the sludge particles.

Sulfate. Sulfate analyses were performed according to Standard Methods (1), Method B: Gravimetric Method with Drying or Residue. Billerica sludge had the maximum value of 1240 mg/l SO_4. The results are tabulated in Table 8.

BOD-COD. Biochemical Oxygen Demand (BOD) and Chemical Oxygen Demand(COD) results are presented in Table 9. The BOD values for the filtrate and decant samples were low. The Murfreesboro sludge had the lowest BOD, 7.8 mg/l. The maximum BOD was in Billerica sludge which also had the highest total solids content.

The COD values ranged from a minimum value of 3330 mg/l for Albany sludge to a maximum of 440,000 mg/l for Billerica. The large amounts of activated carbon present and the high (6.30 percent) total solids content are two possible explanations for the high COD value for Billerica sludge. The COD values for the decant and filtrate samples ranged from 124 to 289 mg/l.

RESULTS OF THE GRAVITY DRAINAGE STUDY

The theoretical formula (Equation 40) previously derived relates the drainage rate of a wastewater sludge on sand or other highly permeable material to the solids content of the sludge, the head, specific resistance, coefficent of compressibility, filtrate density, and dynamic viscosity of the filtrate. The degree of accuracy with which this formula fits the experimental data will in part be dependent upon the accuracy with which the

TABLE 8. AVERAGE VALUES OF PHOSPHATE AND SULFATE FOR THE SLUDGE, FILTRATE, AND DECANT SAMPLES

Sample	Orthophosphate, mg/l PO_4	Polyphosphate, mg/l PO_4	Sulfate, mg/l
Albany			
Sludge	2.64	54.0	209
Filtrate	0.34	0.83	18.2
Decant	0.08	5.4	5.35
Amesbury			
Sludge	1.4	395	150
Filtrate	0.15	1.6	7.20
Decant	0.15	1.2	33.8
Billerica			
Sludge	2.6	1803	1240
Filtrate	0.15	1.6	23.8
Decant	0.40	4.45	51.2
Murfreesboro			
Sludge	134	61	156
Filtrate	0.24	0.88	128
Decant	0.25	1.25	69.0

TABLE 9. BIOCHEMICAL OXYGEN DEMAND AND CHEMICAL OXYGEN DEMAND FOR SLUDGE, FILTRATE, AND DECANT SAMPLES

Sample	BOD, mg/l	COD, mg/l
Albany		
Sludge	160	3,330
Filtrate	9.6	160
Decant	7.9	240
Amesbury		
Sludge	180	18,500
Filtrate	2.7	124
Decant	1.2	98
Billerica		
Sludge	190	440,000
Filtrate	2.0	167
Decant	2.0	289
Murfreesboro		
Sludge	7.8	3,350
Filtrate	0	134
Decant	7.1	124

dependent variables are measured.

Experimental errors incurred in the determination of the solids content must be considered minimal (<5 percent) since the procedure utilized multiple samples. The solids determinations were used in both Equation 40 and in the determination of specific resistance, and values inserted here were in fact approximations for the volume of filtrate per unit weight of solids. Greater accuracy in laboratory determinations for solids content was thus not justified.

The initial head was directly measured to 1 mm. Instantaneous values for head were calculated from the initial head and the instantaneous volume of filtrate. The volume could be measured to within 2 ml which represented a head interval of 2.5 mm, certainly not a source of significant error. A greater error occurred occasionally with the appearance of bubbles in the filtrate discharge tubes below the nozzles. Sometimes the bubbles attained 2-3 cm (.8-1.2 in) length, thus causing a corresponding reduction in the calculated head. However, the heads were invariably greater than 30 cm (11.8 in), hence the bubbles created minimum disturbance.

Values for filtrate density and dynamic viscosity were originally checked and judged to be identical to values for water at the same temperature. A series of preliminary tests indicated this conclusion was sound since any deviations of filtrate characteristics from water were clearly smaller than the effects of temperature fluctuation. These fluctuations, minimized by the air-conditioning system in the laboratory, approximated $\pm$ 3°C during the course of an experiment. Mean temperatures were 24°C, leading to values of 0.00919 gm/cm-sec for dynamic viscosity, and 1.0 gm/cm^3 for density, which appear in both the calculations for gravity dewatering time and specific resistance.

In Experiments I-III, a phenomenon of "surging" occurred whereby an extremely high rate of dewatering occurred with a penetration of solids into the sand. Also, great difficulty was encountered with the placing of supernatant on top of the thick sludge. Turbulence caused a mixing of the two, with a poor, partial separation developing after 24 hours at which time each experiment began. The initial solids content, specific resistance, and coefficient of compressibility were determined from the sludge initially applied, and as shown, these values were to be used in the theoretical equation. Unfortunately they were clearly altered by the addition of supernatant. It might also be mentioned that additional settling after drainage began did not improve the data. Additional settling was minor due to the short drainage times, and also due to temperature currents. Experiments I-III were run in late summer with the columns some 61 cm (2 feet) from an external wall. The outdoor heat created a warmer backside on the columns leading to a flow pattern inimical to settling. Later experiments run in the fall were not influenced by this problem.

Quon (3) witnessed surges which he believed were caused by the adsorption of air in the sand by the filtrate, thus increasing the effective porosity which in turn increased the rate of drainage. Since the supporting media was saturated with water before each experiment, the phenomenon which

Quon observed did not appear to apply.

Visual observations of surging which did occur indicated that the filtrate turbidity sharply increased as a result. Further, it was noted that larger sludge particles penetrated into the sand at the edges of the column-sand interface. This leads one to suspect that the sand-column interface served as an easier exit for particles and that the column diameter may influence the occurrence if not magnitude of the surges. The relatively thin layers of sludge in Experiments I-III exhibited a "punching" of the surface near the edges, adding credence to this theory.

Further substantiation was indicated by Experiments IV-VI, which were charged with homogeneous mixtures providing thicker sludge cakes. Surging was significantly reduced, and it may be assumed that this was due to lower pressure gradients across the sludge cakes. It should also be mentioned that disturbance of the sand surface during the filling with sludge alone was definitely less than in those cases where supernatant was then later added. An uneven sand surface would probably encourage surging, for a cake would build of uneven thickness.

In Experiment VI 10 piezometer tubes spaced along the length of a single column were used as a measure of pressure differences in the sludge column. Initial head of the sludge on the Ottawa sand was 96 cm. During the experiment it was proven that a large pressure difference which is proportional to the head loss occurs at the sludge-sand interface. Therefore, the build-up of a thin sludge cake was responsible for most of the head loss in the column and would thus be the determining factor which controlled drainage rates. This follows standard filter theory for compressible materials, hence justifying the assumption made in developing the theoretical derivation that the drainage rate is proportional to the build-up of a thin sludge cake.

Based upon Experiment VI which provided proof of the existence of a thin sludge layer at the sludge-sand interface, a theory was proposed to explain the surging phenomenon, namely, that this layer structurally bridged the distance between individual sand particles. If the distance between particles were large, a small amount of stress (from viscous drag) would cause a break in the sludge cake to occur, allowing an early release of filtrate. As the liquor passed through, new sludge particles would eventually heal the break and stop the surge. However, this may await a low drainage rate at which viscous drag is at a minimum, i.e., possibly the passages were plugged only at the end of dewatering. If the distances between individual sand particles were small, more stress would be needed to collapse the bridging sludge cake, and once a break occurred less solids would be needed to fill the break.

To explore the rigid sludge cake theory, the effective size of each sand was measured. The effective size is an approximate measure of the sand grain diameters. A small effective size would indicate a small distance between individual sand particles and a large effective size would indicate a large distance between particles. Table 10 indicates that Franklin sand possessed the smallest effective size and Hermitage sand the largest. The sludge supported by Franklin sand in Experiment IV

TABLE 10. PHYSICAL CHARACTERISTICS OF SUPPORTING SAND

Sand Source	Sand Designation	D_{10}(mm)	D_{60}/D_{10}	Media Factor
Franklin Treatment Plant	F	0.16	1.25	0.75
Ottawa Standard Sand	O	0.60	1.23	0.60
Hermitage Hill Treatment Plant	H	0.78	1.41	0.45

did not surge in the twenty-five days (Figure 27) of the experiment except for column 3 on the 14th day. The sludge supported by the Ottawa sand (Figure 28) surged in all three columns around the 17th day of the experiments. And finally, the sludge supported by the Hermitage sand surged in the vicinity of the 14th day (Figure 29).

Data from Experiments IV and V, plotted in Figures 27-32, presented sufficient data before surging to test the validity of Equation 40. The theory, however, predicted longer drainage times in all cases, but a study revealed that a constant correction factor applied for each type of sand.

One would not expect the value of R_c, calculated from Buchner funnel testing, to fully represent a value of specific resistance of a sludge on different supporting media such as a sand. Approximately 40-50 percent of the gross sand surface is porous; that of a Buchner funnel less so, even though filter paper is used. To illustrate extreme cases of the role of the supporting media, it is clear that impermeable supporting media will allow no dewatering, whereas very coarse supporting media will retain no solids, resulting in a zero resistance to flow.

To account for the relationship between the sludge and the supporting media, but mindful of dimensional correctness, a media factor must be introuced into Equation 40. This media factor can be considered as a function of the ratio of a representative sludge floc diameter to an equivalent diameter of a sand grain: the sand grain representing the effect of the supporting media or some equivalent parameter of the Buchner funnel, or filter leaf, or any other dewatering device. The value of the media factor, m, would be larger for finer sands and smaller for coarse sands. As a function of ratio of diameters, m would be dimensionless.

The values found for the media factor by curve fitting, and listed in Table 10 exhibit the correct directional relationship with the corresponding D_{10} size; that is, the decrease in media factor (or drainage time) results from an increase in the sand size. However, such an increase in sand size inevitably increases the turbidity and color of the filtrate.

A plot of the experimental data and theoretical data (Figure 30,

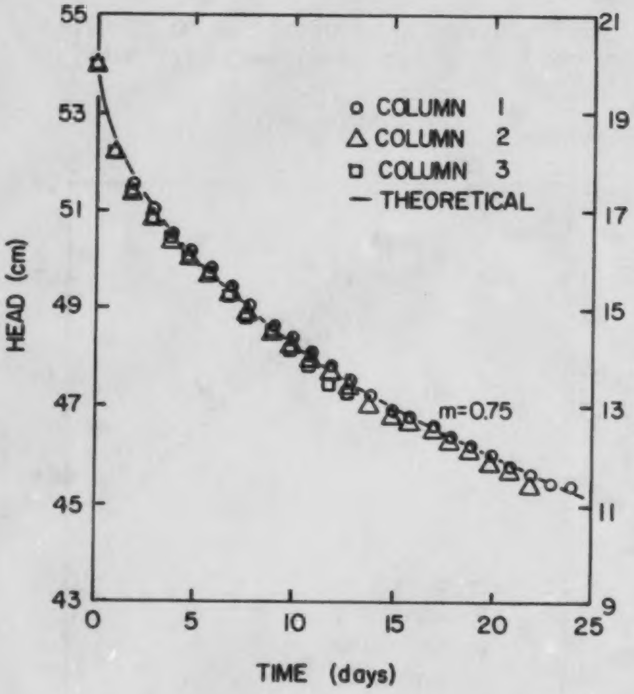

Figure 27. Experiment IV, triplicate tests with 20 cm of sludge on Franklin sand.

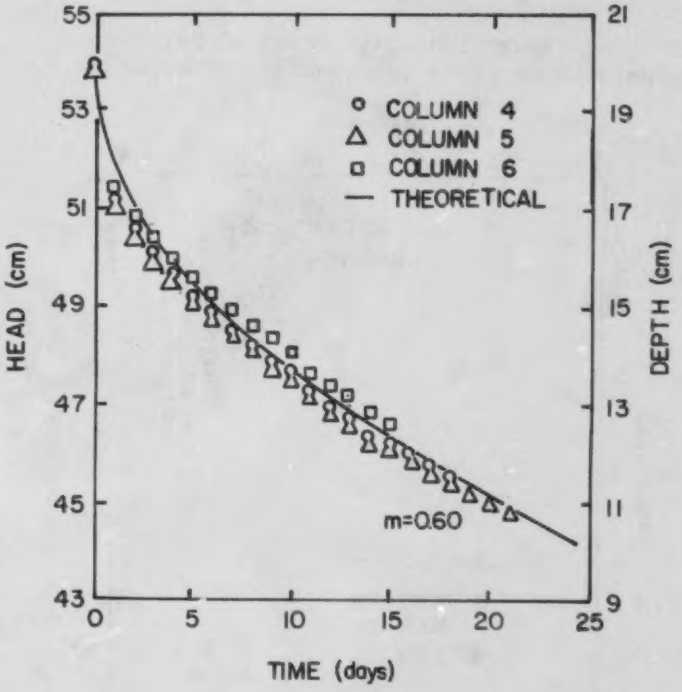

Figure 28: Experiment IV, triplicate tests with 20 cm of sludge on Ottawa sand.

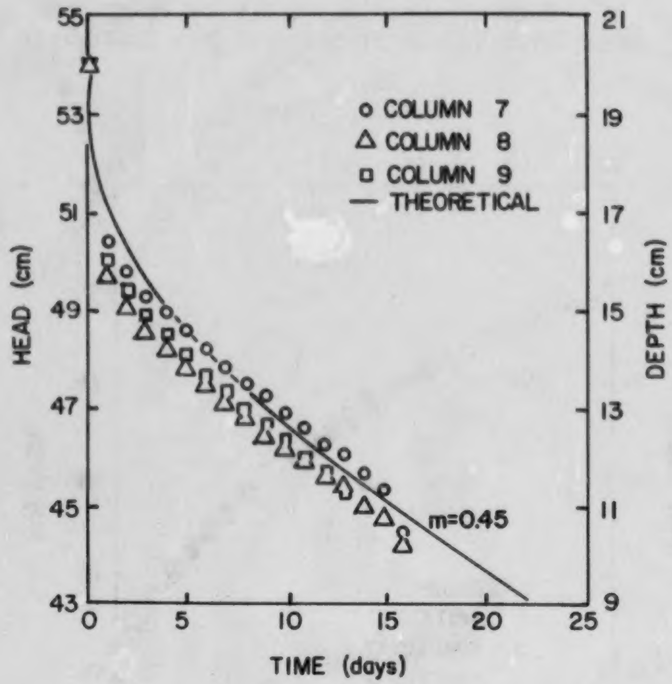

Figure 29: Experiment IV, triplicate tests with 20 cm of sludge on Hermitage sand.

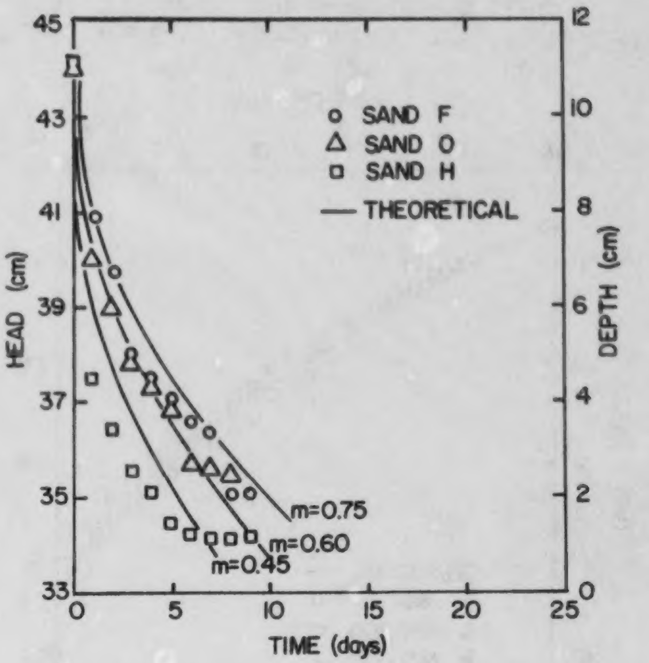

Figure 30: Experiment V, 11 cm of sludge applied on three different sands.

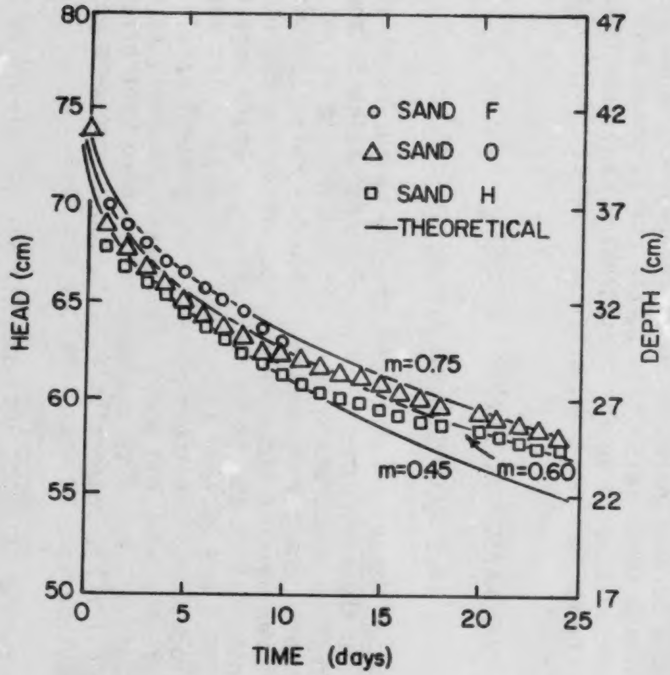

Figure 31: Experiment V, 41 cm of sludge applied on three different sands.

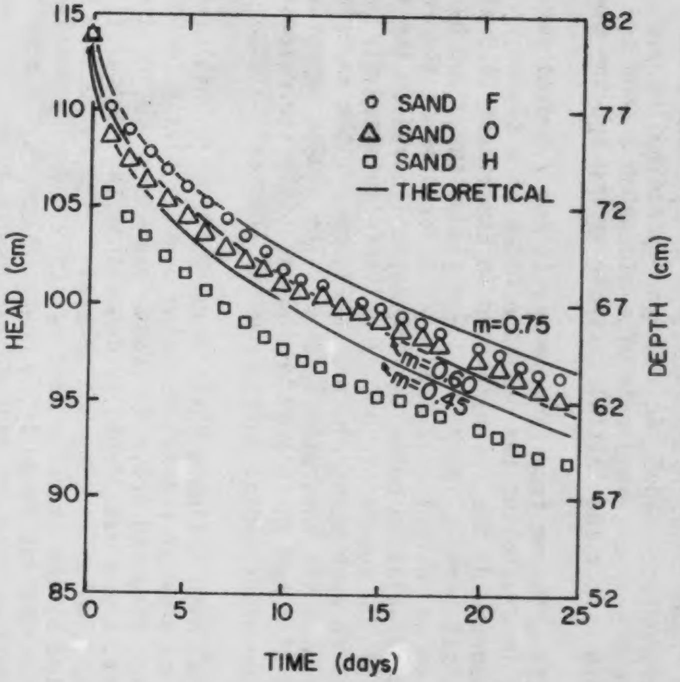

Figure 32: Experiment V, 81 cm of sludge applied on three different sands.

Figure 31, and Figure 32) substantiated the conclusions drawn from Experiment IV that the mathematical model (Eq. 40) incorporating the media factor could approximate the actual drainage rate of a sludge on a sand bed and that the type of sand did effect the initial filtrate volume and the time of surge.

The results obtained from Experiments IV and V proved the applicability of Equation 40 in predicting the drainage rates of a sludge on a sand bed. The sludge supported by the Franklin sand in Experiment IV drained according to the theoretical curve (Figure 27). The sludge supported by the Ottawa sand, because of an initial filtrate release, drained at the rate determined by Equation 40 but plotted below the theoretical curve in the first few days (Figure 28). If the volume of initial filtrate released divided by column area were added to each point plotted in Figure 28, the experimental curves would coincide with the theoretical curve. The sludge supported by the Hermitage sand also had an initial unpredicted filtrate release or surge, which offset the experimental curve from the theoretical curve.

The initial high drainage rates resulted from an initial retarded cake formation due to some of the solids being drawn into the supporting media instead of being retained above the sand interface. During the course of six experiments, there was strong evidence that the initial filtrate release as well as the time of surging was related to the supporting media. The sludge supported by the Franklin sand not only had very little filtrate release but also did not surge in 25 days. However, the same sludge supported by the Hermitage sand did release a sizeable amount of filtrate at the beginning of the experiment and surging occurred at approximately 14 days.

As previously mentioned, if head loss due to the initial filtrate release were added to each point on the head versus time curves for the Ottawa and Hermitage sands respectively, the curves would then coincide with the head versus time curve for the Franklin sand with the same initial head, thus justifying identical media factors for all the sands tested.

RESULTS OF THE EVAPORATION AND DRYING STUDIES

Preliminary Results of Evaporation and Drying

Evaporation of Water. Preliminary studies on the evaporation of water were conducted in the environmental chamber to determine if there was any significant effect on evaporation rates attributable to either location in the environmental chamber or to liquid depth. Deionized water was evaporated in three sets of three cylindrical plastic pails (27.5 cm diameter and 35.5 cm depth, 11 in and 14 in respectively, which were filled to depths of 9.6, 19.3 and 29.1 cm (3.8, 7.6, 11.5 in). A set was placed at each of three locations: on the floor near the control panel, on a table in the center of the room, and on the floor near the door, as shown in Figure 33. Relative humidity and temperature were controlled at 47 percent and 24^{o}C (76^{o}F), respectively. The containers were weighed to the nearest gram at intervals of approximately 1.5 days.

The average rate of water loss (gm/hr) was calculated by fitting a

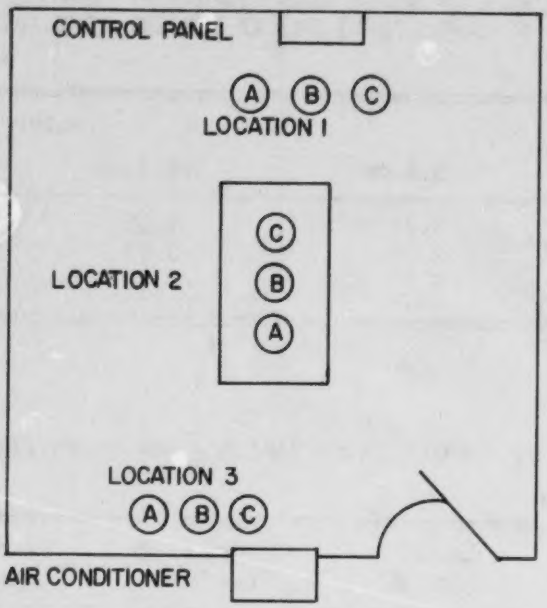

Figure 33: Location of containers in evaporation study.

straight line to the weight-time data, the slope of which was obtained from linear regression analysis. The data are summarized in Table 11. A two-way analysis of variance of the drying rates showed no significant difference between depths and locations at the 5 percent level. A summary of the analysis of variance is shown in Table 12.

Drying Studies. Two preliminary drying studies were conducted using Billerica sludge. Sludges with solids content of 2.35 and 6.12 percent were dried in glass pans .5 cm thick with inside dimensions of 35 x 22 x 4.5 cm (13.8, 8.7, 1.8 in). The initial sludge depths were 3.0 cm (1.2 in). Pans of distilled water were evaporated as controls. Temperature and relative humidity were controlled at 22 ± 1°C (72 ± 0.5°F) and 38 ± 1 percent, respectively. The sludge mass was determined on a triple-beam balance at intervals of approximately one day. When the change in mass was less than one gram per day, the sludges were assumed to be at equilibrium. Results of the two drying studies are summarized in Table 13.

Curves showing the sludge mass-time relationships are shown in Figure 34. The constant-rate drying period accounted for approximately 75 percent of the water loss and 75 percent of the total drying duration for each sample. During the early stages of drying sample D-1 appeared to have a thin film of moisture on the surface while sample D-2, of lower solids content, had clear supernatant present. The first critical moisture content

TABLE 11. RATE OF WATER LOSS (gm/hr) OF DE-IONIZED WATER AT 24°C (76°F) AND 47 PERCENT RELATIVE HUMIDITY

Location	Water Depth 9.6 cm	 19.3 cm	 29.1 cm
1	3.77	4.05	4.39
2	2.74	3.53	4.36
3	2.77	3.18	3.67

TABLE 12. ANALYSIS OF VARIANCE FOR EVAPORATION DATA

Source of Variation	Sum of Squares	Degrees of Freedom	Mean Squares	F Test
Location	2.1	2	1.05	6.20
Depth	1.6	2	0.80	4.70
Error	0.7	4	0.17	
Totals	4.4	8		

TABLE 13. RESULTS OF BILLERICA SLUDGE, AT TWO DIFFERENT SOLIDS CONTENTS, DRIED AT 22°C (72°F) AND 38 PERCENT RELATIVE HUMIDITY FOR 3.0 cm (1.2 in) INITIAL DEPTHS

Sample Number	D-1	D-2
Initial Solids, %	6.12	2.35
Critical Moisture Content, %	400	350
Critical Solids Content, %	20.0	22.2
Solids at Equilibrium, %	90.0	79.5
Moisture at Equilibrium, %	11.0	26.0
I_c, gm/cm^2-hr	0.0062	0.0070
Evaporation ratio, %	76.5	86.5

was not reached, however, until after the sludges had appeared very dry and many cracks had formed. The equilibrium moisture contents were low with an average value of only 18 percent. At equilibrium, the sludges had shrunk to only a few small, warped pieces, approximately 0.5 cm (0.2 in) thick.

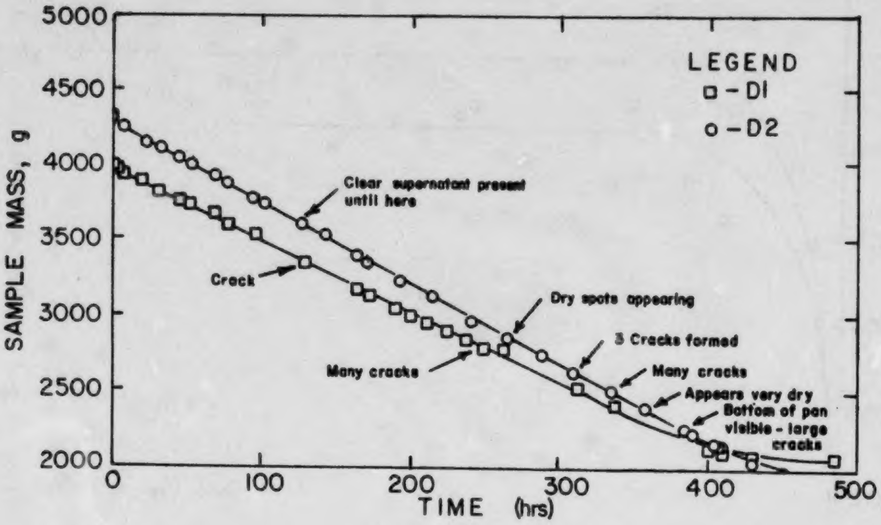

Figure 34: Sample mass versus time for Billerica sludge drying at 22^{0}C (72^{0}F) and 38% relative humidity.

The average drying rate for a long constant-rate drying period was determined by fitting straight lines to the sludge mass-time data. The average drying rates for samples D-1 and D-2 were 0.0062 and 0.0070 gm/cm^2-hr, respectively. When tested by comparison of regression lines the two drying rates were shown to be most affected by the initial solids concentrations. The average evaporation rate of water for the same conditions was 0.0081 gm/hr-cm^2. The evaporation ratios (the ratio of sludge drying intensity to evaporation rate of water) for samples D-1 and D-2 were therefore 76.5 and 86.5 percent, respectively.

Drying-rates for the entire drying duration were calculated by Equation 84 and are shown in Figure 35. The initial decrease in the drying rate was due to the samples having been stored at a higher temperature than the experimental drying conditions. The drying rate decreased while the surface temperature fell to the ultimate value. This initial adjustment period was so short that it was ignored in subsequent analysis of the drying times.

The first critical moisture content was reached at a higher moisture content (shorter drying time) for the sample (D-1) with the higher proportion of solids. This conforms with the general theory for critical moisture content in that sample D-1 had a higher solids content, therefore a higher value for mass of total solids, W_{TS}. A second critical moisture content could not be clearly established for either sample.

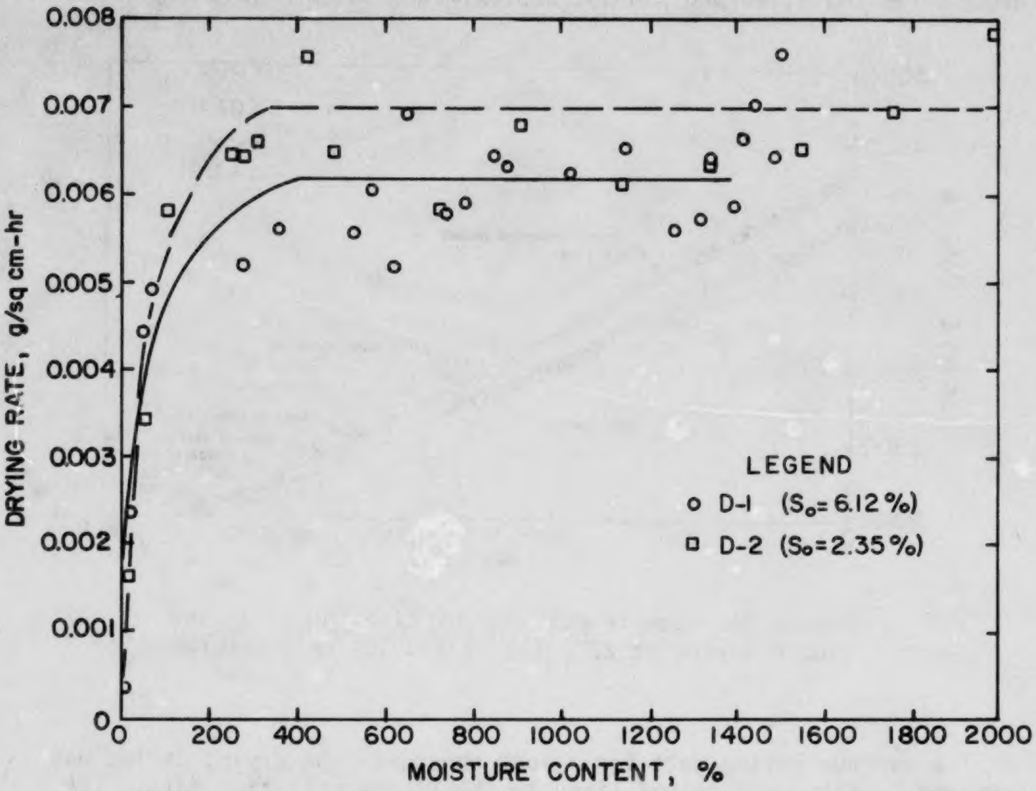

Figure 35: Drying rate curves for Billerica sludge drying at 22^{0}C (72^{0}F) and 38% relative humidity.

RESULTS OF DRYING

Drying studies were conducted to determine the drying rates and evaporation ratios of thin layers of sludge under controlled drying conditions. During the drying of water treatment sludges, shrinkage and formation of cracks occurred which changed the drying surface area. In order to show the relative magnitude of shrinkage, pans containing the four types of sludge were dried in the oven at 103^{0}C (217^{0}F) for approximately two days. Sludge mass was determined periodically to provide values for solids content. The relative amount of shrinkage and crack formation is shown in Figure 36. The softening sludge (Murfreesboro) settled rapidly leaving a clear supernatant to be evaporated during most of the drying period. The Billerica sludge had

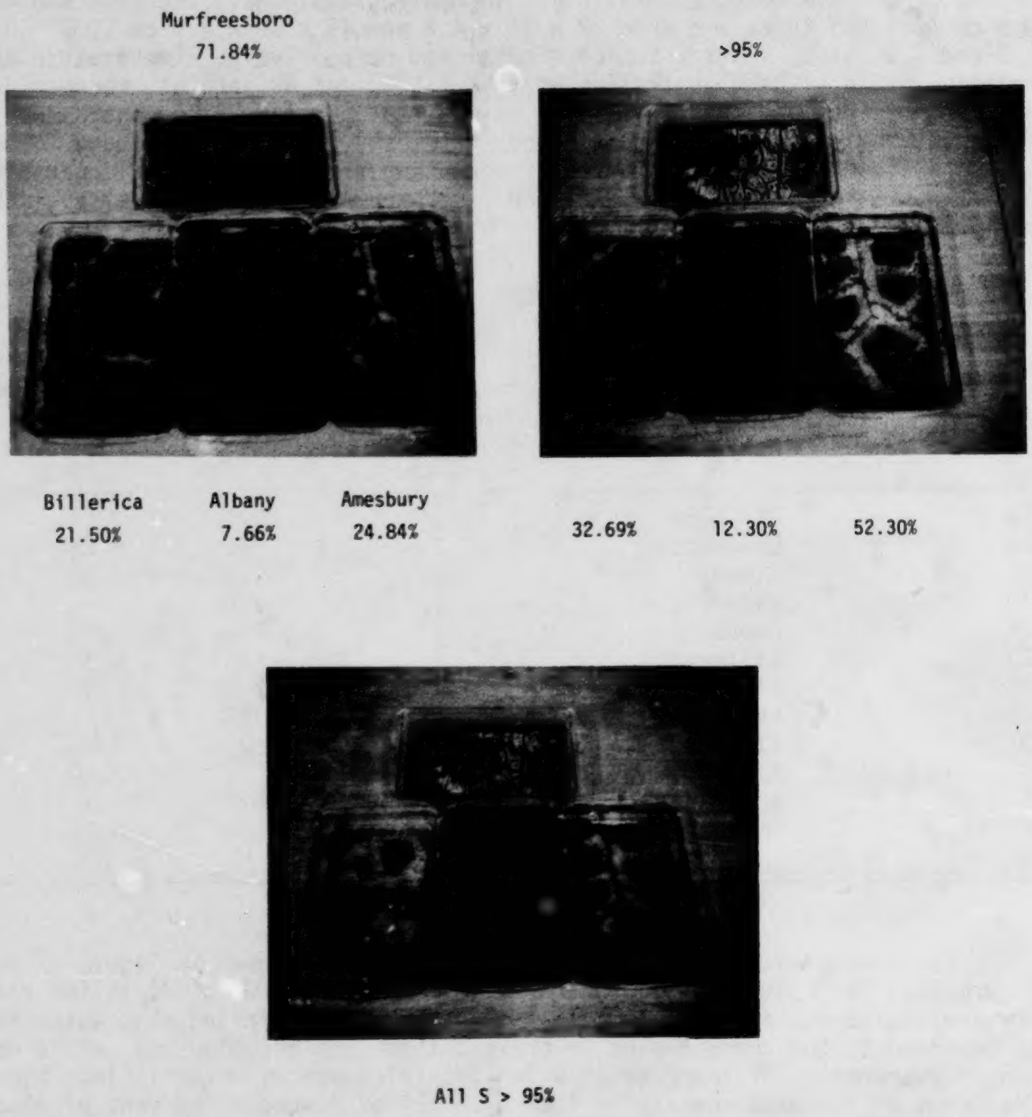

Figure 36: Four types of water treatment sludge at various solids contents.

less shrinkage, probably due to the large amounts of activated carbon present.

Drying-Rate Studies. Drying-rate study D-3 was conducted to study the drying and evaporation ratios of thin layers of sludge under controlled drying conditions. Albany, Billerica, and Amesbury sludges were dried at depths of 2 and 4 cm (0.8 and 1.6 in) in heavy glass pans. The pans had walls 0.5 cm (0.2 in) thick and were 22 x 35 x 4.5 and 19 x 30 x 4.5 cm (0.8, 13.8, 1.8 and 7.5, 11.8, 1.8 in) inside dimensions, respectively. Temperature and relative humidity were controlled at 24°C (75°F) and 65 percent, respectively. All Billerica samples had an initial solids content of 6.20 percent. Two different solids contents were studied for Amesbury and Albany sludge. The higher solids content was obtained by decanting some of the clear supernatant from the original sludge samples. The experimental conditions are tabulated in Table 14.

TABLE 14. EXPERIMENTAL ARRANGEMENT FOR DRYING STUDY D-3 CONDUCTED AT 24°C (75°F) AND 60 PERCENT RELATIVE HUMIDITY

Sample Number	Material	Initial Depth, cm	Area cm^2	S_o, %
1A	Amesbury	2	770	3.15
1B	Billerica	2	770	6.20
1C	Albany	2	770	0.92
1D	Water	2	770	-
2A	Amesbury	4	570	3.15
2B	Billerica	4	570	6.20
2C	Albany	4	770	0.92
2D	Water	4	770	-
3	Albany	2	570	1.40
4	Albany	4	570	1.40
5	Amesbury	4	570	4.47
6	Amesbury	2	570	4.47

The sludge mass-time curves for the samples are shown in Figure 37 and Figure 38. Two control pans of water filled to 2 cm (0.8 in) depth for ease of handling served as controls. Toward the end of the drying run, water had to be added to the control pans to prevent them from becoming dry. This was due to evaporation of the 2 cm (0.8 in) initial depth of water in less time than some of the pans containing 4 cm (1.6 in) of sludge. The pans of sludge were divided between two tables located near the center of the environmental chamber. Each table contained one control pan of water. No difference in drying rates could be attributed to the different locations; however, as a precautionary measure, the evaporation ratios for sludge samples on a given table were calculated using as the denominator the values of the control pan of that table. Results are presented in Table 15.

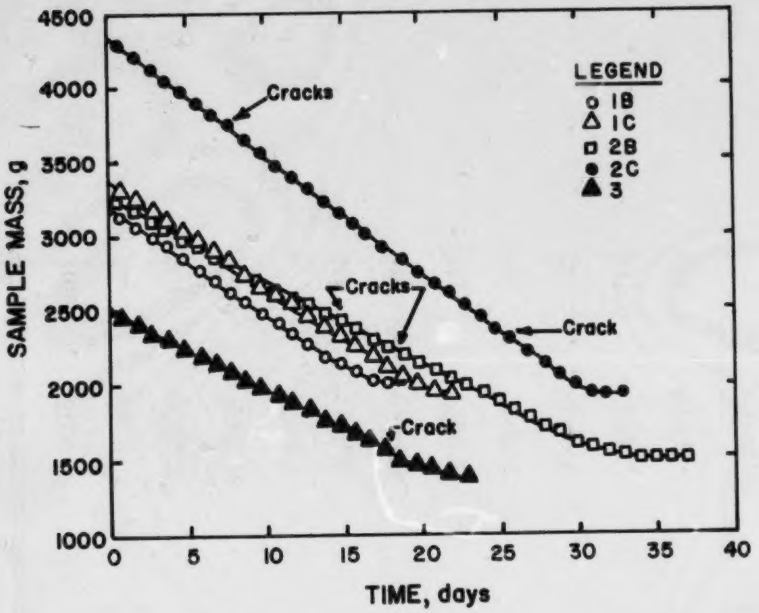

Figure 37: Sample mass versus time curves for sludges (D-3) drying at 24°C (75°F) and 60% relative humidity.

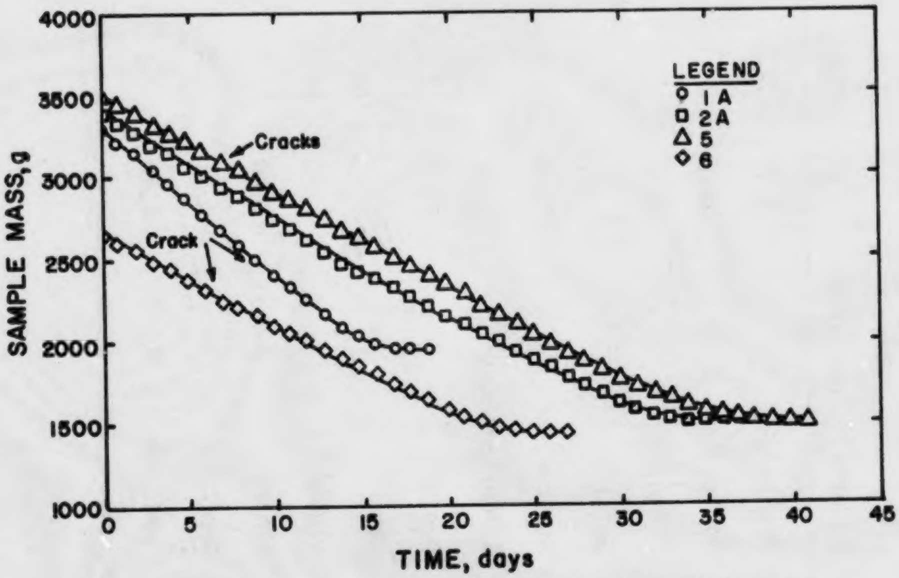

Figure 38. Sample mass versus time curves for sludges (D-3) drying at 24°C (75°F) and 60% relative humidity.

TABLE 15. SUMMARY OF RESULTS FOR DRYING STUDY D-3 CONDUCTED AT 24°C (75°F) AND 60% RELATIVE HUMIDITY.

Column Number	Material	Initial Depth, cm	Solids, % S_o	S_{CR}	S_e	U_{CR}, %	Constant-Rate Drying I_c, gm/hr-cm^2	E, %
1A	Amesbury	2	3.15	16.1	76.5	640	0.0045	118
1B	Billerica	2	6.20	21.8	81.1	360	0.0039	103
1C	Albany	2	0.92	6.1	75.0	840	0.0038	84
1D	Water	2	-	-	-	-	0.0038	-
2A	Amesbury	4	3.15	15.4	76.5	600	0.0044	116
2B	Billerica	4	6.20	23.6	82.5	270	0.0042	93
2C	Albany	4	0.92	13.2	80.8	780	0.0043	96
2D	Water	4	-	-	-	-	0.0045	-
3	Albany	2	1.40	14.3	75.0	460	0.0038	84
4	Albany	4	1.40	24.4	78.8	380	0.0040	105
5	Amesbury	4	4.47	15.4	75.3	480	0.0042	93
6	Amesbury	2	4.47	17.2	73.5	440	0.0038	84

As indicated in the sludge mass-time curves, the constant-rate drying period was dominant. The constant-rate period accounted for 80 to 85 percent of water loss and 65 to 75 percent of the drying duration.

The sludges shrunk vertically and appeared to have a free water surface in the early stages of drying. When a solids content of 7 to 10 percent was reached, cracks formed which increased the exposed surface area. The increased surface area would increase the drying rate, possibly offsetting any decrease in the drying rate due to the surface becoming dry. After cracks were formed in the sludge samples, horizontal shrinkage became more pronounced. At equilibrium the sludge samples had shrunk to irregularly shaped pieces approximately 0.5 cm thick (0.2 in) with a maximum dimension of 2 cm (0.8 in). The pieces appeared completely dry and were warped, exposing the bottom and therefore exposing a maximum surface area.

Evaporation ratios ranged from 84 to 118 percent. Pans with lower initial solids content generally dried at a faster rate than samples with higher initial solids. The larger evaporation ratios can be attributed to heat advection since these samples generally contained a larger amount of solids, W_{TS}.

Curves showing the drying rate-moisture content relationship are shown in Figures 39 and 40. After the initial temperature adjustment, the sludges remained in the constant-rate drying period while 80 to 85 percent of the water was lost. Only 15 to 20 percent of the water was lost during the falling-rate drying period. The falling-rate period was studied for theoretical interest only since the sludges could have been removed from a drying bed before the critical moisture content was reached. No distinct second critical moisture content was established, therefore, the entire falling-rate drying period was considered as one period. Both a straight line and a parabola were fitted to the falling rate portion by regression analysis. As a rule, the parabola was associated with a higher correlation coefficient. Values for the first critical moisture content ranged from 270 to 840.

Critical Moisture Content. Both straight lines and parabolas were fitted by regression analysis to the drying intensity-moisture content data in order to obtain values for the first critical moisture content. As a rule, the parabola provided a better fit and gave a higher correlation coefficient. The intersection of the parabola with the constant rate curve was taken as the critical moisture content.

Relationship for Drying Time. A relationship for calculating the drying duration in the falling-rate portion was developed assuming the relationship between drying intensity and moisture content was parabolic. This relationship can be expressed as

$$I^2 = 4pU \tag{130}$$

or

$$I = 2p^{1/2}U^{1/2} \tag{131}$$

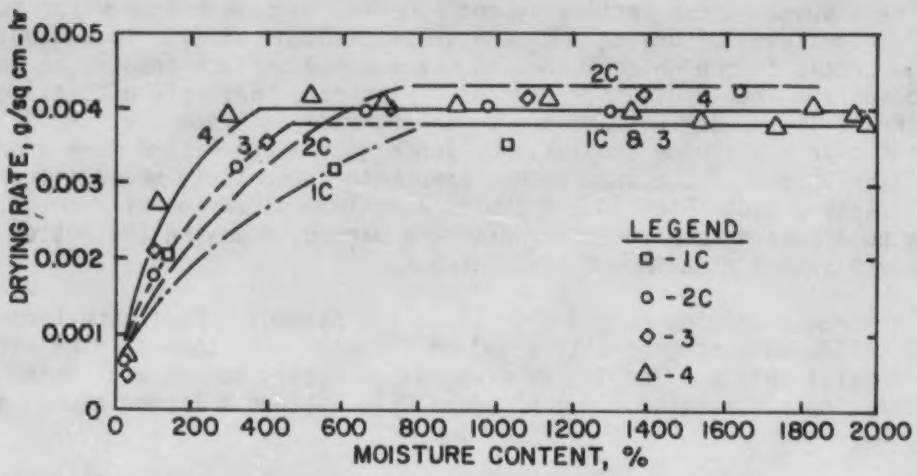

Figure 39. Drying rate curves for sludges (D-3) drying at 24^{O}C (75^{O}F) and 60% relative humidity.

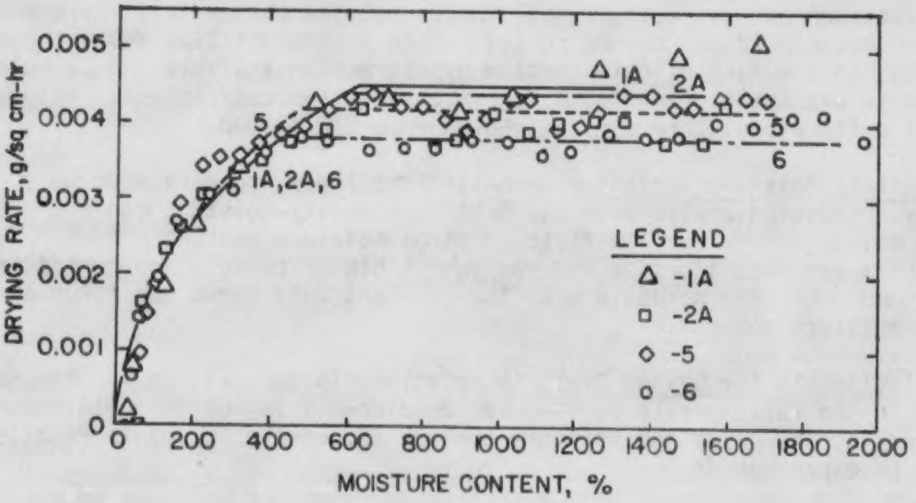

Figure 40: Drying rate curves for sludges (D-3) drying at 24^{O}C (75^{O}F) and 60% relative humidity.

$$= I_c \left(\frac{U}{U_{CR}}\right)^{1/2}$$

where

$$2p = I_c / U_{CR}^{1/2} = \text{Constant} \qquad (132)$$

From Equation 54,

$$t = \frac{W_{TS}}{100A} \int_{U_t}^{U_o} \frac{dU}{I} \qquad (54)$$

Substituting Equation 131 into Equation 54 and performing the integration gives the drying duration in the falling-rate period as

$$t_f = \frac{2W_{TS}\, U_{CR}^{1/2}}{100\ A \cdot I_c} \left(U_o^{1/2} - U_t^{1/2}\right) \qquad (133)$$

$$(U_t \leq U \leq U_{CR})$$

For a sample drying in both the constant and falling-rate period, the total drying duration would be

$$t = \frac{W_{TS}}{100AI_c} \int_{U_{CR}}^{U_o} dU + \int_{U_t}^{U_{CR}} \left(\frac{U}{U_{CR}}\right)^{1/2} dU \qquad (134)$$

$$= \frac{W_{TS}}{100A\ I_c} \left[U_o - U_{CR} + 2U_{CR}^{1/2} \left(U_{CR} - U_t^{1/2}\right)\right] \qquad (135)$$

$$(U_t \leq U_{CR} \leq U_o)$$

RESULTS OF THE COMPLEX SLUDGE DEWATERING STUDIES

Preliminary Studies. A preliminary investigation was conducted to compare simultaneously the drying and dewatering (drying and drainage) of water treatment sludge. Dewatering study DW-1 consisted of two columns of Albany sludge dewatering at 24°C (75°F) and 46 percent relative humidity. Column 1 was permitted to drain while undergoing drying but Column 2 was subjected to drying only. Column 1 contained 8.0 cm (3.1 in) of Ottawa sand supported by 2.5 cm (1.0 in) of coarse sand and 8.0 cm of small stone. The experimental arrangement is given in Table 16 along with experimental results.

The sludge mass-time curves for both columns are shown in Figure 41. Both samples remained in the constant-rate drying period for practically the entire dewatering run. The average drying rate for Column 1 was 0.0057

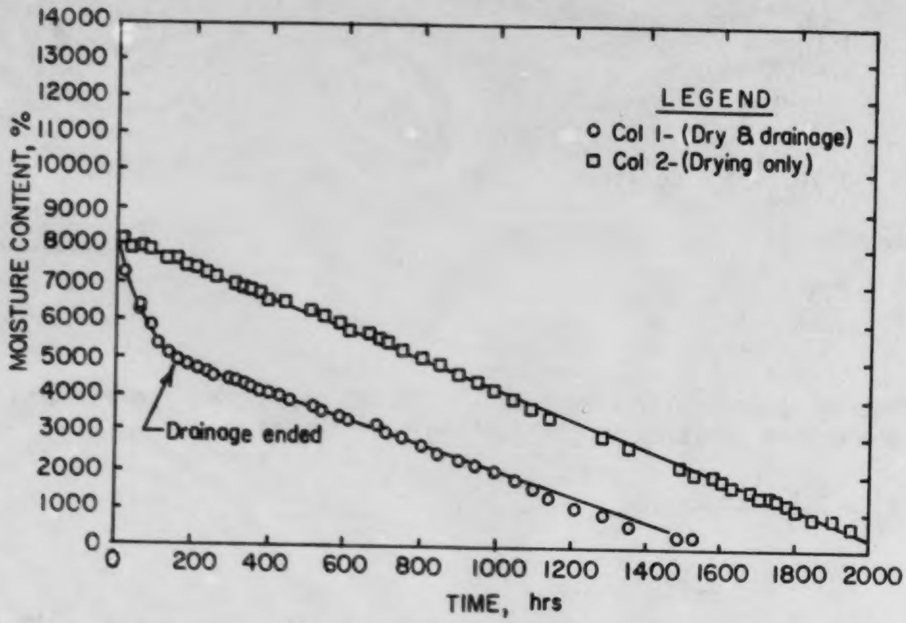

Figure 41: Sample mass versus time curves for Albany sludge dewatering at 24°C (75°F) and 46% relative humidity.

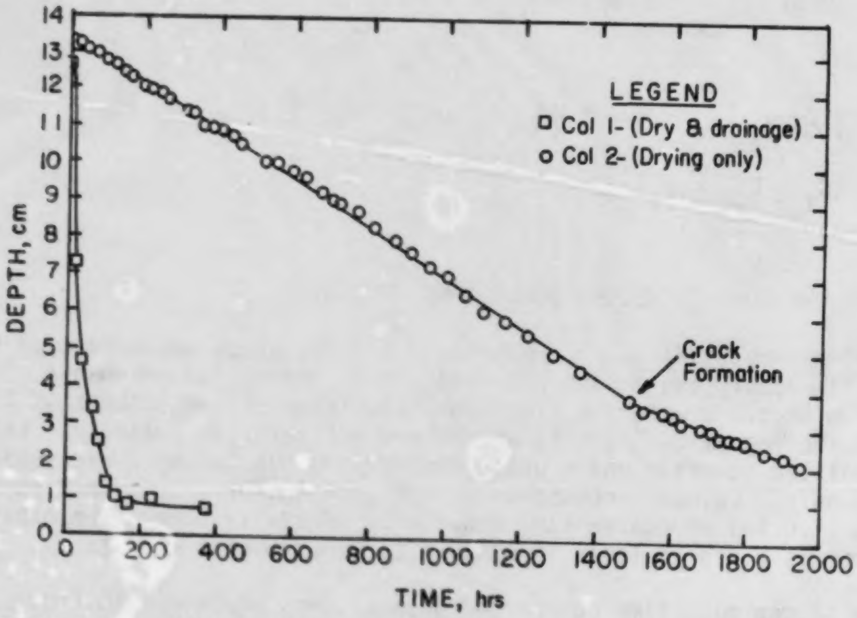

Figure 42. Change in depth of Albany sludge dewatering at 24°C (75°F) and 46% relative humidity.

gm/hr-cm^2 as compared to 0.0063 gm/hr-cm^2 for Column 2.

TABLE 16. RESULTS OF ALBANY SLUDGE, DW-1, DEWATERING AT 24^{o}C (75^{o}F) AND 46 PERCENT RELATIVE HUMIDITY

Column	1	2
Drainage permitted	Yes	No
Initial solids, %	1.22	1.22
Initial sludge depth, cm	13.5	13.5
Final solids content, %	75.5	73.8
I_c, gm/cm^2-hr	0.0057	0.0063
Support media	sand-stone	none

Shrinkage-time curves for both samples are shown in Figure 42. The depth-time curve for Column 2 was linear over most of the dewatering period, indicating constant-rate drying. Vertical shrinkage in Column 2 diminished at a solids content of 4.6 percent and horizontal shrinkage began with cracks forming throughout the depth of the sludge cake.

Dewatering Study DW-2. Dewatering study DW-2 consisted of three columns of Albany sludge draining and drying simultaneously and one column of water used as a control. In addition, three large pails of water in various locations within the environmental chamber were evaporated concurrently as controls. Temperature and relative humidity remained constant at 24° ± 0.5°C (75 ± 1°F) and 30 ± 2 percent, respectively.

The dewatering columns contained 45.7 cm (18 in) of sludge on 11.5 cm (4.5 in) of Ottawa sand supported by 3.8 cm (1.5 in) of stone. The initial solids content of the sludge was 1.3 percent. The initial depth of water in the control column was adjusted to 30 cm (11.8 in) in order to eliminate any "freeboard" effects caused by the surfaces of the columns being at different elevations after drainage had occurred in the sludge columns. No significant difference in evaporation rates was seen in the three large pails of water, thus indicating constant drying conditions. The average evaporation rate for the three pails was 0.0064 gm/hr-cm^2.

The mass of the dewatering columns was determined periodically after drainage ended. The sludge mass-time curves for the columns are shown in Figure 43. Column 3 was omitted from the data analysis since some water was accidentally lost early in the study. The sludge columns remained in the constant rate drying period throughout the drying run. The average drying rate for the two columns of sludge was 0.00524 gm/hr-cm^2 and the average evaporation ratio was 87.5 percent. At the end of the drying run the columns were dismantled and the sludge cakes carefully removed. The sludge cakes appeared dry and could be readily picked up by hand. However, the average

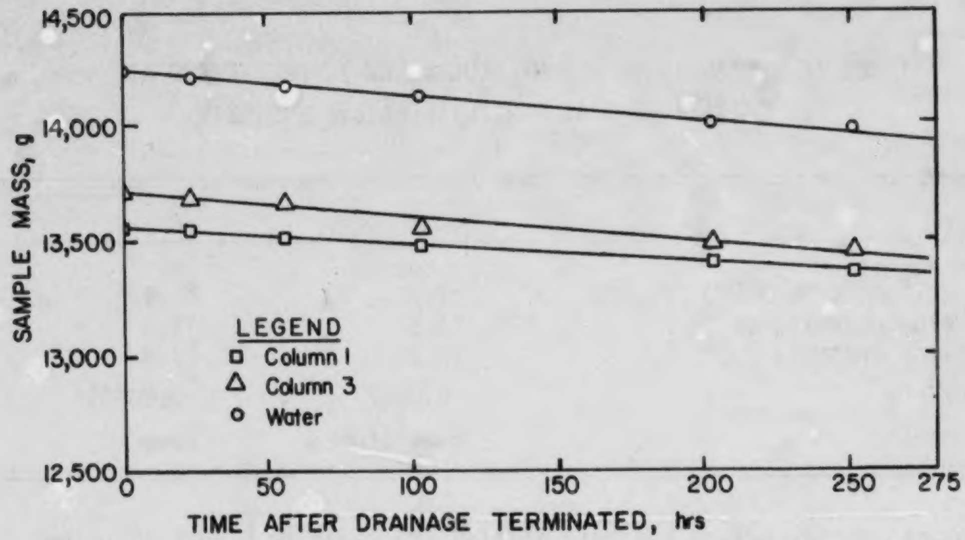

Figure 43: Sample mass versus time curves for drying period of dewatering study DW-2.

solids content was only 10-12 percent, demonstrating that this particular sludge contained large amounts of bound water. A thin layer approximately 5 mm thick and lighter in color encased the sludge mass causing the sludge cake to appear to be drier on the outside than in the interior. This layer was removed from one cake, cut into small pieces and a gravimetric solids content analysis performed. The solids content was 10.7 percent in the interior and 12.3 percent in the outer layer.

The accumulated volume of filtrate for each of the three sludge columns is shown in Figure 44 and the variation of total head (H_o) is shown in Figure 45. The predicted head values using empirical media factors and Equation 46 are shown as solid lines.

Dewatering Study DW-3. Dewatering study DW-3 consisted of 9 columns of sludge and 2 columns of water dewatering under controlled conditions. Temperature and relative humidity were maintained at 25 ± 1°C and 35 ± 2 percent. Air was uniformly supplied to each column to expedite the dewatering process. Each column contained 9 cm of Ottawa sand supported by 2.5 cm of stone. The experimental conditions and results are shown in Table 17.

The two columns of water (columns 4 and 8) had an average drying rate of 0.0097 gm/hr-cm^2 as calculated from the slope of the sludge mass-time data. There was no significant difference in the drying rates of the two columns of water, thus indicating constant drying conditions. The evaporation rate for water at 24°C (75°F) and 35 percent relative humidity, with negligible wind and sunlight, is 0.05 cm/day from Figure 14. Converted to comparable

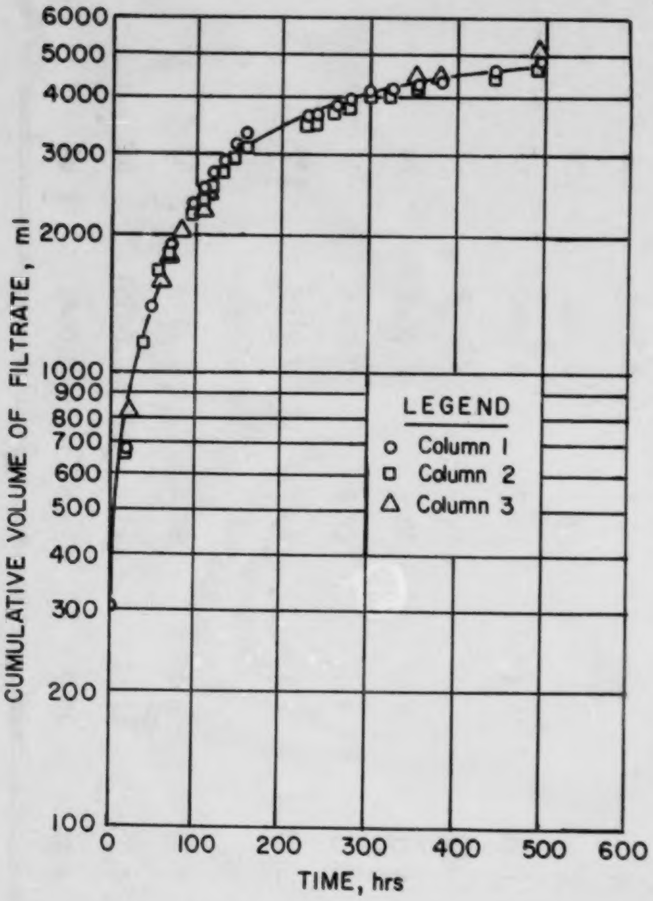

Figure 44: Cumulative volume of filtrate versus time for Albany sludge dewatering on Ottawa sand (DW-2).

units, this would be 0.0021 gm/cm^2-hr, considerably less than the control column value of 0.0097 gm/cm^2. If the vertical air stream alone accounted for the difference in drying rates, the equivalent horizontal wind velocity from Figure 14 would be 12 km per hour (7.5 mi per hour) for the control columns.

Dewatering with and without drainage was studied with Billerica sludge in columns 5 and 6, and column 1, respectively. The drying rates for columns 5 and 6 (drying and drainage) were lower than column 1 (drying only). This could have resulted from the higher solids content in columns 5 and 6 due to drainage or the larger amount of freeboard due to the smaller initial depth. Columns 5 and 6 differed significantly in their drying rates, column 6

TABLE 17. DEWATERING STUDY DW-3, RESULTS OF FOUR SLUDGES DEWATERING AT 24°C (75°F) AND 35% RELATIVE HUMIDITY

Column Number	Material	Initial depth inches	Solids, %			I_c gm/cm^2-hr	E, %
			Initial	After Drainage	Final		
1*	Billerica	18	6.10	-	12.4	0.0128	136
2*	Albany	18	1.86	-	3.7	0.0120	128
3	Albany	12	1.86	5.8	15.2	0.0070	74
4*	Water	12	-	-	-	0.0093	-
5	Billerica	12	6.10	10.4	20.6	0.0075	79
6	Billerica	12	6.10	9.1	22.8	0.0085	91
7	Amesbury	12	3.67	7.1	20.6	0.0115	122
8*	Water	12	-	-	-	0.0096	-
9	Amesbury	12	3.67	6.2	33.4	0.0148	157
10	Murfreesboro	12	4.80	41.0	81.0	0.0055	58
11	Murfreesboro	12	4.80	29.2	92.5	0.0060	64

*Denotes Drying Only.

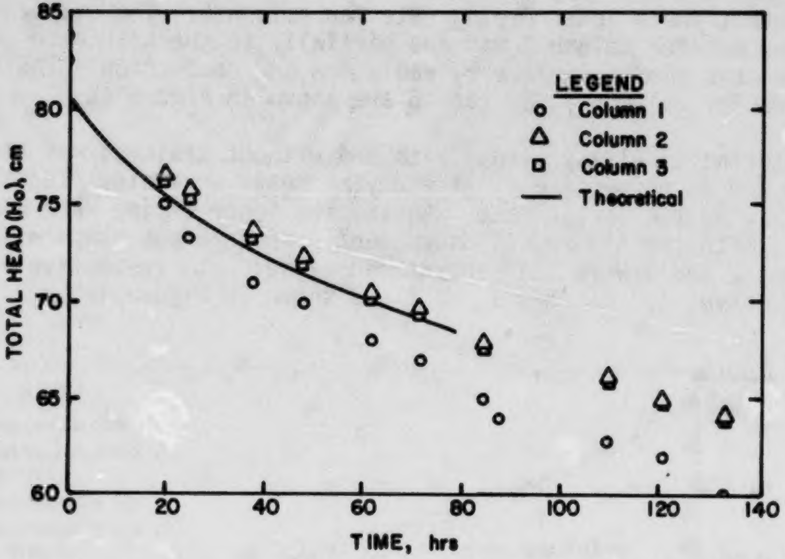

Figure 45: Drainage curves for 45.7 cm of Albany sludge (DW-2) dewatering on Ottawa sand.

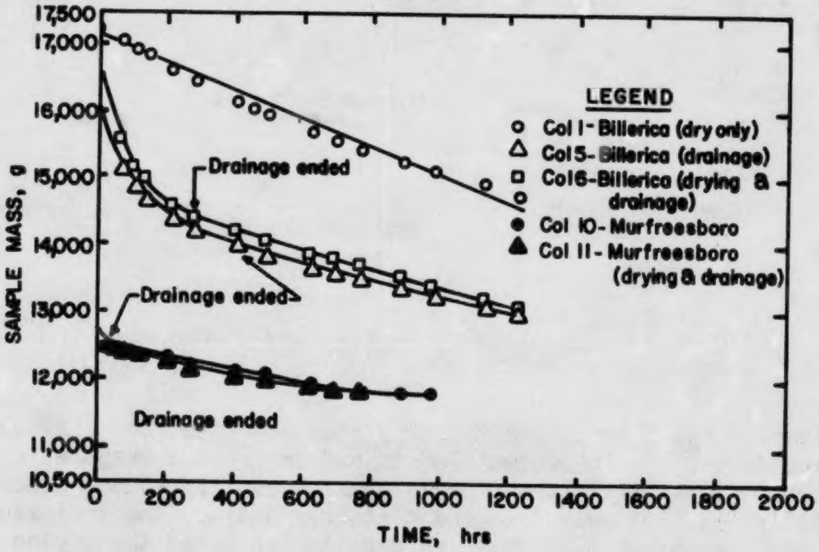

Figure 46: Sample mass versus time curves for sludges (DW-3) dewatering at 24°C (75°F) and 35% relative humidity.

having the faster rate. The amount of water lost by drainage was larger for column 5 than the drainage volume from column 6. This resulted in a higher solids content and a lower drying rate for column 5. The evaporation ratio of 137 percent for column 1 was due partially to the high rate of heat transfer to the dark sludge surface by radiation and conduction. The sludge mass-time curves for columns 1, 5, and 6 are shown in Figure 46.

Dewatering of Albany sludge with and without drainage was studied in columns 3 and 2, respectively. The drying rates were significantly different, column 2 having the larger rate. Again, the lower drying rate occurred in the column with the higher solids content. The average evaporation ratios for columns 2 and 3 were 128 percent and 74 percent, respectively. Sludge mass-time curves for columns 2 and 3 are shown in Figure 47.

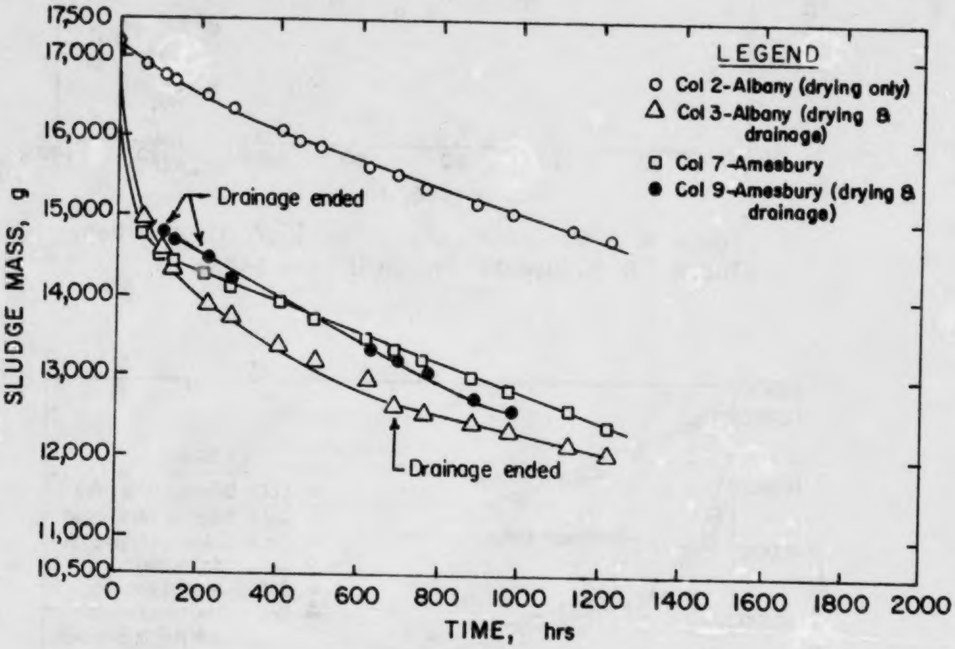

Figure 47: Sample mass versus time for sludges (DW-3) dewatering at 24°C (75°F) and 35% relative humidity.

Columns 7 and 9 contained Amesbury sludge dewatering by simultaneous drying and drainage. These two sludges had an average evaporation rate of 140 percent. Immediately after drainage stopped, the sludge cakes shrunk horizontally, pulling away from the container walls. The shrinkage left a large exposed porous surface which greatly increased the drying area. The sludge was dark in color, thus, some of the increased drying rate may be attributed to heat advection. The mass-time curves for columns 7 and 9 are shown in Figure 47.

Murfreesboro sludge was dewatered by drying and drainage in columns 10 and 11, respectively. The sludge dewatered very rapidly, drainage being completed in approximately 20 hours. Although the sludge initially contained 4.8 percent total solids, the solids settled rapidly to a dense layer approximately 3 centimeters thick, leaving a large clear supernatant. The solids content was approximately 35 percent and the depth of sludge cake was 2.3 cm when drainage ended. Although some vertical cracks appeared, the sludge cake did not have a large exposed drying surface. The average evaporation rate was 62 percent, the smallest of any sludges investigated. The sludge mass-time curves for columns 10 and 11 are shown in Figure 46.

The variation of total head (H_0) for the sludge samples is shown in Figure 48 along with predicted H_0 values from Equation 47. The time span covered by Equation 47 is considerably less than the total time span for total drainage. This is due to two factors: first, approximately 25 percent of the filtrate came from the distilled water used initially to saturate the sand columns; second, Equation 47 does not cover the entire drainage period but is valid only until the decreasing sludge surface coincides with the increasing sludge cake. The remaining drainage, affected by consolidation and shrinkage, is unaccounted for by the drainage model.

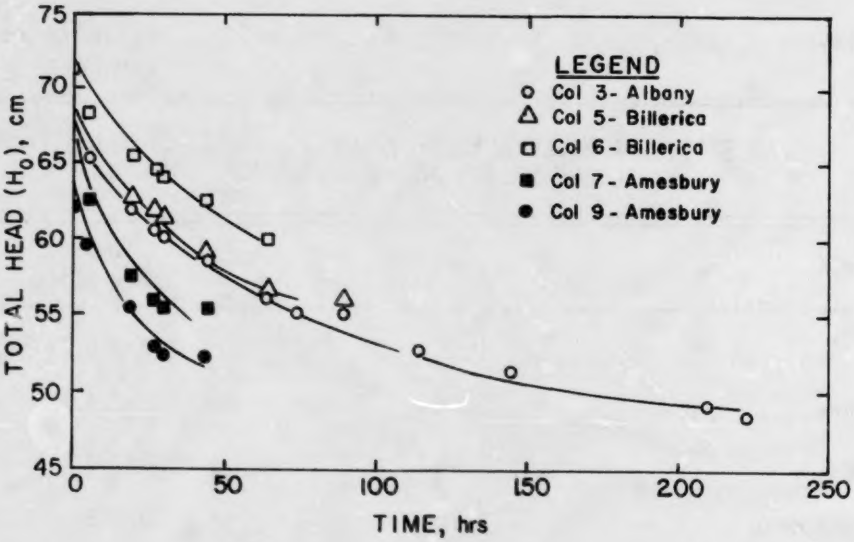

Figure 48: Drainage curves for 30.8 cm of sludge (DW-3) dewatering on Ottawa sand.

MOISTURE AND SOLIDS PROFILES

Preliminary Measurements. The gamma-ray attenuation method of moisture and solids profile measurement required prior determination of attenuation

TABLE 18. ATTENUATION COEFFICIENTS AT 0.661 Mev FOR THE VARIOUS MATERIALS

Material	μ, cm^2/gm	Standard Deviation	Reference
Albany sludge	0.0780	0.0048	Data
Amesbury sludge	0.0792	0.0050	Data
Billerica sludge	0.0781	0.0031	Data
Average value for sludges	0.0784	-	Data
Ottawa sand	0.0765	0.0060	Data
Water	0.0842	0.0007	Data
Water	0.0839	-	Adrian
Water	0.0815	0.0008	Davidson, *et al*.
Soil (average value)	0.0775	-	Reginato and Van Bavel

TABLE 19. PARTICLE DENSITY VALUES, g/cm^3, FOR WATER TREATMENT SLUDGE SOLIDS AND OTTAWA SAND

Source	ρ, gm/cm^3	Standard Deviation
Billerica	1.95	0.025
Amesbury	2.64	0.049
Albany	2.36	0.023
Murfreesboro	2.75	0.019
Ottawa sand	2.64	0.009

coefficients and particle densities. The energy spectrum of the Cs-137 source was determined as a check on the calibration and performance of the counting equipment. The familiar Cs-137 spectrum, as shown in Figure 49, was determined.

The attenuation coefficients were determined by measuring the attenuation of the gamma beam through water in the small plastic boxes. A plot of N/N_0 for 16 minute counts through water is shown in Figure 50. The slope of the line is equal to $\mu\rho$. The values for attenuation coefficients obtained are shown in Table 18 along with the values from the literature.

Particle density measurements of sand and dry sludge solids were made by the specific gravity method. The results are presented in Table 19.

Moisture Movement in Sand. Moisture profiles were determined for the sand layers of the dewatering columns by the attenuation method. The sand layers remained saturated until drainage from the sludge layers terminated. After drying caused cracks to appear in the sludge layer, or the sludge cake receded from the column walls, the water in the sand layer was lost. The sand layers were devoid of water at the termination of the drying period.

The method for measuring water content in sand was tested using Ottawa sand in the small plastic boxes. Values of water content in the sand as determined from Equation 117 are shown in Table 20 along with values obtained by volumetric measurement. There was a 2.6 percent difference between the two methods. The sludge variation in water content (θ) at various depths was attributed to differences in the bulk density of the compacted sand.

TABLE 20. SUMMARY OF WATER CONTENT MEASUREMENTS FOR OTTAWA SAND BY THE ATTENUATION METHOD

Ratio of distance from bottom to total length, x/L	Water content (θ), gm/cm^3
0.20	0.36
0.40	0.34
0.60	0.37
0.80	0.42
Average (Attenuation Values)	0.37
Average (Volumetric Measurement)	0.38
Difference in two methods, %	2.6

Profiles of water content in the supporting sand layers were vertical during the initial dewatering stages, as shown for column 3 in Figure 51 and column 5 in Figure 52. Water content remained constant, during the

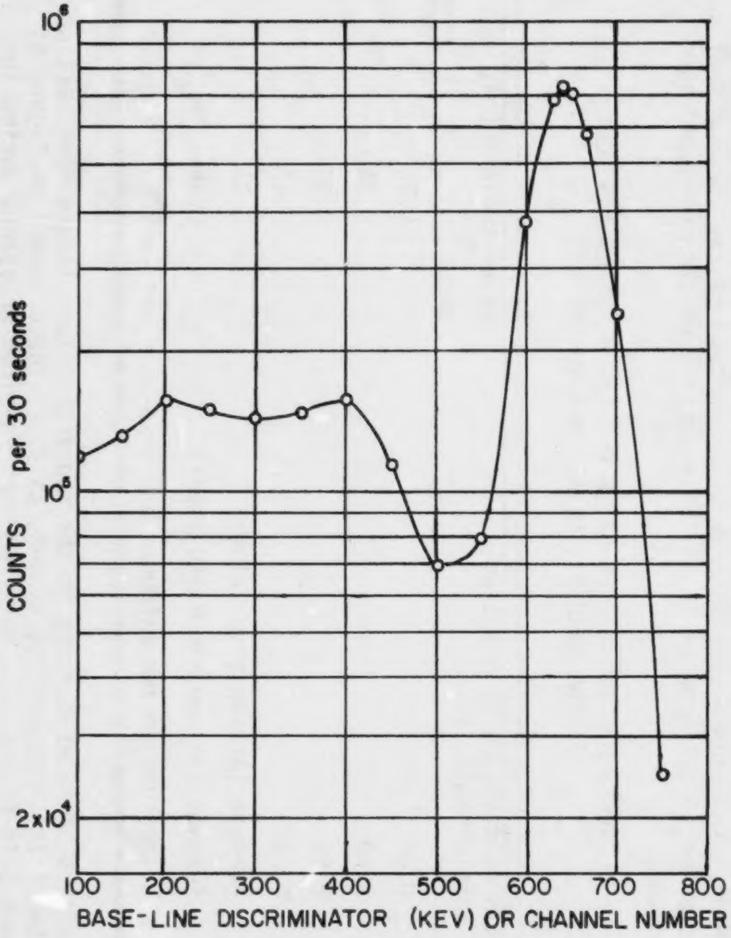

Figure 49: Energy spectrum for 250 millicuries Cs-137 source.

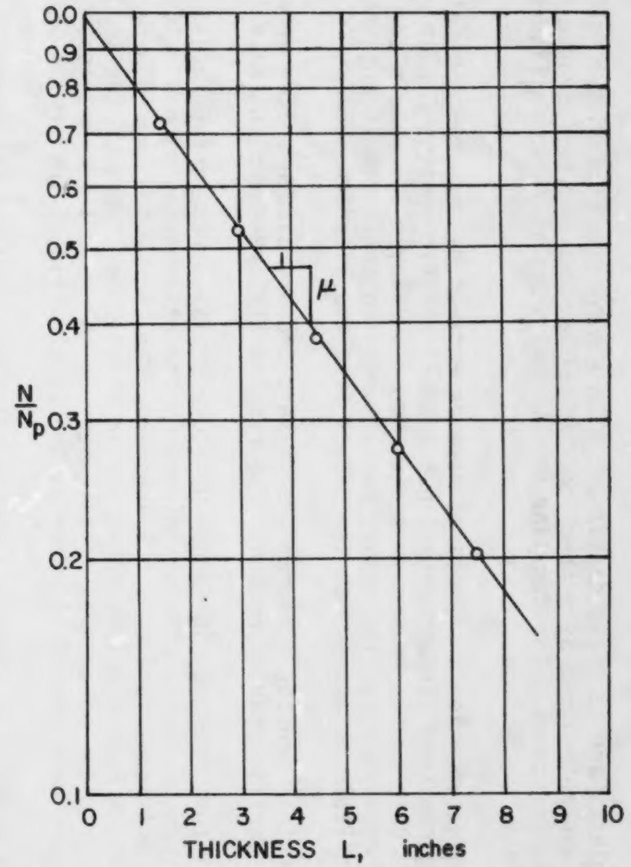

Figure 50: Variation of the ratio N/N_p with thickness of water at 0.661 Mev.

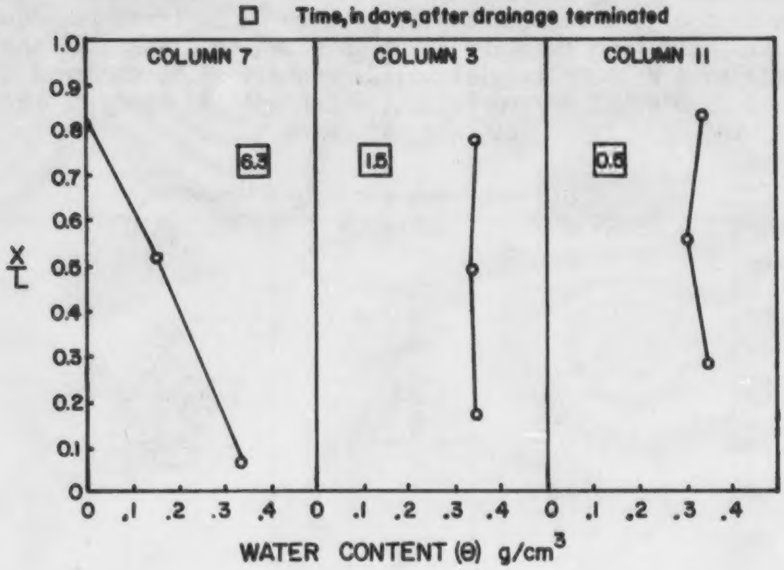

Figure 51: Profile of water content in sand layers (DW-3) after drainage terminated.

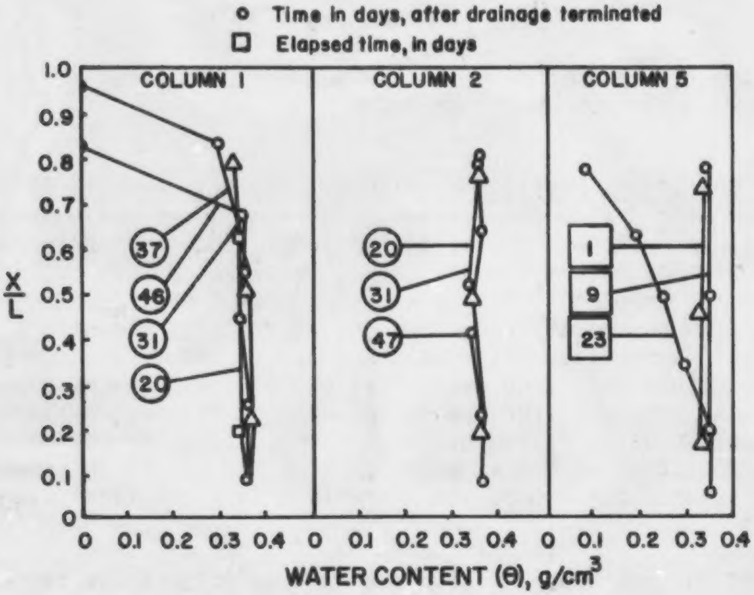

Figure 52. Profiles of water content in sand layers for dewatering study DW-3.

drying of sludge when drainage was not permitted, as shown in column 2 in Figure 52, when dewatering occurred by drying only. After enough water was lost from the sludge to cause the sludge cake to recede from the container walls, water was lost from the sand layer as shown in Figures 52 and 53. Column 2, containing a lower initial solids content (1.86 compared to 6.1 percent for column 1) did not dry sufficiently during this study to shrink horizontally, thus the sand layer remained saturated.

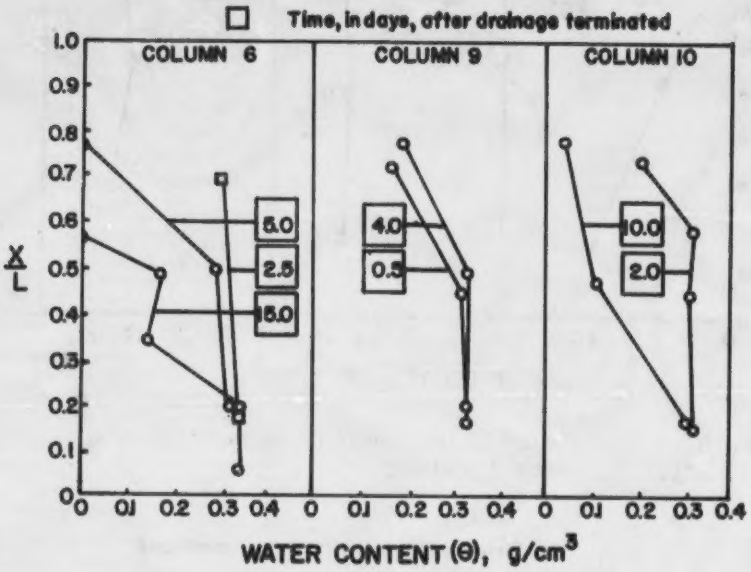

Figure 53: Profiles of water content in sand layers (DW-3) after drainage terminated.

Moisture and Solids Profiles in Sludge. The moisture and solids profiles of sludge undergoing drying and dewatering were measured periodically by the attenuation method. Since the mass of the samples had been determined periodically, the average values for solids and moisture content could be calculated. Measurements obtained in the early stages of dewatering agreed well with gravimetric measurements and showed no significant variations in the moisture and solids profile. As dewatering progressed, the sluge cake receded from the column walls and horizontal and vertical cracks appeared. Since theoretical equations for the solids content had been derived on the basis of the column being filled with water or solids, the net result of shrinkage and formation of cracks was to change the sludge thickness, making the gamma ray attenuation method inapplicable during the final stages of dewatering.

The method for measuring moisture and solids content was tested using Billerica sludge in the small plastic boxes. The sludge was thoroughly mixed initially and an aliquot taken for solids content measurement by the gravimetric method (oven drying). The solids profile as determined by the attenuation method is shown in Figure 54 along with the average solids content

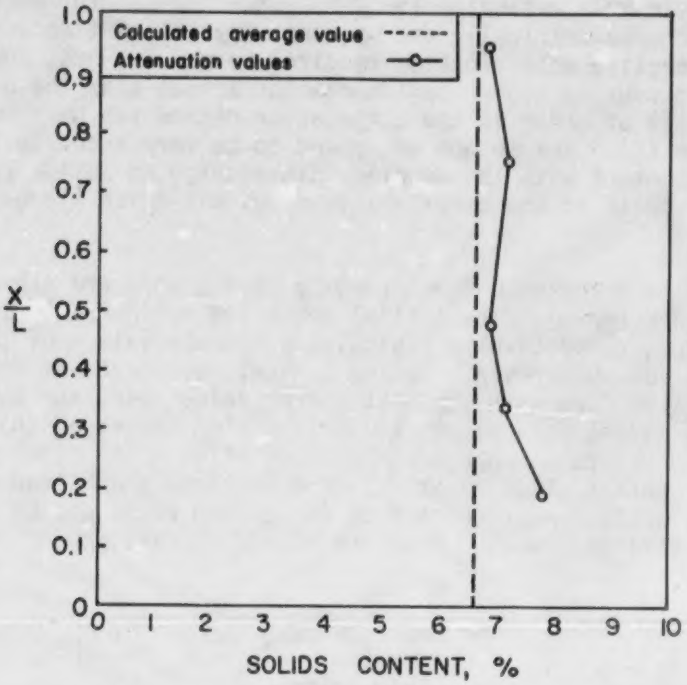

Figure 54: Variation of solids content with depth for Billerica sludge.

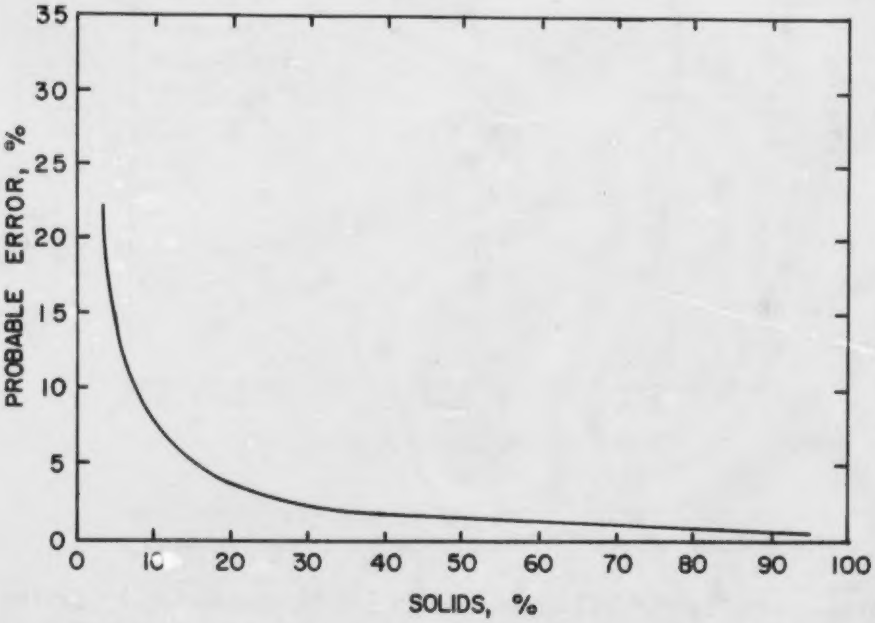

Figure 55: Error analysis.

determined by gravimetric methods. The difference between the average solids content determined gravimetrically and by gamma-ray attenuation was 6.0 percent. Since the profile determination required some 1.5 hours, some sedimentation occurred causing higher solids concentrations near the bottom of the sample. An analysis of error in the attenuation method was performed and is described in Clark (4). The method was found to be very accurate for high values of solids content with the accuracy diminishing as solids content decreased. The results of the error analysis for Billerica sludge are shown in Figure 55.

Solids profiles for sludge dewatering by drying only are shown in Figure 56 for Albany sludge (DW-3). The initial depth and solids content were 40.6 cm and 1.86 percent, respectively. Calculated average values of the solids content are shown for comparison. During the initial stages of drying, the solids profile was uniform with somewhat higher values near the bottom of the column due to sedimentation. As the drying time increased the solids became more varied due to shrinkage and consolidation. The final profile shows the solids content after horizontal and vertical cracks had formed. Values for solids content near the top of the column could not be determined after the sludge cake had receded from the sludge surface, changing the thickness.

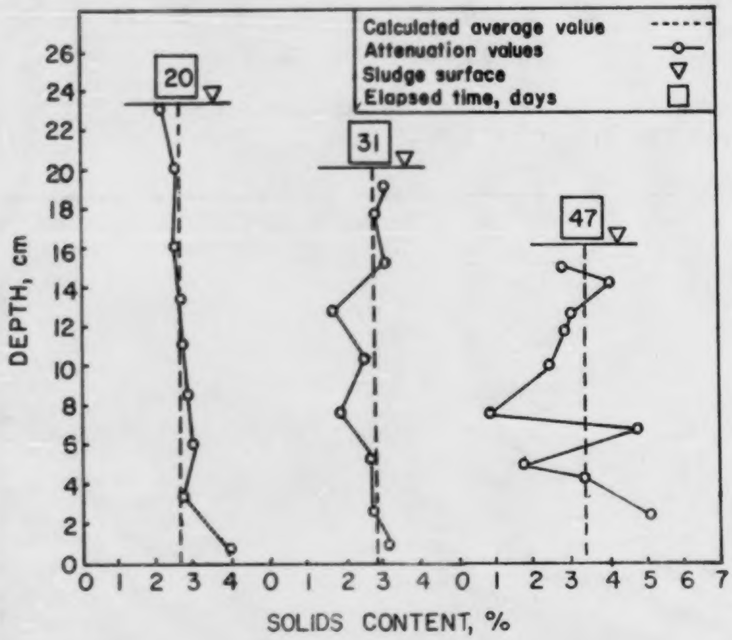

Figure 56: Variation of solids profiles with time for Albany sludge (DW-3) drying on Ottawa sand.

Solids profiles for Billerica sludge (DW-3) dewatering by drying only are shown in Figure 57. The initial depth and solids content were 40.6 cm and 6.10 percent, respectively. The sludge cake shrunk both horizontally and vertically during dewatering.

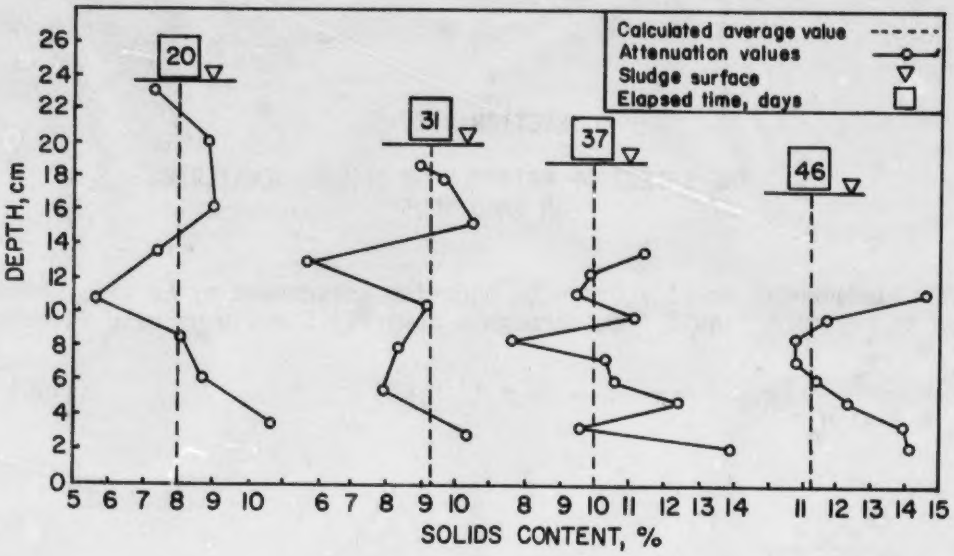

Figure 57. Variation of solids profile with time for Billerica sludge (DW-3) drying on Ottawa Sand.

REFERENCES

1. Standard Methods for the Examination of Water and Wastewater, 12th ed., American Public Health Association, New York, 1965.

2. Nebiker, J. H., Sanders, T. G., and Adrian, D. D. An Investigation of Sludge Dewatering Rates. Journal Water Pollution Control Federation, August, 1969, Part 2.

3. Quon, J. E. and Tamblyn, T. A. Intensity of Radiation and Rate of Sludge Drying. Journal of the Sanitary Engineering Division, A.S.C.E., 91, No. SA2, April, 1965.

4. Clark, E. E. Water Treatment Sludge Drying and Drainage on Sand Beds. Ph.D. dissertation, University of Massachusetts, Amherst, 1970.

SECTION VIII

THE EFFECT OF RAINFALL ON SLUDGE DEWATERING ON SAND BEDS

The fundamental gravity drainage equation, discussed by Lo (1), which is used to describe liquid flow through a compressible sludge cake is:

$$t = \frac{\mu C R_c}{(\sigma+1) H_c^{\sigma}} [H_o^{\sigma+1} + \sigma H^{\sigma+1} - (\sigma + 1) H_o H^{\sigma}] \qquad (136)$$

where

$$C = \frac{g S_c S_o}{100(S_c - S_o)}$$

μ = filtrate viscosity (poises)

R_c = specific resistance of cake at reference head loss, $H_c (T^2/M)$

σ = coefficient of compressibility

H_o = initial hydraulic head (L)

H_c = reference hydraulic head (L)

H = hydraulic head at time t (L)

ρ = density of water (M/L^3)

S_o = initial solids content of sludge (%)

S_c = solids content of cake (%)

In this section, the effect of rainfall on the rate of drainage is incorporated into the drainage equation in order to establish a drainage model with daily rainfall as a stochastic input.

The addition of rainfall on the surface of sludge may not only prolong the drainage time but may also dilute the suspended sludge. According to the basic equations, this diluting effect will increase the rate of drainage. As a result, the following assumptions are important to the behaviour of the dewatering system. For simplicity in analysis, two models (mixing and ponding) were studied to represent two extreme conditions of water on the surface of the sludge. In the ponding model it was assumed that water and sludge were immiscible, resulting in ponding of rainfall on the surface as supernatant.

Mixing model for sludge drainage. It is assumed that R_1 units of rainfall are added to the surface of draining sludge at time t_1, in which a cake has been formed at sludge depth H_1 as shown in Figure 58.

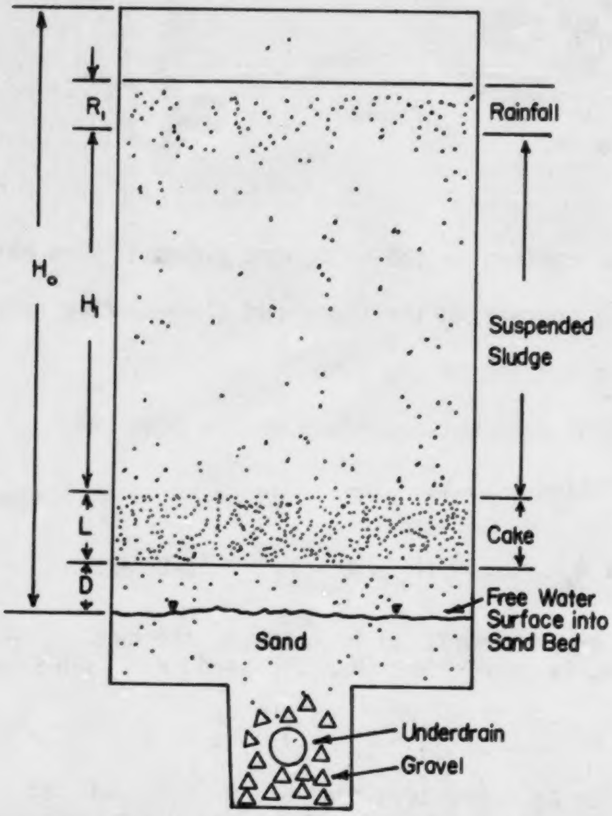

Figure 58: Definition sketch of mixing drainage.

It is seen that filter resistance after time t_1 will gradually increase as filtration proceeds and the amount of cake formed increases. Based on the basic drainage equation, friction losses can be written in terms of specific resistance and the discharged filtrates. If H_{f1} represents the friction loss of the formed cake and H_{f2} the friction loss of the forming cake, these two equations will be:

$$H_{f1} = \frac{dv}{dt}[\mu \; C \; R \; (H_0 + D - H)/ \; (\rho \, g \, A)] \qquad (137)$$

$$H_{f2} = \frac{dv}{dt} [\mu\ C\ R'\ (H_1 + D + R_1 - H)/(\rho\ g\ A)] \quad (138)$$

$$C = \rho\ g\ S_o\ S_c/(S_c - S_o) \cdot 100 \quad (139)$$

$$C' = \rho\ g\ S'_o\ S_c/(S_c - S'_o) \cdot 100 \quad (140)$$

$$R = R_c\ (\frac{H_o}{H_c})^\sigma \quad (141)$$

$$R' = R_c (\frac{H}{H_o})^\sigma \quad (142)$$

where

S_o = solids content in the suspended sludge before raining

S'_o = solids content in the suspended sludge after raining

S_c = solids content in the cake

D = depth of free water surface on the sand bed

Since total friction loss $H_f = H_{f1} + H_{f2}$

$$\frac{dv}{dt} = \rho\ g\ A\ H_f / \{(\mu\ CR)\ (H_o + D - H_1) + (\mu\ C'\ R')\ (H_1 + D + R_1 - H)\} \quad (143)$$

The term dv/dt may be rewritten in terms of the head as -AdH/dt and the total friction loss H_f is none other than the head, H. Then Equation 143 becomes:

$$\frac{dH}{dt} = -\ \rho g\ H / \{(\mu\ CR)\ (H_o + D - H_1) + (\mu\ C'\ R')\ (H_1 + D + R_1 - H)\} \quad (144)$$

This equation can be integrated from $H = H_1 + R_1 - E_1$ at $t = t_1$ to $H = H$ at $t = t_2$ where E_1 is the height of sludge lost due to evaporation during the period t_1. The equation becomes

$$t_2 - t_1 = \frac{\mu\ R_c}{100\ H_c^\sigma\ \sigma(\sigma+1)} [\sigma(\sigma+1)\ \frac{S_c\ S_o}{(S_c - S_o)}\ H_1^\sigma\ (H_o + D - H_1)$$
$$\log\ (\frac{H_1 + D + R_1 - E_1}{H}) + (\sigma+1) \frac{S'_o\ S_c}{S_c - S'_o}\ (H_1 + D + R_1)$$
$$((H_1 + D + R_1 - E_1)^\sigma - H^\sigma)\ - (\frac{S'_o\ S_c}{S_c - S'_o}((H_1 + D$$
$$+ R_1 - E_1)^{\sigma+1}\ - H^{\sigma+1})] \quad (145)$$

Where S'_o, the solids content in the suspended sludge after raining, will depend on the amount of rainfall, the height of suspended sludge and the initial solids content. An attempt has been made to express this post-rain solids content in terms of known parameters.

By definition, the post-rain solids content can be written as

$$S_o = \frac{W_s\ 100}{W_w + \rho\ g\ A\ R_1 + W_s}$$

or

$$W_s = \frac{S'_o}{100 - S'_o} (W_w + \rho\ g\ A\ R_1) \qquad (146)$$

where W_s = the weight of dry solid material in the suspension after raining

W_w = the weight of water in the suspension before raining.

Since the solid material will be the same before or after raining, the W_s may also be expressed in terms of the initial solids content as:

$$W_s = \frac{S_o}{100 - S_o} W_w \qquad (147)$$

Substituting the above equation into Equation 146 gives

$$\frac{S_o}{100 - S_o} W_w = \frac{S'_o}{100 - S'_o} (W_w + \rho\ g\ A\ R_1) \qquad (148)$$

W_w, the amount of water in the suspension, can be expressed as the total amount of water on the drying bed minus the amount of water in the cake and the amount discharged as filtrate. Since the total volume of water in the sludge was found to be

$$A\ H_o \left(\frac{\rho_s \left(1 - \frac{S_o}{100}\right)}{\frac{S_o \rho}{100} + \rho_s \left(1 - \frac{S_o}{100}\right)} \right)$$

therefore

$$W_w = \rho\ g\ A\ H_o \left(\frac{\rho_s \left(1 \quad \frac{S_o}{100}\right)}{\frac{S_o}{100}\rho + \rho_s \left(1 - \frac{S_o}{100}\right)} \right) - W_{sc} \frac{100 - S_c}{S_c}$$
$$- A\ \rho\ g\ (H_o - H) \qquad (149)$$

where W_{sc} denotes the dry solid material in the cake, and ρ_s the density of total solids. Since C_o has been defined in the previous section as the dry solid material in the cake per unit volume of filtrate, W_{sc} can be replaced by the term $C_o\ A\ (H_o - H)$. Equation 149 then becomes

$$W_w = \rho\ g\ A\ H_o\ \left(\frac{\rho_s\ (1 - \frac{S_o}{100})}{\frac{S_o}{100}\ \rho + \rho_s\ (1 - \frac{S_o}{100})}\right) - C_o\ A\ (H_o - H_1).$$

$$\left(\frac{100 - S_c}{S_c}\right) - A\ \rho\ g\ (H_o - H_1) \qquad (150)$$

Inserting $C_o = \frac{\rho\ g\ S_o\ S_c}{100\ (S_c - S_o)}$ into Equation 150

$$W_w = \rho\ g\ A\ H_o\ \left(\frac{\rho_s (1 - \frac{S_o}{100})}{\frac{S_o}{100}\ \rho + \rho_s\ (1 - \frac{S_o}{100})}\right) + \frac{\rho\ g\ S_o\ A}{100(S_c - S_o)}$$

$$(H_o - H_1)\ (100 - S_c) - A\ \rho\ g\ (H_o - H_1) \qquad (151)$$

Substituting Equation 151 into Equation 148 yields

$$\frac{S_o}{100 - S_o} = \frac{S_o'}{100 - S_o'}\ [(H_1 - \frac{S_o\ \rho\ H_o}{S_o\ \rho + \rho_s\ (100 - S_o)} + \frac{S_o (100 - S_c)\ (H_o - H_1)}{100 (S_o - S_o)})]/$$

$$[(H_1 - \frac{S_o \rho\ H_o}{S_o\ \ \rho + \rho_s (100 - S_o)} + \frac{S_o (100 - S_c)\ (H_o - H_1)}{100\ (S_c - S_o)})] \qquad (152)$$

If $G = H_1 - \frac{S_o\ \rho\ H_o}{S_o\ \rho + \rho_s (100 - S_o)} + \frac{S_o (100 - S_c)\ (H_o - H_1)}{100\ (S_c - S_o)}$

Then

$$S_o' = \frac{S_o\ G}{(G + R - \frac{S_o}{100}\ R_1)} \qquad (153)$$

Equation 153 is an expression of the post-rain solids content in terms of known parameters S_o, H_o, H_1, R_1, ρ_s, ρ.

For the general case, the above drainage equation can easily be extended to the condition in which there are many rainy days adding various amounts of rainfall to the surface of the sludge.

If the friction loss due to resistance of the various cakes formed after each rainfall is denoted as H_{fn}, $n = 0, 1 \ldots n$ then,

$$\begin{aligned} H &= h_{f1} + h_{f2} + \ldots\ldots + h_{fn} \\ &= dv/dt\,[\mu\, C_o\, R_c\, (H_1/H_c)^{\sigma} (H_o + D + R_1 - H_1) + \\ &\qquad \mu\, C_1\, R_c\, (H_2/H_c)^{\sigma}\, (H_1 + D + R_2 - H_2) + \\ &\qquad \ldots\ldots + \ldots\ldots + \qquad (154) \\ &\qquad \mu C_{n-1}\, R_c\, (H_n/H_c)^{\sigma}\, (H_{n-1} + D + R_n - H)]/\rho\, g\, A \end{aligned}$$

Rearranging this equation;

$$\frac{dv}{dt} = \frac{\rho\, g\, A\, H}{\dfrac{\mu\, R_c}{100\, H_c^{\sigma}}\left[\sum_{n=0}^{n+1} C_n\, H_{n+1}\, (H_n + D + R_{n+1} - H_{n+1})\right]} \qquad (155)$$

which after integration yields:

$$\begin{aligned} t_{n+1} = t_n + \frac{R_c}{100H_c^{\sigma}}\{([\sum_{n=0}^{n} \frac{S_n\, S_c}{S_c - S_n}(H_{n+1})\, (H_n + D + R_{n+1} - H_{n+1}) \\ \log\left(\frac{H_n + R_n + D - E_n}{H}\right)] + \frac{S_n\, S_c}{S_c - S_n}\,[(H_n + D + R_n - E_n)^{\sigma} \\ - H^{\sigma}])\} \qquad (156) \end{aligned}$$

where S_n is;

$$S_n = \frac{S_{n-1}\left(H_n - \dfrac{S_n\, \rho\, H_{n-1}\rho}{S_{n-1}\, \rho + \rho_s(100 - S_n - 1)} + \dfrac{S_{n-1}(100 - S_c)\, (H_{n-1} - H_n)}{100\, (S_c - S_{n-1})}\right)}{\left(H_n - \dfrac{S_{n-1}\, H_{n-1}\, \rho}{S_{n-1} + \rho_s(100\, S_{n-1})} + \dfrac{S_{n-1}\, (100 - S_c)\, (H_{n-1} - H_n)}{100\, (S_c - S_{n-1})} + R_n - \dfrac{S_{n-1}}{100} R_n\right)} \qquad (157)$$

Ponding model for sludge dewatering. In the development of this model, rainfall is assumed immiscible with the sludge and therefore is ponded on the surface as supernatant. The equation which calculates the drainage rate of the sludge is derived below.

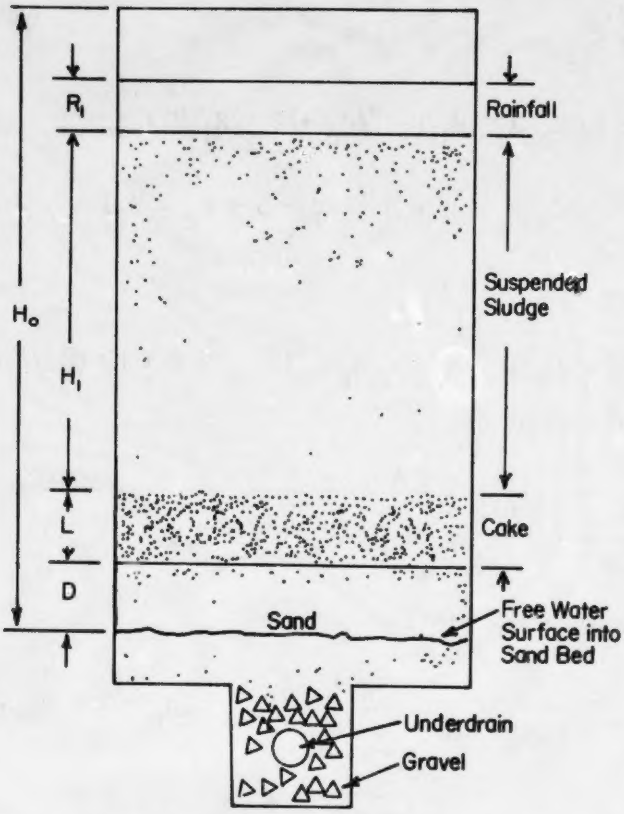

Figure 59: Definition sketch of ponding drainage.

Let R_1 units of rainfall be ponded on the surface of sludge at time t_1 while the sludge depth is known as H_1, shown on Figure 59. It is seen that the resistance to the flow of supernatant will include resistance from the sludge suspension, from the formed cake and from the supporting material. If the resistance from the suspended sludge and the supporting material are neglected, the rate of drainage can be expressed as:

$$\frac{dV_s}{dt} = \frac{\rho g A h_f}{\mu C RV/A} \tag{158}$$

where

$$\frac{dV_s}{dt} = -A\frac{d(H_1 + D + R_1)}{dt} \tag{159}$$

if H_1 is considered as a constant for a short period, then

$$dV_s = -A\ dR_1 \tag{160}$$

and

$$h_f = H_1$$

then

$$\frac{dR_1}{dt} = \frac{-\rho\ g\ (H_1 + D)}{\mu\ C\ R_c (H_1/H_c)^\sigma\ (H_o + D - H_1)} \tag{161}$$

Integrating the above equation from $R_1 = R_1$ at $t = 0$, to $R_1 = R$ at $t = t$, yields,

$$R = R_1 - \frac{\rho\ g\ (H_1 + D)t}{\mu C\ R_c\ (H_1/H_c)^\sigma\ (H_o + D - H_1)} \tag{162}$$

where $C = \dfrac{\rho\ g\ S_o\ S_c}{(S_c - S_o)100}$

or $$R_1 - R = \Delta R = \frac{\rho\ g\ (H_1 + D)\ t}{\mu\ C\ R_c (H_1/H_c)^\sigma\ (H_o + D - H_1)}$$

or $$\Delta R = \frac{(H_1 + D)\ t}{\dfrac{\mu\ S_o\ S_c}{100(S_c - S_o)}\ (H_1/H_c)^\sigma\ R_c\ (H_o + D - H_1)} \tag{163}$$

Equation 163 allows determination of the amount of supernatant drained at a certain period of time, while the depth of the sludge is assumed constant. This means that the dewatering of sludge is temporarily halted during the course of draining the supernatant. Of course this is not true in a real sense, but the error may be not significant if the time of drainage is chosen to be small.

Verification of drainage models. After developing the mixing and ponding models, tests were made to see if these two models yielded the same results under various rainfall conditions. The aim of this investigation was to test the sensitivity of the assumption about mixing and ponding models which represented two extreme conditions of rainwater on the surface of sludge. The results indicated that under identical conditions the ponding model usually had a more rapid drainage rate than the mixing model. The reason is simply that the mixing model treated rainwater as sludge while the ponding model did not. A representative comparison is shown in Figure 60. The overall results indicate that the difference in most cases was within 5 percent, demonstrating that the assumption of miscibility of rainwater and sludge does not significantly affect the final results. In the real condition of course, rainwater in sludge will behave somewhat in between these two models.

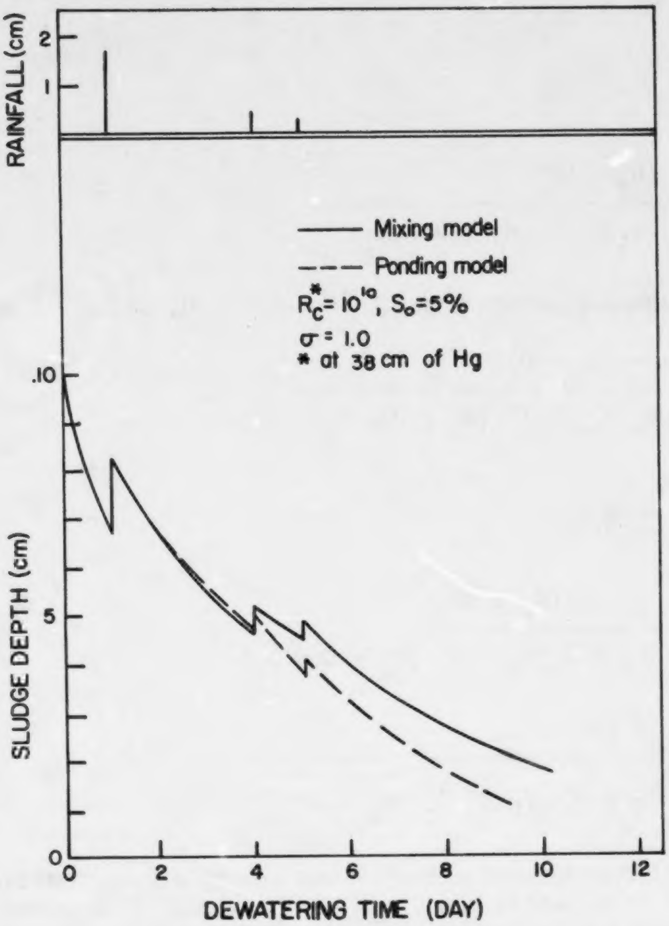

Figure 60: Comparison between mixing and ponding models.

Since the mixing drainage model gives a conservative drainage rate, it lends itself well to computer applications, thus it was chosen as the drainage model to be used to predict the required drainage for water and wastewater sludge in the rest of the study.

To test whether or not this model really describes the behavior of sludge drainage on a sand bed, the mixing model was further investigated in the laboratory by means of column tests. Results shown in Figure 61 indicate that the observed sludge heads on sand beds were very close to that predicted by the mixing model equation, and proved that the model was verified experimentally, provided a media factor of 0.36 and the adjusted specific resistance were used.

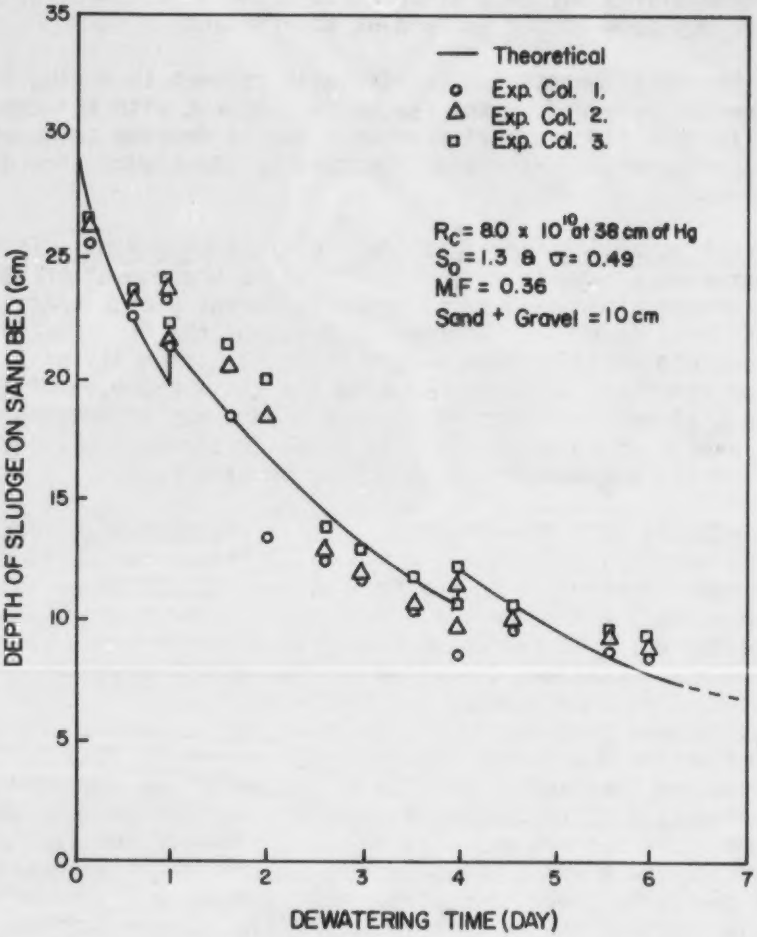

Figure 61: Comparison between mixing drainage model and experimental data.

THE EFFECT OF RAINFALL ON DRYING

The effects of rainfall on the rate of drainage during the constant rate drying period may be determined by the models discussed previously. However, very little information exists which describes the effects of rainwater on the process of drying during the falling rate drying period. In all cases, rainfall will prolong the length of time a drying sludge must remain on the sand bed. A previous investigation (2) indicated that this effect varied considerably, depending upon the time, intensity, and duration of the rainfall. If rain occurs during the falling rate drying period, a portion of the rainwater is absorbed by the sludge. The remainder depending upon such factors as number and depth of cracks, cake moisture content and sludge cake permeability may be drained through the sludge cake to appear as filtrate, or may pond on the surface as supernatant.

However, the most important parameter with respect to drying is the amount of rainwater retained by the sludge in contrast with the amount that drains away. In this study experiments were run to develop an equation which would predict the amount of rainwater absorbed by the sludges for different sludge conditions.

Experimental determination of rainfall effects on drying. These experiments were concerned primarily with characterizing the amount of rainwater absorbed by a sludge after each rain, under different sludge conditions. Variables considered were: (1) moisture content of the sludge after rain, (2) moisture content of the sludge before rain, (3) intensity of rainfall and (4) duration of rainfall. In order to make the tests representative of field conditions, initial moisture content of each sludge was intentionally altered to cover the range that would normally be found during the falling rate drying period for water and wastewater sludge drying on sand beds.

Rainfall effects were determined through experiments with intensities of 0.025, 0.125 and 0.25 cm/hr (0.1, 0.5 and 1.0 in/hr) for durations of 1, 2 and 4 hr at each intensity. In the test procedure, 500 ml of well mixed sludge was poured into a fritted glass funnel after which the sludge was allowed to dewater until it reached the desired moisture content. After being weighed, this glass funnel was installed on the testing equipment to receive artificial rainfall at a designated intensity and duration. After treatment, the sludge was removed from the test apparatus and weighed again to measure the increase of weight due to the absorption of rainfall. The results of the experiments revealed that only a portion of rainwater was absorbed by the sludge, the percentage of rainwater retained varied considerably with the initial cake moisture content and with the intensity and duration of rainfall. In general, there was a rapid initial absorption of rainwater by the sludge during the early stage of testing, then the rate of absorption decreased with an increase in the duration of rainfall. The initial intake was even more significant for higher intensities of rainfall. The occurence of this phenomenon is attributed to an initially highly porous sludge surface. Following saturation at the surface, water then migrated from the region of high surface moisture to inner portions of the sludge.

In order to establish the water-absorbing characteristics of sludge, moisture content after rainfall was related by multiple regression analysis to the intensity and duration of rainfall and to the moisture content before rainfall. In general, statistically significant relationships were shown to exist, and the signs of the regression coefficients were consistent with intuitive judgment of cause and effect. The regression equations for water and wastewater sludge are shown below.

(1) Water treatment sludge

$$M = 3.44\ M_o^{0.812} \times I^{0.008} \times D^{0.012} \tag{164}$$

$R^2 = 0.9956$ N = 30

(2) Wastewater treatment sludge

$$M = 5.44\ M_o^{0.751} \times I^{0.062} \times D^{0.041}$$

$R^2 = 0.9759$ N = 27 (165)

where M = moisture content after rain

M_o = moisture content before rain

D = duration of rainfall (hr)

I = intensity of rainfall (in/hr)

It is interesting to note that the exponents for intensity and duration were close to each other for each type of sludge. This suggests that the effects of intensity on the moisture content after rainfall seemed very similar to the effects of duration; therefore, these two factors were combined into a new variable: depth of daily rainfall. This combination is fortuitous in a practical sense because daily rainfall records are more readily available than are records of continuous rainfall. When the moisture content after rainfall was related to the parameters of initial moisture content and daily rainfall, the equations obtained were:

(1) For water treatment sludge

$$M = 3.55\ M_o^{0.807} \times R_d^{0.0095}$$

$R^2 = 0.9953$ N = 30 (166)

(2) For wastewater sludge

$$M = 4.93\ M_o^{0.766} \times R_d^{0.056}$$

$R^2 = 0.9727$ N = 27 (167)

Where R_d = daily rainfall (inches)

Comparison between moisture contents predicted by Equations 166 and 167 and the experimental values is shown in Tables 21 and 22.

TABLE 21. THE EFFECT OF RAINFALL ON WASTEWATER SLUDGE DRYING DURING THE FALLING RATE PERIOD

Rainfall in Inch (R_d)	Moist. Cont. Before Rain (M_o)	Experimental Moist. Cont. After Rain (M)	Calculated Moist. Cont. After Rain (M)	Residual
.1	267.5	310.7	313.3	-2.7
.1	272.2	326.5	317.5	9.1
.1	276.6	305.3	321.4	-16.1
.2	243.6	292.3	303.2	-10.9
.2	269.6	338.5	327.7	10.8
.2	174.7	236.7	235.0	1.6
.4	289.6	364.7	359.8	4.9
.4	179.1	243.6	249.0	-5.4
.4	330.2	396.3	397.8	-1.6
.5	250.8	326.9	326.4	.6
.5	317.2	381.7	390.6	-9.0
.5	290.7	371.7	365.4	6.3
1.0	257.5	342.2	346.2	-4.0
1.0	280.0	381.0	369.2	11.8
1.0	201.4	289.3	286.8	2.6
2.0	195.6	287.7	291.5	-3.8
2.0	278.4	383.5	382.1	1.5
2.0	329.9	420.9	435.1	-14.3
1.0	272.9	375.4	361.9	13.5
1.0	345.0	436.2	433.1	3.0
1.0	297.5	398.8	386.6	12.2
2.0	285.4	392.6	389.4	3.2
2.0	321.6	463.3	426.7	36.7
2.0	254.5	359.6	356.7	2.9
4.0	245.5	358.2	360.7	-2.4
4.0	369.6	469.1	493.5	-24.3
4.0	342.5	452.9	465.5	-12.6

TABLE 22: THE EFFECT OF RAINFALL ON WATER TREATMENT SLUDGE DRYING DURING THE FALLING RATE PERIOD

Rainfall In Inch (R_d)	Moist. Cont. Before Rain (M_o)	Experimental Moist. Cont. After Rain (M)	Calculated Moist. Cont. After Rain (M)	Residual
.1	580.0	592.9	604.6	-11.7
.1	560.0	578.6	587.7	-9.1
.1	572.3	583.7	598.1	-14.4
.2	548.3	572.6	578.1	-5.5
.2	521.7	548.9	555.4	-6.5
.2	559.1	572.3	587.3	-15.1
.2	362.6	405.7	413.9	-8.2
.4	540.0	569.4	571.4	-2.0
.4	526.6	562.0	559.9	2.1
.4	508.6	546.3	544.4	1.9
.5	575.4	596.3	601.7	-5.4
.5	564.3	585.7	592.3	-6.5
.5	571.4	594.3	598.3	-4.0
1.0	546.3	576.9	577.3	-.5
1.0	546.9	576.3	577.8	-1.5
1.0	556.0	584.3	585.6	-1.3
1.0	418.6	466.3	465.6	.7
2.0	548.9	577.4	579.9	-2.5
2.0	544.3	579.1	576.0	3.1
2.0	457.4	505.7	500.5	5.2
1.0	568.6	591.4	596.3	-4.9
1.0	564.3	597.1	592.7	4.5
1.0	568.6	595.7	596.3	-.6
2.0	530.0	564.9	563.8	1.1
2.0	544.0	585.7	575.8	9.9
2.0	537.7	577.1	570.4	6.7
2.0	423.7	471.4	470,5	.9
4.0	538.6	578.9	571.5	7.3
4.0	547.7	584.3	579.4	4.9
4.0	518.6	560.3	554.3	6.0

REFERENCES

1. Lo, K. Digital Computer Simulation of Water and Wastewater Sludge Drying on Sand Beds. Ph.D. dissertation, University of Massachusetts, Amherst, 1971.

2. Randall, C. W. and Koch, C. T. Dewatering Characteristics of Aerobically Digested Sludge. Journal of the Water Pollution Control Federation, Research Supplement, May, 1969.

SECTION IX

SIMULATION OF DEWATERING ON SAND BEDS

Because of the stochastic nature of rainfall and its resultant effect on drainage and drying on open sand beds, a simulation approach was employed to test the performance of a particular design under conditions representative of a given area of the country. To achieve this simulation, drainage and drying models were developed, as discussed previously, which related sludge characteristics and weather to the amount of water lost by drying and drainage. Synthetic rainfalls were used as input to determine the response of the models.

Local evaporation data were another important input to the models for they not only represented water losses during the constant rate drying period but also determined drying rates during the falling rate period. Therefore, the time required for drainage and drying was treated as a function of local meteorological conditions and the nature of the sludge.

SCOPE OF THE SIMULATION

The computer simulation included four different types of wastewater sludge and two types of water treatment sludge. The wastewater sludges were anaerobically digested primary sludge, primary and trickling filter digested sludge, primary and activated sludge and aerobically digested sludge. Alum sludges from the Albany, New York, and Amesbury, Massachusetts treatment plants were used to represent the water treatment sludges. These two alum sludges exhibited significant differences in drainage rates permitting them to serve as the upper and lower limits of sludge properties. Softening sludge was not considered in this study because this sludge settles so rapidly that a lagoon disposal method might be more suitable. The sludge parameters related to dewatering are presented in Table 23.

So as to take into account weather conditions encountered across the United States, six cities were chosen to represent six different meteorological conditions. Table 24 shows the normal weather data for these cities, and indicates the variation they experience in annual precipitation.

In recognition of decreased drainage and drying in cold weather, winter months at each location were excluded from simulation. The occurrence of freezing in selected cities, shown in Table 25, is based upon Environmental Science Service Administration records (7). Excluding the periods during which freezing occurs is a conservative approach since some drainage and

TABLE 23. CHARACTERISTICS OF SLUDGES

	Types of Sludge	Solids Content	Specific Resistance* Sec^2/gm	Coefficient of Compressibility	Reference
Water Sludge	Alum Sludge (Albany)	1.3%	8.0×10^9	0.49	Lo (1)
	Alum Sludge (Amesbury)	1.5%	5.8×10^8	0.99	Adrian (2)
Waste Water Sludge	Primary Anaerobically Digested Sludge	9.5%	2.6×10^{10}	0.68	Nebiker (3)
	Anaerobically Digested Sludge Mixed with Activated Sludge	3.6%	4.8×10^{10}	0.66	Sanders (4)
	Anaerobically Digested Sludge Mixed with Trickling Filter	6.1%	8.25×10^9	0.8	Quon (5)
	Aerobically Digested Sludge	4.5%	1.15×10^9	0.97	Cummings(6)

*At pressure P = 38.1 cm of Hg

TABLE 24. NORMAL MONTHLY WEATHER DATA - SELECTED CITIES

Stations	Jan.	Feb.	Mar.	Apr.	May	Jun.	Jul.	Aug.	Sep.	Oct.	Nov.	Dec.
Phoenix, Arizona	2.90	3.50	5.40	7.40	10.4	13.5	14.8	13.5	11.7	8.20	5.10	3.10*
	0.61	0.82	0.68	0.37	0.16	0.06	0.68	0.90	0.36	0.40	0.50	0.98**
	4.0	4.0	3.0	2.0	1.0	1.0	5.0	5.0	2.0	3.0	2.0	4.0***
San Francisco, California	1.3	1.5	2.1	2.5	2.7	2.9	2.7	2.5	2.9	2.9	2.4	1.7*
	4.03	3.91	2.78	1.49	0.59	0.15	0.01	0.01	0.13	1.07	2.27	4.07**
	11.0	10.0	10.0	6.0	4.0	2.0	1.0	1.0	1.0	5.0	7.0	11.0***
Boise, Idaho	0.79	1.2	2.4	3.8	5.3	7.1	10.6	10.1	6.3	3.5	1.8	0.92*
	1.33	1.35	1.34	1.10	1.09	0.84	0.18	0.21	0.46	0.94	1.35	1.29**
	12.0	11.0	10.0	8.0	9.0	7.0	2.0	2.0	3.0	7.0	10.0	12.0***
Miami, Florida	3.0	3.4	4.1	4.9	5.0	4.8	5.3	5.1	4.3	4.1	4.3	2.7*
	2.15	1.73	2.15	3.44	4.27	5.55	4.36	5.06	6.72	7.88	2.16	1.73**
	8.0	6.0	6.0	7.0	11.0	13.0	15.0	15.0	18.0	15.0	9.0	7.0***
Boston, Massachusetts	0.97	1.1	1.4	2.2	3.1	4.2	5.0	4.5	3.6	2.9	1.9	1.3*
	3.50	2.93	3.43	3.46	2.91	3.48	3.18	3.23	2.99	2.79	3.49	3.37**
	12.0	10.0	12.0	11.0	11.0	10.0	10.0	10.0	9.0	9.0	10.0	11.0***
Duluth, Minnesota	0.26	0.32	0.69	1.4	2.1	2.4	3.7	4.2	3.6	2.4	1.0	0.31*
	1.01	1.02	1.54	2.21	2.95	3.72	3.31	3.19	3.03	1.96	1.67	1.00**
	10.0	8.0	10.0	9.0	12.0	13.0	11.0	11.0	11.0	9.0	9.0	9.0***

*Monthly evaporation in inches.

**Monthly precipitation in inches.

***Number of rainy days.

TABLE 25. OCCURRENCE OF FREEZING AT SELECTED CITIES

(Based on records from 1921 to 1950)

Station	Occurrence of Freezing 0^oC Mean Fall Date	Mean Spring Date	Mean Number of Days Minimum Temperature 0^oC or less
Phoenix	Dec. 6	Feb. 2	17
San Francisco	Dec. 22	Jan. 17	less than 10
Miami	-	-	-
Boise	Oct. 16	Apr. 29	128
Boston	Oct. 25	Apr. 16	94
Duluth	Oct. 3	May 13	189

drying still occur during such intervals.

All six sludges were simulated for their performance on sand beds in various locations with at least six different application depths. The starting depth was 10 cm for each sludge; its value was increased by 5 or 10 cm increments wherever possible.

ESTIMATION OF THE SIMULATION SAMPLE SIZE

Sample size for a simulation study must not be so large as to be too costly or so small as to be unreliable. In this study, the sample size (the number of sludge applications to be generated for the simulation experiment) was determined according to Equation 168 given by Chow and Ramaseshan (8), for which levels of precision and confidence are specified.

$$n > (t_\beta/\alpha)^2[(1-P_n)/P_n] \tag{168}$$

where P_n = the proportion of the sample from a population that belongs to the group under consideration

α = percentage of error level

β = percentage of confidence level

t_β = the standard normal deviate corresponding to the confidence level

In this study, a confidence level of 80 percent results in a standard normal deviate of 0.842 for the equation. With a selected error level of 15 percent, the value of the proportion of generated dewatering times that were different from the actual dewatering time was 15 percent. The desired sample size is calculated as:

$$N = \left(\frac{0.842}{0.15}\right)^2 \quad \left(\frac{1-0.15}{0.15}\right) = 180$$

Because the dewatering time varied widely depending upon location, type of sludge, and applied depth, 180 application times might mean a 20-year simulated operation under one condition and only 10 years under another. The longer the period of simulation, the greater the chance of encountering higher intensities of rainfall. The chance of a 10 year simulation having a 20-year storm history was only 30 percent. Consequently, the use of the number of applications as the criterion for sample size was biased based on the hydrological point of view. In order to correct this, the sample size was chosen to be at least 200 events to be applied over a 20 year simulation period. This dual criteria for sample size control provided the required level of accuracy and also ensured that a 20-year storm or higher was considered in the simulation; therefore, a bed design based on the results of this study is expected to have a useful life of 20 years or more.

SIMULATION PROCEDURE

Input parameters to the sludge dewatering simulation experiment were the physical properties of the sludge. Output of the stochastic system was affected by changes in the quantities and types of input. The models were operated in the computer in accordance with the following rules:

1. The total amount of daily rainfall was considered to fall on the ground instantaneously at zero hour of each day of rain.

2. The drainage process for wastewater sludge was terminated when the moisture content reached the first critical point (U_{CR}). For water treatment sludge the drainage was stopped according to Clark's expression (1)

   $$S_d = 4.3 + 0.7\ S_o$$

   where S_d = solids content at which drainage stops

   S_o = initial solids content

3. The final solids content for wastewater sludge was selected as 35 percent, while 20 percent was selected for water treatment sludge. The values were considered to be representative of past practice.

The simulation started at the beginning of each day with the addition of the daily rainfall to the sludge surface; if it was not a raining day, a zero amount of rainfall was added. Then by applying the drainage model

(Eqs. 156 and 157), the depth of sludge on the drying bed at the end of 24 hours of dewatering was obtained. This depth of sludge, after subtracting the amount of water lost by drying, was used as an entry value for the drainage model in the second day's operation. The procedure was repeated until the drainage-terminate moisture content was obtained. Moisture content of sludge was calculated by Equations 64 and 133 for wastewater and water sludge respectively, with Equations 166 and 167 accounting for rainfall effects. A result of this operation is shown in Figure 62.

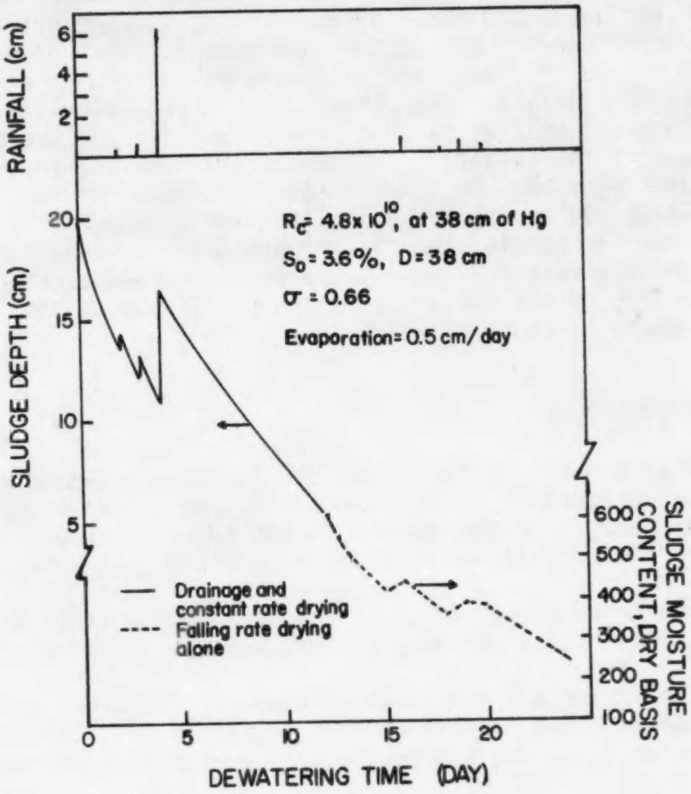

Figure 62: Sample operation of drainage and drying models.

VERIFICATION OF SIMULATION

Verification of the degree to which simulated sludge dewatering time conformed to known data was carried out by comparing the dewatering performance obtained from simulation with observed data. Haseltine (9) reported data for covered beds at wastewater treatment plants in California, New York, and other areas; and open beds in Pennsylvania. Comparative parameters for the rainfall generation model were drawn from weather records for nearby locations. Haseltine had not reported rainfall data for the particular periods corresponding to his field observations of net bed loadings. For this reason the weather pattern existing when Haseltine collected his data was assumed the same as the average obtained from a 20 year simulation.

The comparison for covered beds is shown in Table 26. The results indicate that the reported net bed loading at the various plants was within the limit established by the expected dewatering time for the 20 year simulation at different application depths. The results for open beds in Table 27 and 28 show that the reported dewatering times for various application depths were slightly less than the expected dewatering time from the 20-year simulation, but the observed values still fell within the range of the simulated dewatering times. Statistical tests between the observed and simulated values were not considered because of the small sample from which observed data were drawn.

OUTPUT OF SIMULATION

The output of this simulation was a random variable (the required drying time) and its associated probability distribution. A sample output is shown in Table 29. Essentially, it describes the natural phenomena of sand bed dewatering in terms of outcomes of various frequencies. For example, following application of 20 cm of mixed digested primary and activated sludge in Boise, Idaho, it would be possible to remove the sludge at 35 percent solids content twice within fourteen days, forty times within 15 days, and so on, over a twenty-year period. The mean period for which the sludge had to remain on the beds was 19.9 days with a standard deviation of five days. The shape of the frequency distribution shows that the low limit of dewatering time was 14 days, with short dewatering times occurring more frequently than long ones, suggesting that dewatering time might be described by the Poisson distribution.

Overall outputs for the entire simulation are presented in summary form in Lo (1). They include the data for mean and range of dewatering times and their corresponding standard deviations. Net bed loadings calculated from the mean dewatering time are also included.

TABLE 26: COMPARISON BETWEEN COMPUTER SIMULATION AND FIELD OBSERVATIONS FOR COVERED BEDS AT VARIOUS LOCATIONS.

				Computer Simulation					
				Solids(%)		Net Bed Loading for Applied Sludge Depth, in			
Plants	On	Off	Net Bed Loading	On	Off	4	6	8	10
Butler, PA	6.1-9.2	26.7-37.9	1.05-1.99	7.0	35.0	1.42	0.94	0.75	0.63
Grove City, PA	3.6-4.8	38-50	0.66-1.0	4.3	40.0	2.14	1.33	1.07	0.85
Dayton, Ohio	4-5	36-56	1.04-1.71	5.0	40.0	1.79	1.18	0.91	0.81
Huntington, NY	8.4	27.0	2.92	8.4	27.0	1.44	0.93	0.71	0.66
Rockville, NY	5.4	24.5	1.66	5.4	24.5	3.35	1.58	1.13	0.89
Salinas, CA	5.4	62.8	1.35	5.4	62.8	1.49	1.08	0.92	0.83
San Antonio, Tex.	4.0	45.5	0.86	4.0	45.5	2.14	1.41	1.20	1.0
Springfield, Ill.	9.2	54.1	2.66	9.2	54.1	1.08	0.82	0.80	0.74

$R_c = 8.25 \times 10^9$ at P = 38 cm of Hg.

M.F. = 0.36

$\sigma = 0.66$

TABLE 27. COMPARISON BETWEEN 20-YEAR COMPUTER SIMULATION RESULTS AND HASELTINE'S (9) FIELD OBSERVATION FOR OPEN SAND BEDS AT GROVE CITY, PA

Field Observations					20-yr. Computer Simulation Results					
								Total Drying Time(Days)		
Depth Applied (in)	Solids on (%)	Solids off (%)	Total Dry Time (day)	Net Bed Loading	Depth Applied (in)	Solids on (%)	Solids off (%)	Exp Dry Time	Range of Dry Time	Net Bed Loading
8/12	3.4	34.1	18	0.86	8 1/2	3.4	34.1	22.6	12-59	0.68
9	3.55	40.1	19	1.05	9	3.55	40.0	36.6	19-58	0.54
9	3.5	34.1	16	1.05	9	3.5	34.1	26.1	15-57	0.64

$R_c = 8.25 \times 10^9$

M.F. = 0.36
σ = 0.66

TABLE 28. COMPARISON BETWEEN 20-YEAR COMPUTER SIMULATION RESULTS AND HASELTINE'S (9) FIELD OBSERVATION FOR COVERED SAND BEDS AT GROVE CITY, PA.

Field Observations					20-yr. Computer Simulation Results					
								Total Drying Time		
Applied Depth (in)	Solids on (%)	Solids off (%)	Total Drying Time (day)	Net Bed Loading	Applied Depth (in)	Solids on (%)	Solids off (%)	Exp. Dry Time	Range of Dry Time	Net Bed Loading
10	3.8	41.8	20	1.26	10	3.8	41.8	26.8	25-29	0.93
10	4.1	42.4	20	1.37	10	4.1	42.4	29	29-31	0.94

$R_c = 8.25 \times 10^9$

M.F. = 0.36
σ = 0.66

TABLE 29. THE OUTPUT OF SIMULATION OF MIXED DIGESTED PRIMARY AND ACTIVATED SLUDGE DEWATERING ON SAND BEDS AT BOISE, IDAHO WITH 20 cm APPLICATION

Dewatering Time (days)	Frequency of Occurrence	Probability	Cumulative Probability
14.0	2.0	0.01000	0.01000
15.0	38.0	0.19000	0.20000
16.0	20.0	0.10000	0.30000
17.0	21.0	0.10500	0.40500
18.0	24.0	0.12000	0.52500
19.0	12.0	0.06000	0.58500
20.0	15.0	0.07500	0.66000
21.0	9.0	0.04500	0.70500
22.0	9.0	0.04500	0.75000
23.0	6.0	0.03000	0.78000
24.0	4.0	0.02000	0.80000
25.0	8.0	0.04000	0.84000
26.0	8.0	0.04000	0.88000
27.0	7.0	0.03500	0.91500
28.0	1.0	0.00500	0.92000
29.0	4.0	0.02000	0.94000
30.0	2.0	0.01000	0.95000
31.0	2.0	0.01000	0.06000
32.0	4.0	0.02000	0.98000
33.0	1.0	0.00500	0.98500
34.0	1.0	0.00500	0.99000
37.0	2.0	0.01000	1.00000

The expected mean dewatering time is 19.9 days.
The standard deviation of dewatering time is 5.0 days.
The net bed loading is 0.81 lb/ft^2/30 days. (Based on the mean dewatering time).

REFERENCES

1. Lo, K. Digital Computer Simulation of Water and Wastewater Sludge Dewatering on Sand Beds. Ph.D. Dissertation, University of Massachusetts, Amherst, 1971.

2. Adrian, D. D. et al. Source Control of Water Treatment Waste Solids. Report No. EVE-7-58-1, Environmental Engineering, Department of Civil Engineering, University of Massachusetts, Amherst, 1968.

3. Nebiker, J. H., Adrian, D. D. and Lo, K. Evaluation of Chemical Conditioning for Gravity Dewatering of Wastewater Sludge. In Report No. EVE-7-68-1, Environmental Engineering, Department of Civil Engineering, University of Massachusetts, Amherst, 1968.

4. Sanders, T. G. A Mathematical Model Describing the Gravity Dewatering of Wastewater Sludge on Sand Drainage Beds. M. S. Thesis in Civil Engineering, University of Massachusetts, Amherst, 1968.

5. Quon, J. E. and Tamblyn, T. A. Intensity of Radiation and Rate of Sludge Drying. Journal, Sanitary Engineering Division, ASCE, April, 1965.

6. Cummings, P. W. Digital Computer Simulation of Wastewater Treatment. M.S. Thesis in Civil Engineering, University of Massachusetts, Amherst, 1969.

7. Statistical Abstract of the United States, 1969. U. S. Department of Commerce, 1969.

8. Chow, V. T. and Ramaseshan, S. Sequential Generation of Rainfall and Runoff Data. Journal, Hydraulics Division, ASCE, July, 1965.

9. Haseltine, R. R. Measurement of Sludge Drying Bed Performance. Sewage and Industrial Wastes, 23(9): 1065-1083, 1951.

SECTION X

PEFORMANCE OF SAND DRYING BEDS

In the previous section, dewatering times for various sludges at different locations were determined. Little mention was made of the required bed area and the expected bed performance under each condition. In general, knowing the dewatering time, depth of application and solids content of the applied sludge will enable the design engineer to size the drying bed if the known dewatering time is a single value variable. Due to the effect of weather, however, the dewatering time as obtained in the preceeding section was shown to be a random variable which exhibits a wide range of outcomes for a given sludge and location. Therefore, the design engineer is required to choose from a number of courses of action. The practical consequence of adopting any particular course depends not only upon the choice made but also upon local meteorological conditions. Referring to the data shown in Table 29 for example, it is shown that the time required to dewater a 20 cm application of mixed digested primary and activated sludge in Boise, Idaho ranged from 14 days to 37 days. If the design engineer chose 15-days as the design dewatering time, the calculated bed area would be 1.45 square feet per capita, based on the method suggested by the Water Pollution Control Federation (1). However, the designed bed would be undersized according to the data shown in Table 28 in that during a twenty year period the sludge would have to remain on the bed longer than 15 days, 80 percent of the time. As a result, the yield of dry solids from the bed, or the bed performance, would not satisfy the design requirements.

AN APPLICATION OF STATISTICAL DECISION THEORY

Before seeking the relationship between dewatering time, bed area and bed performance, a new random variable N was introduced to represent the total number of bed applications per year. N was obtained by substituting the results of the dewatering time obtained in the previous chapter into the equation:

$$N = \frac{T}{T_d + T_p} \qquad (169)$$

where N = total number of bed applications per year

T = total dewatering time available (day/year)

T_d = the required dewatering time per application (day)

T_p = the required bed preparing time (day)

In order to measure the consequence of an engineer selecting a larger number of bed applications than "Nature" allowed, it was assumed that there existed a loss function which reflected a penalty for the loss of bed performance brought about by taking too short a design dewatering time. Consequently, some amount of dry solids was left undewatered. If the amount of undewatered solids is represented by the random variable Z,

$$Z(n) = \begin{cases} (A_n - N)\ A_r\ H\ S_o\ \rho & A_n > n \\ 0 & A_n > n \end{cases} \tag{170}$$

where A_n = the number of bed applications considered by the designer

N = the random variable of bed applications which represents the "state of nature"

A_r = the required bed area in ft^2 (for wastewater sludge it is the area needed per capita, per year; for water treatment sludge, it is the area needed per pound of dry solids per day)

H = the depth of sludge in ft

S_o = the solids content of the applied sludge

ρ = the density of sludge

Then the expected value of the total solids left undewatered per year can be calculated as;

$$\begin{aligned} E\ (Z) &= \sum_{K=o}^{\infty} Z\ (K)\ P_n\ (K) \\ &= \sum_{K=o}^{A_n-1} (A_n - N)\ A_r\ H\ S_o\ \rho\ P_n\ (K) + \\ &\quad \sum_{K=A_n}^{\infty} 0\ P_n(K) \\ &= (A_n\ A_r\ H\ S_o\ \rho)\ (P\ [n < A_{n-1}]) - \\ &\quad (A_r\ H\ S_o\ \rho)\ (\sum_{K=o}^{A_{n-1}} K\ P_n(K)) \end{aligned} \tag{171}$$

where $P[n < A_n\text{-}1]$ is the probability that the random variable N is less than A_{n-1}. Its value can be calculated or found in statistics tables under the chosen probabilistic model.

Using the data in Table 29 as an example, it can be shown that

A_n = 12 bed applications per year,

$A_r = 0.135\ m^2 (1.45\ ft^2)$ per capita,

$H = 0.20\ m\ (0.66\ ft^2)$,

$S_o = 0.034$, and

$\rho = 1000\ kg/m^3\ (62.4\ lb/ft^3)$

a fifteen day design dewatering time results in 2.4 kg (5.3 lb) per capita per year as the expected dry solids left undewatered.

PERFORMANCE INDEX

For the purpose of expressing bed performance as a function of inputs such as bed area, application depth and local weather conditions, a term called performance index (PI) was introduced to measure the weighted average of sludge dewatered by drying beds each year under various conditions. It was defined as

$$PI(\%) = \frac{\text{Wt of sludge dewatered} \times 100}{\text{Total wt. of sludge}} \tag{172}$$

By applying Equation 171 to the above relationship, the performance index is written as:

$$PI(\%) = [W_d - \{A_n A_r H S_o \rho (P_n (n < A_{n-1})) - A_r H S_o \rho (\sum_{K=0}^{A_n - 1} K P_n (K))\} \times 100]/W_{ts} \tag{173}$$

where W_d = weight of dry solids expected to be dewatered under the design condition without consideration of "the state of nature". The terms enclosed in parenthesis { } represent the dry weight of undewatered sludge.

W_{ts} = total dry solids expected per year

In words the equation states that the performance index depends upon the inputs A_n, A_r, and H. The design engineer may increase or decrease the output by increasing or decreasing the quantities of all inputs used, or increase it to some maximum level by increasing the quantity of one input while holding the quantities of other inputs constant. Since this equation expresses the physical relation between the inputs of resources (such as the bed area, the number of applications and the applied depth) and their output (PI -- the percentage of the total dry solids dried on the drying beds) per unit of time, it is often called a production function. Since this particular production function also involves a random variable N to describe the "state of nature", the function is then appropriately called a stochastic production function (2).

The overall performance for sludge dewatering on sand beds at various locations is shown in tables prepared by Lo (3). In each table, the data show the corresponding performance index for each possible dewatering time and bed area.

REFERENCES

1. ASCE & WPCF, Sewage Treatment Plant Design. Manual of Engineering Practice, No. 36, 1959.

2. Mass, A., et al. Design of Water-Resource Systems, Harvard University Press, 1962.

3. Lo, K. Digital Computer Simulation of Water and Wastewater Sludge Dewatering on Sand Beds. Ph.D. Dissertation, University of Massachusetts, Amherst, 1971.

SECTION XI

ECONOMIC ANALYSIS FOR SLUDGE DEWATERING ON SAND BEDS

INTRODUCTION

The objective of this chapter is to utilize computer simulation results presented in previous sections in order to improve sludge dewatering bed design methodology, so that an optimal system can be obtained. The conventional rule-of-thumb procedure for designing dewatering beds, based largely on limited field observations, does not effectively incorporate both engineering and economic analysis. A typical dewatering bed design basis as recommended by the American Society of Civil Engineers (1) is 1.0 to 1.5 square feet (.09 to 0.14 m^2) per capita for primary digested sludge in the northern United States. It gives no consideration to the cost of land, labor and operation. Furthermore, there has been a tendency in engineering practice to consider these design criteria as professional engineering standards, and the realities upon which they are based are not commonly appreciated. Support is presented in this chapter for the belief that design criteria may be applied more satisfactorily if they are associated with all relevant cost terms. For example, the engineer might over-design the bed in low land-cost areas in order to reduce the labor costs of operation. In high land-cost areas, he might design to minimize land costs.

In order to join engineering and economics more effectively than has been the case in past, an objective function for sand bed dewatering has been derived which includes design criteria and the associated cost terms. The objective function used in this study is basically the same as suggested by Meier (2) in his study of dewatering bed system design. However, efforts are made in this section to minimize the objective function by utilizing a simulation approach and a marginal analysis approach.

SIMULATION APPROACH

Simulation has been used by Meier and Ray (2) to study the optimum dewatering bed system design. In their study, an objective function Z was suggested:

$$Z = C_1 A_r + C_2 A_r A_n \qquad (174)$$

where Z = total cost of sand bed dewatering

C_1 = cost associated with the required land area

C_2 = cost associated with the number of applications to the land area

A_r = area of land required

A_n = the number of applications

A_r and A_n are functions of the dewatering time. Therefore knowing C_1, C_2, the dewatering time and the depth of sludge application, the total cost of sand bed dewatering can be determined if this dewatering time is a single value variable. Due to the effects of weather, however, the actual dewatering time for a sludge in a particular location has been shown to be a random variable with a wide range of outcomes. For example, the dewatering time shown in Table 29 for 20 cm of digested primary and activated sludge on a sand bed in Boise, Idaho was found to range from 14 days to 37 days. For each possible dewatering time, there was a corresponding combination of A_n and A_r which in turn yielded a different cost. Therefore, the design engineer in this case was left to choose from a large number of possible outcomes. In order to choose a dewatering time that would best represent actual field conditions and serve as a basis for design and comparison between alternatives, the following two criteria were used in this study: expected value of dewatering time, and performance index (PI).

Expected value of drying time. The entire frequency distribution of possible dewatering times for the example of 20 cm of mixed digested primary and activated sludge in Boise, Idaho is shown in Table 29. It indicates that there were 2 times in 20 years when the required dewatering time was 14 days or less, and 40 times when it was 15 days or less, and so on. This frequency distribution may be considered to be the probability distribution* of the random variable, drying time. The expected value of the random variable is

$$E(t) = \sum_{i=1}^{n} P_i t_i \qquad (175)$$

where t_i = the value of the ith possible outcome of the dewatering time

P_i = the probability of occurrence of t_i.

By applying this equation to the data in Table 29, the expected dewatering time was found to be 19.9 days. This means that 19.9 days only represents the average dewatering time for an infinite number of applications. It should be realized that on a single dewatering, one and only one of the dewatering times from 14 to 37 days can occur. Therefore, if one uses this expected dewatering time as a basis of design, it is almost certain that the bed so designed would not be sufficient for certain periods of time during a 20-year period. Nevertheless, this expected value of dewatering time does give a single number which significantly characterizes the random variable over its range of occurrence. In many cases, it alone is an adequate basis for choice among alternatives, especially when all alternatives have approximately the same probability distribution. Based on the above discussion, then, the expected value of drying time is suggested in this study as one of the criteria to be used in determining the variables A_n and A_r. The data concerning these expected drying times for various sludges dewatered in different locations at different depths of application is found in Lo (4).

---

*By the law of large numbers, the frequency distribution would approach the probability distribution as a limit, when the sample size approaches infinity(3).

Performance index (PI). In preceeding paragraphs the expected dewatering time was suggested as a criterion for determining the variables A_n and A_r. The advantages of using this familiar statistic are:

1. it makes use of all outcomes, and develops a weighted sum in which the contribution of each outcome is afforded an equal weight.

2. the assertion drawn from Tchebycheff's inequality (5) regarding any probability distribution with a finite standard deviation, namely that the probability that an outcome of dewatering time larger than K days away from its mean is at most $1/K^2$,

3. that it is relatively easy and straightforward to determine; also it gives the option of using only the mean or the mean plus one or more standard deviations as criteria.

On the other hand, the main disadvantage of using this expected dewatering time is that it is affected by its probability distribution, by which the expected drying time from a positively skewed distribution (like the Poisson distribution) is considerably smaller than that from a symmetric distribution (like the normal distribution) over the same range of occurrence. Consequently, two outcomes with the same expected dewatering time would not yield the same performance level (PI) if their probability distributions were different. In order to avoid this problem, an alternative decision criterion based upon the concept of performance index was suggested. The actual probability distribution generated by computer simulation was treated as an empirical discrete distribution so that the performance index would not be affected by the shape of the distribution. One may design the bed based on any expected performance level. However, 100 percent performance index is not recommended for use because it is overly conservative.

Since the rainfall distribution appeared highly skewed regardless of geographical location, the shorter dewatering times occurred most frequently, and longer dewatering times occurred more and more infrequently. As a result, the performance index determined by the expected dewatering time was found to be very high. In most cases it was in the range of 90 percent to 95 percent. Based upon the above observation, therefore, it was recommended that the concepts of expected dewatering time and performance index be used jointly to design the bed in such a way that the target performance index is in close agreement with the expected dewatering time.

Economic factors. Upon completing the criteria for determining A_n and

A_r, consideration has been given to economic parameters C_1, the cost associated with the required land, and C_2 the cost associated with the number of applications per land area. Items which must be included in C_1 would be land construction and maintenance costs as well as the land salvage value and rehabilitation cost at the end of the economic life span. For example if one assumes

land cost	\$10,000/Acre
construction cost	\$10,000/Acre
maintenance cost	\$ 1,000/Acre/Year
repair of bed cost	\$ 5,000/Acre/Year
salvage value	\$10,000/Acre
rehabilitation cost	\$ 2,000/Acre/30 Years
economic life	30 years

and selects an appropriate interest rate, the value of C_1 can be readily calculated as follows:

land cost (6%, 30 Years)	= \$ 726/Acre
construction cost (6%, 30 Years)	= \$ 726/Acre
maintenance cost	= \$1,000/Acre
repair cost (6%, every 10 Years)	= \$ 320/Acre
salvage value (6%, 30 Years)	= \$ 125/Acre
rehabilitation cost (6%, 30 Years)	= \$ 25/Acre
Total C_1	= \$2,672/Acre/ Year(\$6600/Hectare/ Year)

C_2 considers the costs of applying and removing sludge and varies with the method of removal. Cake removed by hand requires a low capital investment, but requires more labor than that removed by machine. In addition, machine removal causes a greater loss of sand and requires frequent sand renewal. The depth of application may also affect removal costs. A shallow application may result in a thin layer of cake which might impede the removal operation. Unfortunately, there is very little information in the literature concerning sludge removal. Conversation with the operators at the Northampton, Massachusetts, sewage treatment plant revealed that it took 2 man-days to remove sludge from 7 beds by machine. In 2 man-days sludge could be removed from 2 beds by hand. The dimension of the bed was 25 feet by 150 feet. On the average the bed required sand renewal after every 8 applications for either machine or hand removal.

Using this information and assuming that the cost of labor is \$4/hr, and that the sand renewal operation is \$50/bed, C_1 can be determined for a plant utilizing hand methods to remove sludge as:

Labor Cost:

$$\frac{2 \text{ man-day} \times 8 \text{ hr/man-day} \times 4 \text{ \$/hr} \times 43560 \text{ ft}^2\text{/AC}}{2 \text{ Bed/day} \times 25 \text{ ft} \times 150 \text{ ft}} = \text{\$370/application Acre}$$

(\$914/application/hectare)

Sand renewal cost:

$$\frac{50\ \$/\text{bed} \times 43560\ \text{ft}\ 2/\text{Ac}}{8\ \text{Apply.} \times 25\ \text{ft} \times 150\ \text{ft}} = \$\ 73/\text{application/Acre}$$

($180/application/hectare)

Total C_1 = $443/application/Acre

($1094/application/hectare)

Determination of optimum system design. By including the calculated C_1 and C_2 in the objective function of Equation 174, simulation results were obtained for the optimum application depth of sludge. The method utilized was to take A_n and A_r for different application depths and calculate the annual cost. The global optimum was then determined as the depth which yielded a minimum cost. The results shown in Table 30 using the output from Boise, Idaho as an example, indicate that the optimum sludge depth would be 25 cm for a digested primary and activated sludge with 95 percent performance index as the target output. The required bed area would be 0.22 m^2(2.32 ft^2) per capita with 6 applications per year. The annual cost of sand bed drying would be $0.281/person.

As an alternative, however, the design engineer may chose to use a mechanical rather than a manual method to remove dry sludge from the bed.

TABLE 30. ANNUAL COST OF SLUDGE DRIED IN BOISE, IDAHO AT DIFFERENT APPLICATION DEPTHS (Sludge Removed by Hand)(1)

Application Depth (cm)	Dewatering Time (day)	Bed Area (ft^2/cap)	No. of Application Per Year	Annual Cost (2)(3) ($/cap)
10	5	1.40	26	0.445
15	12	1.66	14	0.331
20	20-21	1.98	9	0.299
25	30-35	2.32	6	0.281*
30	44-57	2.90	4	0.293
35	58-81	2.32	3	0.301

(1) Type of Sludge: Digested Primary and Activated Sludge.
(2) C_1 = $ 2672/AC = $ 0.061/ft^2
C_2 = 443/AC/Applic. = $ 0.01/ft^2/Applic.
(3) PI = 95%
*Optimum Depth.

Under this alternative situation, the cost of C_2 would reduce to:

labor cost:

$$\frac{2\text{ man-day} \times 8\text{ hr/man-day} \times 4\ \$/\text{hr} \times 43560\text{ ft}^2\text{ Ac}}{7\text{ Bed/day} \times 15\text{ ft} \times 150\text{ ft}} = \$105/\text{application/Acre}$$

($260/application/hectare)

sand renewal cost:

$$\frac{50\ \$/\text{Bed} \times 43560\text{ ft}^2/\text{Ac}}{8\text{ Apply.} \times 25\text{ ft} \times 150\text{ ft}} = \$\,73/\text{application Acre}$$

($180/application/hectare)

$$C_1 = \$178/\text{application/Acre}$$

($440/application/hectare)

Substituting this cost factor into Equation 174 produces the output shown in Table 31, indicating that the optimum depth reduces to 20 cm and the required bed area to 0.18 m^2 (1.98 ft^2) per capita with an increase in applications to 9 per year, while a saving of $0.089/cap/year would be realized by mechanical sludge removal. Therefore the decision of whether or not to use a machine to remove sludge would depend upon whether this saving would cover its annual per capita cost.

TABLE 31. ANNUAL COST OF SLUDGE DRIED IN BOISE, IDAHO FOR DIFFERENT APPLICATION DEPTHS (Dry Sludge Removed by Machine)(1)

Application Depth (cm)	Dewatering Time (day)	Bed Area (ft^2/cap)	No. of Application Per Year	Annual Cost ($/cap)(2)(3)
10	15	1.40	26	0.230
15	12	1.66	14	0.194
20	20-21	1.98	9	0.192*
25	30-35	2.32	6	0.198
30	44-57	2.90	4	0.224
35	58-81	3.32	3	0.242

(1) Type of Sludge: Digested Primary and Activated Sludge

(2) C_1 = $ 2672/AC = $ 0.061/ft^2

C_2 = $ 178/AC/Applic. = $ 0.004/ft^2/Applic.

(3) PI = 95%

* Optimum Depth.

A method has been illustrated in the above example to determine the optimum system design from the results of simulation by relating C_1 and C_2 to their associated variables, A_r and A_p. Appendix C of Lo (4) shows the optimum depths of application for sludges dried in various locations under different cost ratios C_2/C_1.

The way in which this information might be used is first to determine the cost terms C_1 and C_2 following which the design engineer, using expected drying time and/or performance index as the design criterion, could select the optimum depth in such a way that it best accounts for local weather and sludge conditions. After the optimum applied depth and the expected performance index have been determined, the required land area and its corresponding number of applications per year can be found from the data presented in Appendix B of Lo (4) in which ft^2/cap was used as the unit for sizing wastewater sludge dewatering beds and ft^2/lb of dry solids was used as the unit for sizing water treatment sludge dewatering beds.

MARGINAL ANALYSIS APPROACH

A simulation approach has been presented for the determination of optimum dewatering bed system design. An example illustrating this simulation methodology indicated that the 95 percent performance level could be attained in Boise, Idaho by using either a bed area of .022 m^2 (2.32 ft^2) per capita with 6 applications per year or 0.18 m^2(1.98 ft^2) per capita with 9 applications per year. Of course, the applied depth in the latter case was reduced from 25 to 20 cm in order to shorten the necessary dewatering time and make the additional 3 applications possible. This demonstrates that a tradeoff exists between land and labor, since application may be accomplished manually rather than by machine.

Both land and labor are economic resources which command a price at a given time and condition. They have long been analyzed in production theory in order to find an optimum combination that will produce the greatest amount of product for a given cost outlay. In this section, a production theory approach is taken to determine the optimum dewatering bed design, in which the whole process of dewatering is treated from the viewpoint of a firm that attempts to maximize the produce (dry solids) in relation to any given cost outlay by way of securing and combining resource inputs (bed area and applications).

The approach begins with the determination of a production function. In this study, Equation 173 is used as the production function because it expresses the physical relation between resource input and output, leaving price aside. In Equation 173,

$$PI(\%) = [W_d - \{A_n A_r H S_o \rho (P_n (n < A_{n-1})) - A_r H S_o \rho (\sum_{k=1}^{A_{n=1}} K P_n (K))\} \times 100]/W_{ts} \tag{173}$$

where PI = performance index, the percentage of the total dry solids dewatered

A_n = applications per year

A_r = required bed area

H = the applied depth

W_d, S_o, ρ, W_{ts} are parameters

Marginal analysis for one input. In many cases, the engineer may face a restriction on the use of land. For example, it is often desirable to increase the dewatering capacity of an existing plant in which the bed area is fixed, and auxiliary means of dewatering must be employed. Before the results can be analyzed in a least cost fashion, the relationship between the output and the input of sand bed dewatering must be examined in terms of the law of diminishing returns.

The following example should illustrate the law of diminishing returns numerically and graphically. Suppose that for a secondary sewage treatment plant in the Boston area the dewatering bed was fixed as 0.14 m^2 (1.5 ft^2) per capita. If different quantites of input and bed applications per year were applied to the bed, the performance index calculated from Equation 173 would be observed as shown in Table 31. It indicates that the performance index would increase linearly with an increase in the number of applications for the first four units. Then, beginning with 6 applications per year, the law of diminishing returns comes into effect and the marginal physical product of "application" decreases with an increase of the input resource. This marginal physical product of a resource is defined by economists (6,7,8) as the change in total product resulting from a one-unit change in the quantity of the resource used per unit of time. Thus the law of diminishing returns is also frequently called the law of diminishing marginal physical product.

The total product curve of Figure 63 plotted from columns 3 and 4 of Table 32 illustrates that the law of diminishing returns holds in this example. Obviously, the reason is that the weather limits the number of applications allowed each year. For later stages, an increase in number of bed applications would not yield any significant increase of performance index simply because there is only a very slight possibility that the "state of nature" would allow such a high number of applications.

Up to this point, only the physical relation between output and input has been considered. No mention was made of decision making since any recommendation as to the bed's optimum rate of application would depend upon the price of the output and the cost of each application. The dry sludge produced by dewatering beds has no significant cash value in the private market, thus there is no market price for the output. However, the output can be assigned a value represented by the cost of dewatering by an alternative method, or the amount of charge (fine) imposed by a regulatory agency for discharging untreated sludge. For example, assume that the value of the output is \$1.25/capita/year, and the cost of application is \$0.093/capita/m^2/year (\$0.026/capita/1.5 ft^2/year). If the number of applications is increased from 6 to 8 per year the input-output results in Table 31 would yield an additional value of

$$\frac{(47.755 - 35.855) \times 1.25}{100} = \$0.149/\text{capita/year}$$

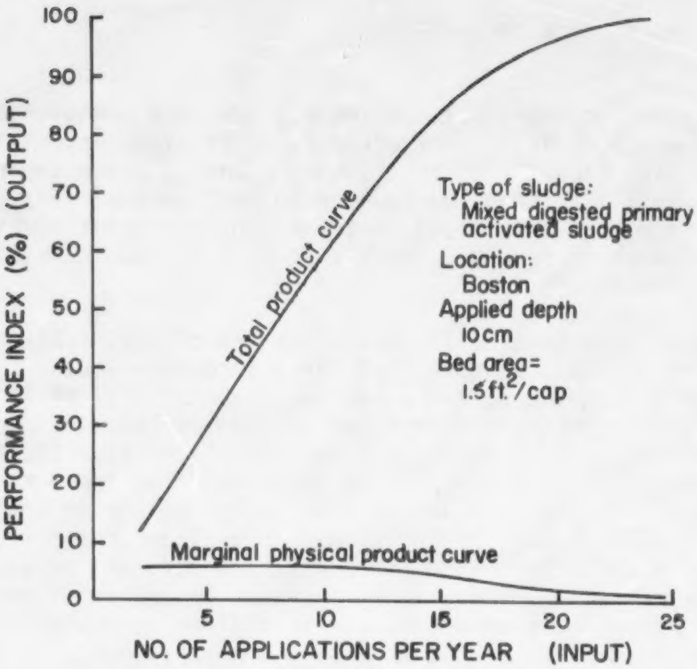

Figure 63: An input/output relation showing the law of diminishing returns.

at an additional cost of

$$2 \times 0.026 = \$0.051/\text{capita/yr}$$

As the value per additional unit of input is greater than the additional unit of input cost, it pays to increase the number of applications and the output. However, in order to find the optimum output the value of the total product and the marginal physical product have to be determined. For this particular example, they were obtained by multiplying 1.25 by the total product and the marginal physical product, and are shown in columns 5 and 6 of Table 32. Economists have proven that the optimum use of a variable input is obtained when the value of marginal physical product is equal to the cost of unit input. The marginal analysis implies (1) that if the last incremental increase in the number of applications does not pay for itself, fewer applications should be used, (2) that if the last increase of applications more than pays for itself, additional applications should be considered, and (3) the number of applications should be stopped at the point at which the last application just pays for itself.

TABLE 32. AN INPUT-OUTPUT* RELATION SHOWING THE LAW OF DIMINISHING RETURNS

(1) Bed Area (ft^2/Cap)	(2) No. of Applic. per year (labor)	(3) Total Product (performance) index	(4) Marginal Physical Product (labor)	(5) Total Value Product ($)	(6) Marginal Value Product ($)
1.5	2	11.954	5.977	0.149	0.075
1.5	4	23.908	5.977	0.299	0.075
1.5	6	35.855	5.972	0.448	0.075
1.5	8	47.755	5.938	0.597	0.074
1.5	10	59.438	5.795	0.743	0.072
1.5	12	70.481	5.404	0.881	0.068
1.5	14	80.211	4.654	1.003	0.058
1.5	16	87.954	3.592	1.099	0.045
1.5	18	93.395	2.433	1.167	0.030
1.5	20	96.729	1.433	1.209	0.018
1.5	22	98.502	0.731	1.231	0.009
1.5	24	99.321	0.324	1.242	0.004
1.5	26	99.651	0.125	1.246	0.002

*Type of Sludge: Mixed digested primary and activated sludge.
Location: Boston
Applied Depth: 10 cm

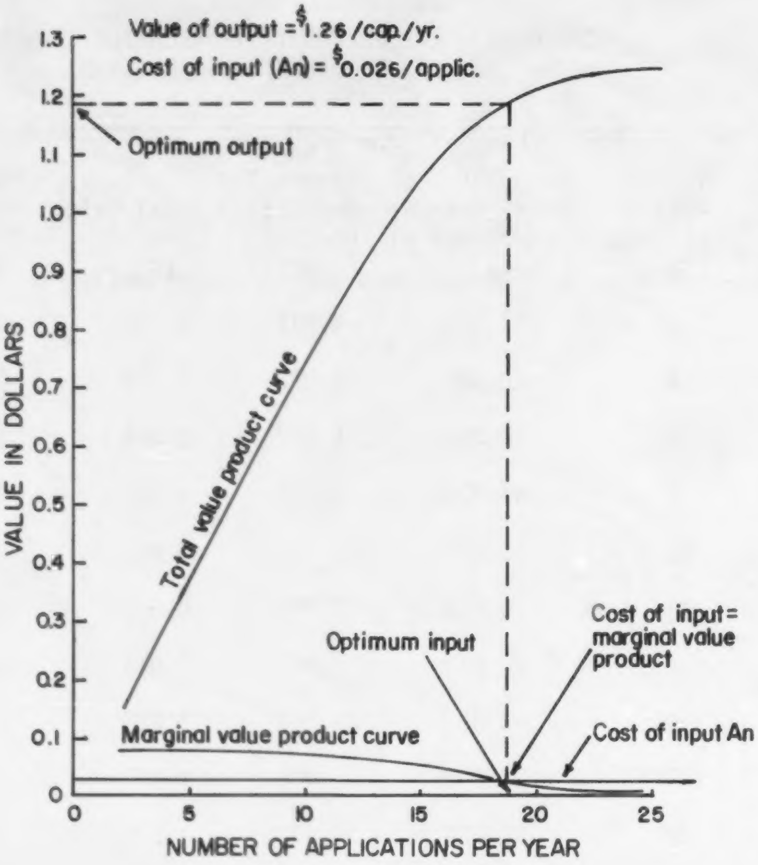

Figure 64: Determination of the optimum input and output.

Applying the above concept to an example produces the results shown in Figure 64 indicating that the optimum number of applications per year is 19 at the applied depth of 10 cm. The results for other application depths are shown in Table 33. Therefore the optimum operation of dewatering beds in Boston with a fixed bed area of 0.139 m^2(1.5 ft^2) per capita is to apply 15 cm sludge on the bed with 13 applications per year at a cost of \$0.026/application. For this optimum condition, the dewatering bed would handle about 82 percent of the sludge (since the performance index is 82 percent), and the untreated sludge is more economically treated by other means at a cost of \$1.25/cap. Therefore, if mechanical methods are used as an auxiliary means of dewatering, the capacity of the equipment should be designed to handle 18 percent of the sludge. Of course, this optimum condition would change when the value of the output and the cost of the input varied.

The fundamental difference between this approach and the simulation approach discussed in the preceding section is that the output in this approach was assigned a cash value, so that the logical optimum point in this

TABLE 33. THE RESULTS OF OPTIMUM SAND BED DEWATERING IN BOSTON WITH A FIXED BED AREA (0.14 m^2/1.5 ft^2) PER CAPITA (1)

Applied Depth of Sludge (cm)	Optimum Bed Applications per Year	Optimum Sand Bed Dewatering (Performance Index)	Cost of Sand Bed Dewatering (at \$0.026/ Application)	Cost of Mechancial Dewatering (at \$1.25/ Capita)	Total Cost per Capita
5	34	99%	0.885	0.013	0.898
10	19	95%	0.495	0.063	0.558
15	13	82%	0.325	0.223	0.548
20	9	71%	0.234	0.363	0.597

(1) Mixed digested primary and activated sludge.

method is the cost of input just equal to the marginal value of output. In the simulation approach the value of output was not considered. The purpose was to find a combination of inputs that fulfilled the target (say 95 percent performance index) at a minimum cost.

Marginal analysis for two inputs. In the previous section, marginal analysis was introduced to increase the economic efficiency for an existing plant which had limited land. This section takes up the more complicated aspect of drying bed optimization including more than one variable.

In designing a new plant, the restriction on land area usually does not exist, therefore the output (performance index) as shown in Equation 173 is conceived of as depending upon two important inputs, the total application per year (A_n), and the bed area (A_r). When two inputs are combined together to produce a given output, two questions are likely to be raised concerning the optimization: the first has to do with the proportion in which the two inputs should be used, the second has to do with the amount of the two inputs which would be produced. These two questions are answered by means of marginal analysis.

Under the concepts of marginal analysis for multi-variables, it is usually considered that different resources can be technical substitutes. Leftwich (6) pointed out that if labor and capital were used in digging a ditch of a certain length, width and depth, they could be substituted for each other within certain limits. But the more labor and the less capital used to dig the ditch, the more difficult it becomes to substitute additional labor for capital. Finally, additional units of labor just compensate for smaller and smaller amounts of capital. In our analysis, the inputs, bed applications per year (A_n) and the bed area (A_r), bear resemblance to the labor and capital example. Theoretically, the output from applying 10 cm of sludge on 2 units of land should be the same as that of two applications on one unit of land. In actuality, however, this substitution is complicated by the fact that the number of bed applications is limited by the duration of the drying season and by the "state of nature". Due to the effects of weather, the allowable number of applications in this study is a random variable, and the probability of an assumed number of applications will be realized decreasing with the increase of its value. In addition, for a given applied depth the calculated performance index will decrease as the number of applications increases. Therefore, a "trade-off" between the number of applications and land area at a given depth of sludge application is not practical in this case because of the complications mentioned above. Nevertheless, it has been shown that a perfect substitution of land and applications was possible if the applied depth was reduced for the purpose of shortening the necessary drying time. A possible increase in bed applications as a trade-off for a smaller bed area thus results. This substitution has been demonstrated clearly in Table 30, in which six different combinations of A_n and A_r were possible to obtain a constant output of 95 percent performance index. By drawing the above information as a smooth curve, an isoquant curve shown in Figure 65 is obtained, with which one can produce the same amount of output by using A_n in one direction and A_r in other direction. By using information contained in Appendix B of Lo (4), a family of isoquant lines may be drawn to indicate the different levels of output.

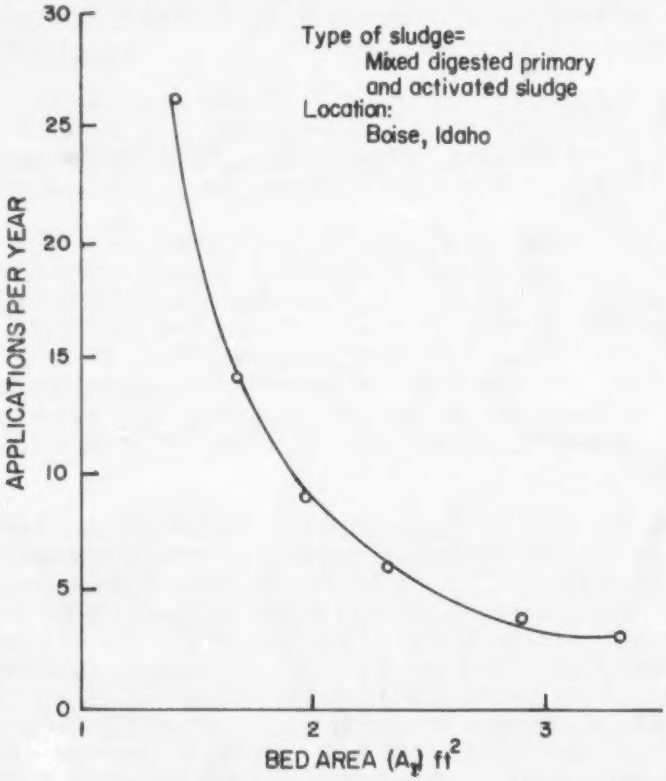

Figure 65: Iso-quant curve showing six different combinations of A_n and A_r which yield a constant output of 95% performance index.

At this point, there is a question concerning how the economizing procedure can be applied to locate the optimum amount of output and the optimum proportions in which two inputs should be used to dry the sludge under given economic conditions. This question is answered by determining the proportions in which the two inputs should be combined and by determining the optimum level of output.

1. Optimum proportion using bed application and bed area. It is obvious that the best way to spend a given amount of money on two inputs is such that they will produce the highest output. In order to achieve this, the cost of drying must first be decided upon before any optimization can be undertaken. A cost function introduced earlier is:

$$Z = C_1 A_r + C_2 A_n A_r \qquad (174)$$

in which C_1 and C_2 are costs associated with the inputs A_r and A_n, respectively. Based on the above equation, an isocost curve can be determined which shows the price per unit of each resource, and shows that different combinations of resources A_n and A_r can be allocated to produce output at a given cost outlay. In Figure 66 each curve represents a given cost outlay.

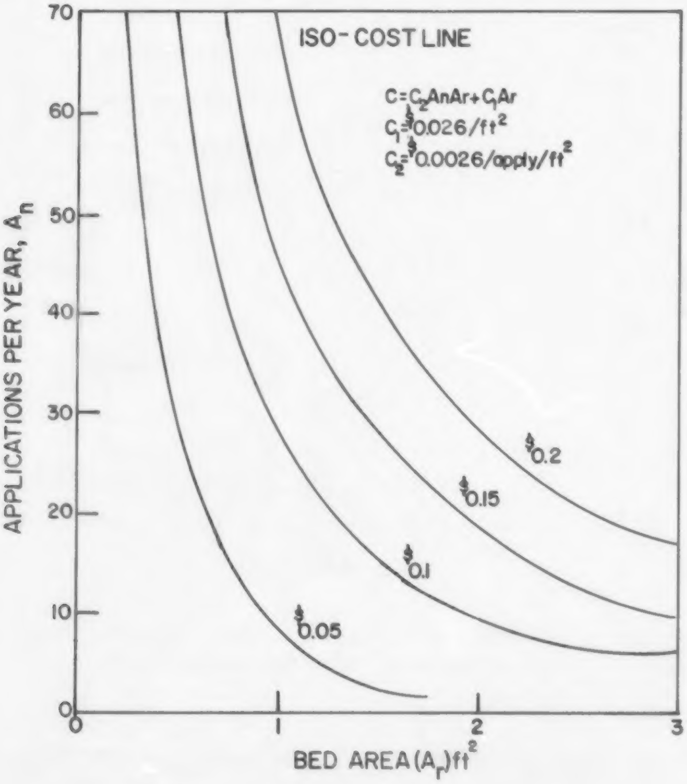

Figure 66: Curves of iso-cost lines.

Up to this point, the problem of optimization was reduced to combining the isoquant and isocost curves, and identifying the highest possible isoquant that its isocost curve would allow, so that the concept of deriving the greatest amount of product from the given cost outlay on resources might be realized.

The point at which the isoquant line is tangent to an isocost line yields the highest value of output attainable for that input. Therefore, it is the point of optimum combination. In Figure 67 it is easily seen that a greater cost outlay would be necessary if some non-optimum resource combination were used to produce the same quantity of output. Since this particular cost function gives a curved isocost line, it is difficult to determine the points of tangency. The curves shown in Figure 67 were set by trial, the isocost curves being drawn in the region of apparent tangency.

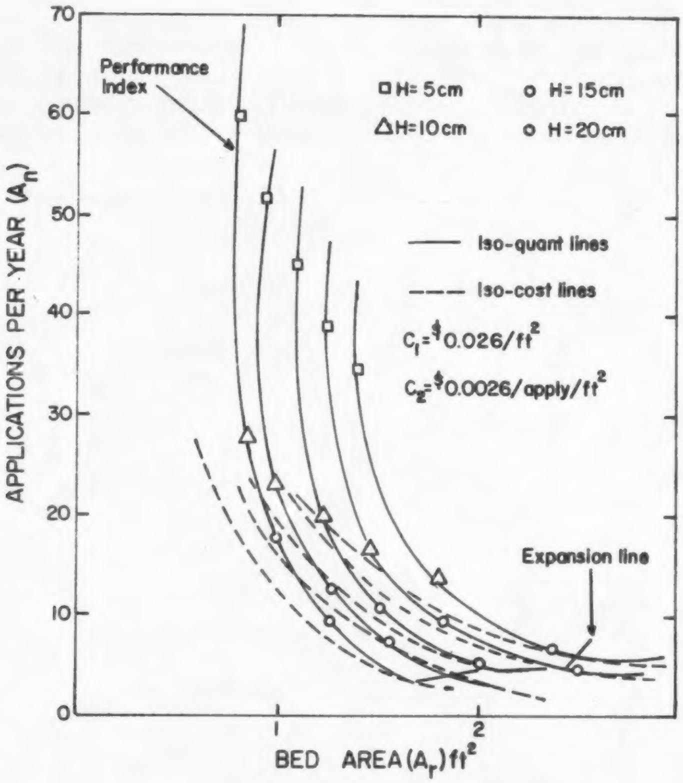

Figure 67: Diagram illustrating procedure for locating the points of optimum proportions.

Two important features should be noted in regard to Figure 67:

a. Change in the cost of resources will shift the isocost curve. For example, an increase in the land cost would shift the curve to the left to favor more applications and less land. When the land cost decreases, the curve shifts to the right favoring more land use and fewer applications. However, at any resource cost level, the tangent point would be the least possible cost of producing the given output.

b. After locating the optimum point on the isoquant curve, the optimum application depth is determined by interpolation because the isoquant curve is drawn from the points at different applied depths.

2. The optimum output level. The line which connects the optimum combination points in Figure 67 is called the expansion line by economists. It indicates the amount of output which should be produced at various investment levels. Since increased investment will result in a higher performance index, the optimum level of sand bed dewatering would obviously depend on the cost of treating the remaining sludge. This may be the cost of mechanically dewatering the excess sludge, or it may be the charge imposed by a regulatory agency. However, the optimum performance index is the least-cost combination of sand bed dewatering and dewatering by other means. The cost of sand bed dewatering for various performance index levels using Boston as an example is presented in Table 34. From this table it is readily apparent that the optimum level for gravity dewatering is at a performance index of 90 percent with the sludge application depth between 15 to 20 cm. At this level the required bed area is 0.19 m^2 (2.0 ft^2) with 8 bed applications per year.

TABLE 34. THE COST OF SLUDGE DEWATERING

Performance Index	Cost of* Sand Bed Drying	Cost of Mechanical Dewatering**	Total Cost per capita	Sludge Application depth (cm)
0%	-	1.250	1.250	-
60%	0.546	0.500	1.046	20
70%	0.623	0.375	1.008	20
80%	0.649	0.250	0.899	15-20
90%	0.728	0.125	0.853	15-20
95%	0.879	0.063	0.942	15-20

*The Cost of Land = $ 0.26/ft^2/yr.
The Cost of Application = 0.026/Application

**The Cost of Mechanical Dewatering = $1.25/Capita.

REFERENCES

1. ASCE & WPCF, Sewage Treatment Plant Design, Manual of Engineering Practice No. 36, 1959.

2. Meier, P. M. and Ray, D. L. "Optimum System Design," in Report No. EVE 13-69-1, Source Control of Water Treatment Waste Solids, Environmental Engineering, Department of Civil Engineering, University of Massachusetts, Amherst, 1969.

3. Ehrenfeld, S. and Vittaner, S. B. Introduction to Statistical Methods, McGraw-Hill, 1963.

4. Lo, K. Digital Computer Simulation of Water and Wastewater Sludge Dewatering on Sand Beds. Report No. EVE 26-71-1, Department of Civil Engineering, University of Massachusetts, Amherst, 1971.

5. Kane, E. J. Economic Statistics and Econometrics, Harper and Row, 1968.

6. Leftwich, R. H. The Price System and Resource Allocation, Holt, Rinehart and Winston, 1966.

7. Bradford, L. A. and Johnson, G. L. Farm Management Analysis, John Wiley & Sons, Inc., 1953.

8. Mass, A., et al. Design of Water Resource Systems, Harvard University Press, 1962.

APPENDIX

EXPERIMENTAL DETERMINATION OF SPECIFIC RESISTANCE AND COEFFICIENT OF COMPRESSIBILITY

Great care was taken to devise an accurate method to determine specific resistance, the basic sludge characteristic used in formulation of the mathematical model descriptive of gravity drainage properties. The lack of standard equipment and a standard procedure for the determination of specific resistance required development of special equipment, description of which follows

EQUIPMENT

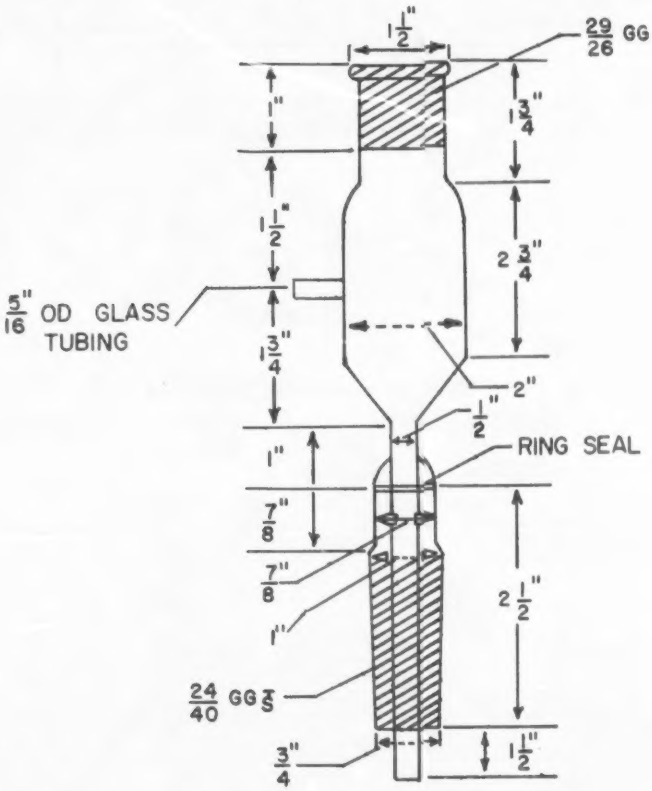

Figure A-1: Vacuum adaptor

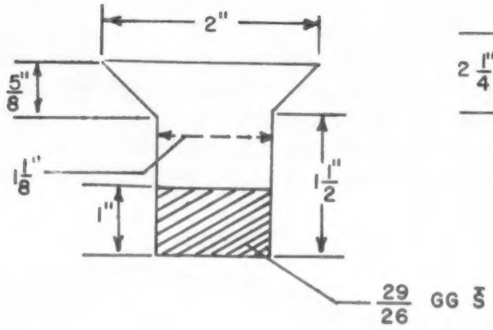

Figure A-2a: Funnel adaptor.

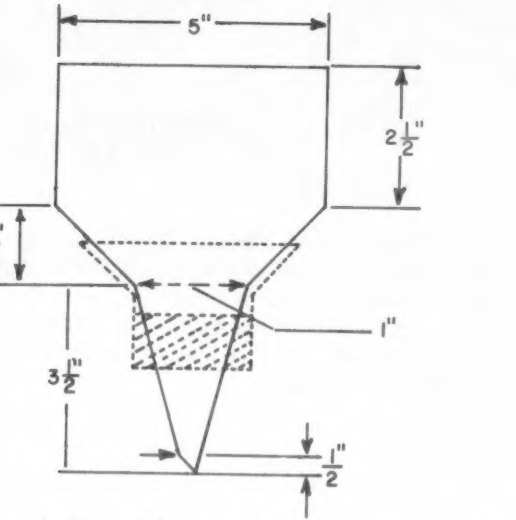

Figure A-2b: Adaptor in place on Buchner funnel (with epoxy cement seal).

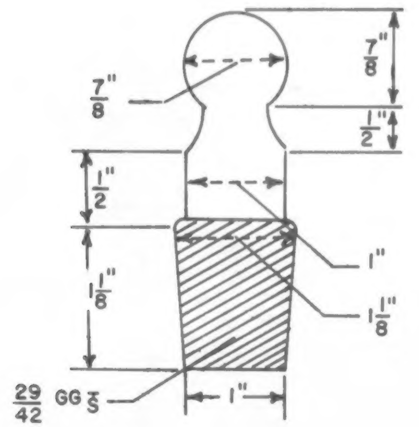

Figure A-3: Vacuum plug (optional).

a. The following custom glass equipment is fabricated:

(1) Join the female portion of a 24/40 S̄ ground glass joint to the open end of a 250 ml buret (1.0 ml subdivisions)

(2) Construct a vacuum adaptor as shown in Figure A-1 taking care that the glass in the narrow neck above the ringseal is not weakened. Anneal the fixture. A small drip extension (not shown) on the effluent end will be helpful.

(3) Use a short male section of a 29/26 S̄ joint, flair the funnel adaptor as shown in Figure A-2a. Anneal the fixture. Join the adaptor to the Buchner funnel with epoxy cement as shown in Figure A-2b.

b. Assembly of equipment

The components are assembled according to the schematic diagram of Figure A-4. Two screw clamps (not shown) may be substituted in series for the pressure control valve. The clamp nearest the manometer may be used to bring the manometer slightly below the desired pressure setting while the second clamp is used to fine-adjust the level.

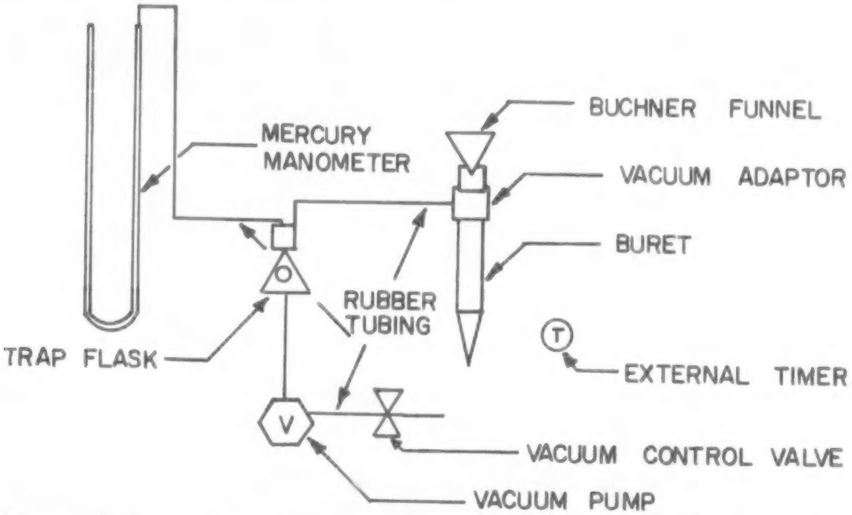

Figure A-4: Schematic flow diagram for specific resistance testing.

LABORATORY PROCEDURES

a. Storage of sludge sample.

The bulk samples are stored in a 20°C constant temperature room in closed containers.

b. Preparation of the test samples.

(1) Bulk samples are thoroughly mixed by gentle stirring to provide homogeneity.

(2) A smaller 32-ounce (95 ml) polyethylene bottle is filled and its contents used throughout the testing. This aliquot is sufficient to perform triplicate solids analysis as well as three specific resistance tests.

c. Laboratory analysis

(1) Solids Determinations.

Solids determinations are run in triplicate 50 ml samples according to Standard Methods (12th Edition) part III, Residue on Evaporation.

(2) Remove the Buchner funnel from the vacuum adaptor and insert the vacuum plug. By means of the pressure control selected, adjust the manometer to a constant pressure level. Since three separate tests will be run in the range from 10 cm Hg to 50 cm Hg, it is suggested that a low pressure test be run first to become familiar with the equipment.

(3) Wet the porous surface of the Buchner funnel and cover with Whatman No. 5 filter paper. Smooth out wrinkles and air bubbles, replace the funnel in the vacuum adaptor, and apply a vacuum to void the paper of excess water.

(4) Measure 100 ml of wet sludge into a graduated cylinder and apply to the filter surface of the Buchner funnel.

(5) Apply a vacuum to the system. Since there will be a time lag between the inception of the vacuum and the actual present value, the timer is not actuated until the present pressure value is reached. Record the initial volume on the data sheet shown in Figure A-5 when the timer is started. Record the pressure and room temperature at this time.

(6) Remove the Buchner funnel at the end of each test, record the depth of sludge cake, and perform triplicate residue (total) tests on the cake as outlined.

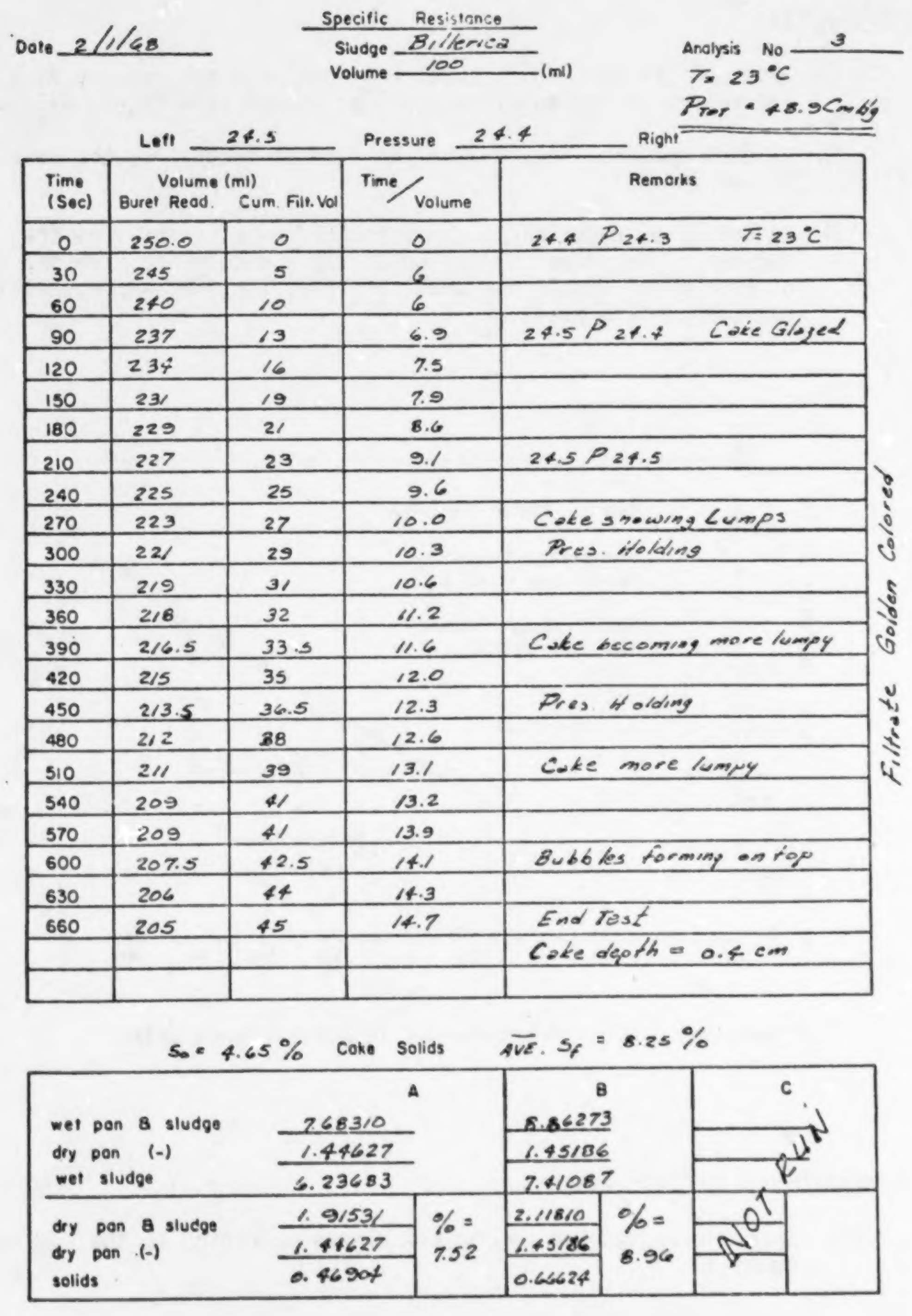

Specific Resistance

Date 2/1/68

Sludge Bilkerica

Volume 100 (ml)

Analysis No 3

T = 23 °C

P_{TOT} = 48.9 Cm Hg

Left 24.5 Pressure 24.4 Right

Time (Sec)	Volume (ml)		Time / Volume	Remarks
	Buret Read.	Cum. Filt. Vol		
0	250.0	0	0	24.4 P 24.3 T = 23 °C
30	245	5	6	
60	240	10	6	
90	237	13	6.9	24.5 P 24.4 Cake Glazed
120	234	16	7.5	
150	231	19	7.9	
180	229	21	8.6	
210	227	23	9.1	24.5 P 24.5
240	225	25	9.6	
270	223	27	10.0	Cake showing Lumps
300	221	29	10.3	Pres. Holding
330	219	31	10.6	
360	218	32	11.2	
390	216.5	33.5	11.6	Cake becoming more lumpy
420	215	35	12.0	
450	213.5	36.5	12.3	Pres. Holding
480	212	38	12.6	
510	211	39	13.1	Cake more lumpy
540	209	41	13.2	
570	209	41	13.9	
600	207.5	42.5	14.1	Bubbles forming on top
630	206	44	14.3	
660	205	45	14.7	End Test
				Cake depth = 0.4 cm

Filtrate Golden Colored

S_o = 4.65 % Cake Solids $\overline{AVE}$. S_f = 8.25 %

	A		B		C
wet pan & sludge	7.68310		8.86273		NOT RUN
dry pan (-)	1.44627		1.45186		
wet sludge	6.23683		7.41087		
dry pan & sludge	1.91531	% = 7.52	2.11810	% = 8.96	
dry pan (-)	1.44627		1.45186		
solids	0.46904		0.66624		

Figure A-5: Sample data and data format for specific resistance test.

DATA ANALYSIS

(1) Subtract the succeeding buret readings from the reading at t = 0 and record in the cumulative volume column (see Figure A-5).

(2) At each reading time, divide the time in seconds by the cumulative volume in ml.

(3) On Cartesian paper plot t/V as the ordinate versus V as the abcissa. The slope "b" may be directly determined from the line of best fit. Figure A-6 shows the plot for the sample specific resistance data provided.

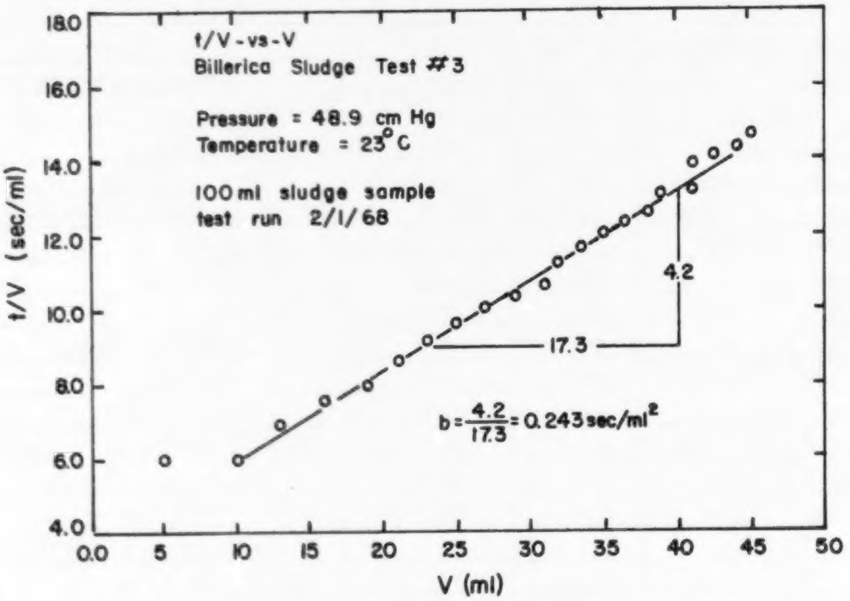

Figure A-6: Plot of sample specific resistance data.

CALCULATION OF SPECIFIC RESISTANCE

(1) Specific resistance may be calculated according to the following equation

$$R = \frac{2\ b\ A^2\ \Delta p}{\mu c}$$

where: R = specific resistance (sec^2/gm)

b = slope of t/V vs. V (sec/ml^2)

A = area of filter paper (cm^2)

Δp = test pressure ($dynes/cm^2$); p is taken as the average test pressure in cm Hg X 13333.22 to convert to $dynes/cm^2$.

μ = dynamic viscosity (poise) or dyne sec/cm^2 may be found in various handbooks or calculated by the formula:

$$\mu = \frac{1.0}{2.1482[(t-8.435) + \{8078.4 + (t-8.435)^2\}^{0.5} -120}$$

where t = test temperature (^oC)

c = weight of solids per unit volume of filtrate ($gm/cm^2 \cdot sec^2$), given by the formula:

$$C = \frac{\rho g}{\frac{100}{S_o} - \frac{100}{S_f}}$$

where: ρ = density of filtrate (assumed water) at the test temperature (gm/cm^3)

g = gravitational constant (980.0 cm/sec^2)

S_o = initial sludge solids content

S_f = sludge solids content after testing

(2) Sample Calculation

$b = 0.243$ (see Figure A-6)

diameter of filter paper = 11.1 cm

pressure = 48.9 cm Hg

temperature = 23^oC

$S_o = 4.65\%$

$S_f = 8.25\%$

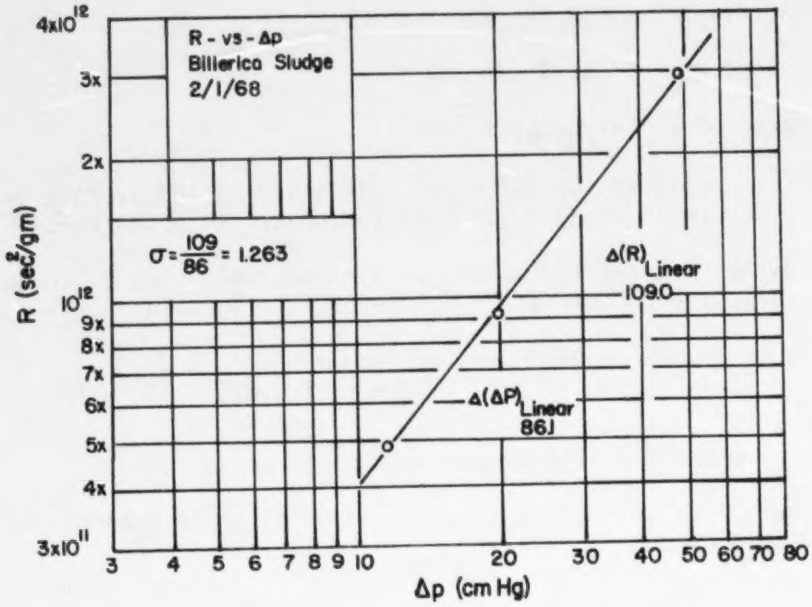

Figure A-7: Graph for calculating coefficient of compressibility.

$$R = \frac{2(0.243)\ (9.364 \times 10^3)\ (48.9 \times 1.33 \times 10^4)}{(9.358 \times 10^3)\ \dfrac{(0.997538)\cdot(980)}{(\frac{100}{0.0465}) - (\frac{100}{0.0825})}}$$

$$R = 3.05 \times 10^9 \ \mathrm{sec}^2/\mathrm{gm}$$

CALCULATION OF COEFFICIENT OF COMPRESSIBILITY

It has been experimentally determined that specific resistance is related to pressure by the following

$$R = R_c\left(\frac{h}{h_c}\right)^{\sigma}$$

where R = specific resistance (sec^2/gm)

R_c = specific resistance at a head h_c

h = test head

σ = coefficient of compressibility (dimensionless)

(1) Before determining the coefficient of compressibility, three or more specific resistance tests must be run, as previously outlined, at pressures of about 10, 20, and 50 cm Hg.

(2) Plot on bi-logarithmic paper each resistance ordinate versus the pressure at which the resistance was run. Determine the slope σ which is the coefficient of compressibility, as shown in Figure A-7.